Aus der Kinderklinik und Kinderpoliklinik im

Dr. von Haunerschen Kinderspital,

Klinik der Universität München

Vorstand: Prof. Dr. Dr. Christoph Klein

Dissertation

zum Erwerb des Doktorgrades der Medizin

an der Medizinischen Fakultät der

Ludwig-Maximilians-Universität zu München

T-cell interaction with leukemia in the bone marrow of pediatric patients with T-cell acute lymphoblastic leukemia

vorgelegt von

Jonas Wilhelm

aus

München, Deutschland

Jahr

2022

Mit Genehmigung der Medizinischen Fakultät

der Universität München

Berichterstatter:	Prof. Dr. Tobias Feuchtinger
Mitberichterstatter:	PD Dr. Hanna-Mari Baldauf
	Prof. Dr. Helga Maria Schmetzer
Mitbetreuung durch die promovierten Mitarbeiter:	Dr. Semjon Willier, Dr. Franziska Blaeschke
Dekan:	Prof. Dr. med. Thomas Gudermann
Tag der mündlichen Prüfung:	28.07.2022

„Leukämie muss heilbar werden.

Immer und bei jedem.“

José Carreras

Inhalt

1. Abstract

Pediatric T-cell acute lymphoblastic leukemia (T-ALL) accounts for 10-15% of pediatric ALL cases. 5-year overall survival is between 70-80%. Clinical breakthroughs of immunotherapeutic approaches for different tumor entities and new developments, emphasize the potential of immune interaction for cancer treatment. T-ALL is a non-immunogenic disease, and the search of possible T-ALL specific target antigens is further complicated by a low mutational burden of the leukemic T-ALL blasts. For the development of suitable immunotherapies for pediatric T-ALL, the knowledge of immune interaction is essential.

In this context we systematically characterized bone marrow (BM) of pediatric T-ALL patients and healthy BM donors as a reference. We compared the expression of differentiation markers and immune checkpoints (IC) of bone marrow T cells (bmT cells) and leukemic blasts (T-ALL patients) or physiological T-cell progenitors (healthy BM donors) in the BM. Since bmT cells are located in the BM microenvironment, they are also referred to as tumor infiltrating lymphocytes (TIL).

In total 72 samples were processed and analyzed: (1) 24 samples from pediatric T-ALL patients from the Hauner children´s hospital (samples of initial diagnosis of patients with/without future relapse and samples of relapse). (2) 34 samples from pediatric T-ALL patients from the CoALL study (initial diagnosis). (3) 14 samples from healthy BM donors as a reference. With a focus on the flow cytometric analysis, bmT cells and blast samples with sufficient cells were further processed and subsequently used for RNA isolation/sequencing and assessment of chromatin accessibility via ATAC-sequencing.
Flow cytometric analysis showed a shift of CD4+ and CD8+ bmT-cell phenotype towards advanced maturation. Co-inhibitory IC were upregulated on CD4+ and CD8+ bmT cells in flow cytometric analysis (CTLA-4, LAG-3, TIM-3). RNA-sequencing of CD8+ bmT cells showed significantly increased expression of genes coding for co-inhibitory markers LAG-3 and CTLA-4. Further, RNA-sequencing of CD8+ bmT cells revealed increased expression of genes coding for Granzyme B, Perforin 1, Granulysin and a decreased expression of the IL21R and RARA, suggesting bmT-cell exhaustion and decreased T-cell effector function in the BM micromilieu as the results of chronic activation. Leukemic T-ALL blasts showed an upregulation of costimulatory molecules (CD28, CD27, OX40, CD70, ICOS) and downregulation of co-inhibitory markers (CD160, TIGIT, 2B4, TIM-3, CD57). To identify blast-T cell interactions – possible target pathways for an immunotherapeutic approach – several combinations of IC on bmT cells and corresponding IC on the leukemic blasts were analyzed. Blast-T cell interaction via the CD112-TIGIT axis is suggested by the expression pattern. The comparison of T-ALL patients suffering from future relapse, led to the identification of potential prognostic markers correlating with

increased risk of relapse: (1) Overexpression of TIM-3 on CD4+ and CD8+ bmT cells as well as (2) overexpression of PD-1 on leukemic blasts are associated with increased risk of relapse.

In conclusion, local immune interaction of leukemic blasts with bmT cells was evaluated in the micromilieu BM for pediatric T-ALL patients compared to the healthy control individuals. Prospective studies will be necessary to examine possible clinical relevance.

2. German Abstract (Zusammenfassung)

Die akute lymphatische Leukämie vom T-Zell-Typ (T-ALL) ist mit 10-15% aller pädiatrischen akuten lymphatischen Leukämien vergleichsweise selten, hat jedoch mit einer 5-Jahres Überlebensrate von 70-80% eine schlechtere Prognose als z.B. B-Zell-Neoplasien. Klinische Durchbrüche und neuste Entwicklungen bei immuntherapeutischen Ansätzen zeigen deren großes Potential. Die geringe Mutationslast der malignen T-Zell-Blasten erschwert die Suche nach möglichen Zielstrukturen. Detaillierte Charakterisierungen der Interaktion mit dem Immunsystem, können jedoch eine Grundlage für neue immuntherapeutische Ansätze bilden.

In dieser Arbeit wurde das Knochenmark pädiatrischer T-ALL Patienten und gesunder Knochenmarkspender als Referenz analysiert. Der Phänotyp der CD4+ und CD8+ T-Zellen, sowie leukämischer Blasten (T-ALL Patienten), bzw. physiologischer T-Vorläuferzellen (gesunde Knochenmarkspender) wurde hinsichtlich der Expression verschiedener Differenzierungsmoleküle und immun-modulatorischer Moleküle (immune checkpoints, IC) charakterisiert. Da die T-Zellen im Mikromilieu Knochenmark lokalisiert sind, können sie auch als Tumor-infiltrierende Lymphozyten bezeichnet werden.

Im Rahmen des Projekts wurden insgesamt 72 Proben aufgearbeitet und analysiert: (1) 24 Proben pädiatrischer T-ALL Patienten des Dr. Haunerschen Kinderspitals (Proben initialer Diagnose von Patienten mit/ohne Rezidiv und Rezidivproben). (2) 34 Proben pädiatrischer T-ALL Patienten der CoALL-Studienzentrale (initiale Diagnose). (3) 14 Proben gesunder Knochenmarkspender als Referenz. Während der Fokus des Projekts auf der durchflusszytometrischen Untersuchung lag, wurden bei ausreichender Zellzahl RNA-Isolation/-Sequenzierung und ATAC-Sequenzierung der verschiedenen Knochenmarkpopulationen durchgeführt.

In der Durchflusszytomie zeigten CD4+ und CD8+ T-Zellen der T-ALL Patienten vermehrt Oberflächenmarker im Sinne einer fortgeschrittenen Reifung. Auf der Zelloberfläche wurden vermehrt co-inhibitorische Moleküle auf CD4+ und CD8+ T-Zellen exprimiert (CTLA-4, LAG-3, TIM-3). Dies konnte für CD8+ T-Zellen bereits auf RNA-Ebene bestätigt werden (signifikant erhöhte Expression der Genkorrelate für LAG-3 und CTLA-4). Die CD8+ T-Zell-Population von pädiatrischen T-ALL Patienten zeigte auf RNA Ebene eine vermehrte Expression der Gene kodierend für Granzyme B, Perforin 1, Granulysin und eine verminderte Expression der Gene IL21R und RARA im Vergleich zu gesunden Knochenmarkspendern. Dies unterstützt die These einer Erschöpfung der Effektorfunktion im Sinne einer chronischen Überaktivierung der T-Zellen im Mikromilieu Knochenmark. Die leukämischen T-ALL Blasten zeigten eine vermehrte Oberflächenexpression co-stimulatorischer Moleküle (CD28, CD27, OX40, CD70, ICOS) und eine verminderte Expression co-inhibitorischer Moleküle (CD160, TIGIT, 2B4,

TIM-3, CD57). Die Interaktion zwischen Blasten und T-Zellen wurde durch Messung verschiedener IC

auf T-Zellen und deren Bindungspartner auf Seite der Blasten untersucht – mit dem Ziel der Identifizierung potenzieller Zielstrukturen für zukünftige immuntherapeutischer Ansätze. Eine mögliche Interaktion konnte bei der CD112-TIGIT Achse gefunden werden. Der Vergleich der T-ALL Patienten nach Rückfall gegenüber denen ohne zukünftigen Rückfall führte zu der Identifizierung möglicher prognostischer Marker: (1) Vermehrte Expression von TIM-3 auf CD4+ und CD8+ T-Zellen und (2) vermehrte Expression von PD-1 auf leukämischen T-Zell Blasten führen zu einem erhöhten Risiko für einen Rückfall Leukämie im Verlauf.

Zusammenfassend konnte eine Interaktion von pädiatrischen T-ALL Blasten mit T-Zellen im Mikromilieu Knochenmark pädiatrischer T-ALL Patienten identifiziert werden. Prospektive Untersuchungen werden eine mögliche klinische Relevanz weiter evaluieren müssen.

3. Abbreviations

Abbreviation	
2B4	2B4 receptor
ALL	Acute lymphoblastic leukemia
AML	Acute myeloid leukemia
APC	Antigene presenting cell
ATAC	Assay for transposase accessible chromatin
BCP-ALL	B-cell progenitor acute lymphoblastic leukemia
BiTE	bispecific T-cell engager
BM	Bone marrow
bmT cell	Bone marrow T-cell
BTLA	B- and T-cell lymphocyte attenuator
CAR T cell	Chimeric antigen receptor T-cell
CCR	Complete cytogenic remission
CD	Cluster of differentiation
CNS	Central nervous system
CoALL study	Cooperative Acute Lymphoblastic Leukemia study
CPI	Immune checkpoint inhibitor
CTLA-4	Cytotoxic T-lymphocyte-associated antigen 4
Isotype Ctrl	Isotype control
DC	Dendritic cell
DMSO	Dimethyl sulfoxide
DNA	Deoxyribonucleic acid
DNAseI	Desoxyribonuclease I
ec	Extracellular
F	Female
FACS	Fluorescence activated cell sorting
FAS	FAS cell surface death receptor
FC	Fold change
FCS	Fetal bovine serum
FDA	Food and Drug Administration
FITC	Fluoresceinisothiocyanat Isomer I
FMF	Fluorescence minus four
FR	Future relapse
FSC-A	Forward scatter-area
FSC-H	Forward scatter-height
GITR	Glucocorticoid-induced TNFR-related protein
GRLY	Granulysin
GvHD	Graft-versus-host disease
GZMB	Granzyme B
HCH	Hauner children´s hospital

HD	Healthy bone marrow donor
Healthy BMD	Healthy bone marrow donor
HSCT	Hematopoetic stem cell transplantation
HVEM	Herpes Virus Entry Mediator
IC	Immune checkpoint
ic	Intracellular
ICOS	Inducible T-cell co-stimulator
iDx	Initial diagnosis
IFN	Interferon
IgG	Immunoglobulin G
IL	Interleukin
IL21R	Interleukin 21 receptor
Int	Intermediate
LAG-3	Lymphocyte-activation gene 3
LR	Late responder
LTCP	Leukemic T-cell progenitors
M	Male
Min	Minutes
MM	Multiple myeloma
MRD	Minimal residual disease
mRNA	Messenger-RNA
MUC1 5E10	Mucin-1 5E10 monoclonal antibody
MUC1 5E5	Mucin-1 5E5 monoclonal antibody
MYB	MYB proto-oncogene
N/A	Not available
NF-κB	Nuclear factor kappa-light-chain-enhancer of activated B cells
NFR	No future relapse
NGS	Next generation sequencing
NK cell	Natural killer cell
NP40	Nonidet P40
ns	Not significant
NT5E	Ecto-5'-nucleotidase
OX40	OX40 receptor
PBMCs	Peripheral blood mononuclear cells
PBS	Phosphate-buffered saline
PCR	Polymerase chain reaction
PD-1	Programmed cell death protein 1
PD-L1	Programmed cell death-ligand 1
Pen-Strep	Penicillin-Streptomycin
PFR1	Perforin 1
RARA	Retinoic acid receptor alpha

RFS	Relapse-free survival
RIN	RNA Integrity Number
RNA	Ribonucleic acid
RPKM	Reads per kilo base per million mapped reads
RPM	Rounds per minute
RPMI medium	Roswell Park Memorial Institute medium
RT	Room temperature
SSC-A	Side scatter-area
T	Treated CoALL T-ALL patients
T-ALL	T-cell acute lymphoblastic leukemia
T_{CM}	Central memory T-cells
TCP	T-cell progenitors
TCR	T-cell receptor
TD buffer	DNA tagmentation buffer
T_{EFF}	Effector T cells
T_{EM}	Effector memory T cells
TIGIT	T cell immunoreceptor with Ig and ITIM domains
TIL	Tumor-infiltrating lymphocyte
TIM-3	T-cell immunoglobulin and mucin-domain containing-3
TME	Tumor microenvironment
TN	Therapy naive CoALL T-ALL patients
$T_{N/SCM}$	Naïve/stem cell-like memory T cells
TNF	Tumor necrosis factor
TRBC1	T-cell receptor beta constant 1
T_{regs}	Regulatory T cells
TRIM39	Tripartite motif containing 39
TRM T cell	Tissue-resident memory T cell
TSA	Tumor specific antigen
T_{SCM}	Stem cell-like memory T cells
TXN	Thioredoxin
U	Units
WBC	White blood cell
Y	Years

4. Introduction

4.1. Pediatric acute lymphoblastic leukemia

Leukemia is the most common childhood malignancy accounting for approximately one-third of pediatric malignancies. Acute lymphoblastic leukemia (ALL) constitutes for 80-85% of all pediatric leukemia cases and most commonly develops from B-cell progenitors (B-cell acute lymphoblastic leukemia, BCP-ALL). However, 10-15% of all pediatric ALL cases originate from T-cell progenitors (T-cell acute lymphoblastic leukemia, T-ALL). T-ALL affects predominantly male children with a median age of nine years (Karrman & Johansson, 2017). Most commonly patients show elevated white blood cell count (WBC) with hematopoietic failure (neutropenia, anemia, thrombocytopenia) (Belver & Ferrando, 2016; Bernbeck et al., 2009). In approximately 60% of T-ALL cases patients present with a mediastinal mass; infiltration of the central nervous system (CNS) can be observed in around 10% of the patients (Karrman & Johansson, 2017). While T-ALL is characterized by a blast count of more than 25% in the bone marrow (BM), T-cell lymphoblastic lymphoma shows limited or no infiltration of the BM. T-ALL and T-cell lymphoblastic lymphoma are considered two different manifestations of the same disease (Basso et al., 2011).

According to the European Group of Immunologic Classification (EGIL) the following subgroups can be distinguished using immunophenotypic features: pro-T-ALL (EGIL T-I), pre-T-ALL (EGIL T-II), cortical T-ALL (EGIL T-III), medullary T-ALL (EGIL T-IV) and EGIL T-γ/δ (Mroczek, Zawitkowska, Kowalczyk, & Lejman, 2021). Early T-cell precursor ALL (ETP-ALL) was first described by the WHO in 2016. ETP-ALL is characterized by immunophenotypic as well as genetic features and is associated with dismal outcome (Arber et al., 2016; Karrman & Johansson, 2017; Lato, Przysucha, Grosman, Zawitkowska, & Lejman, 2021).

The 5-year survival rate in cases of BCP-ALL has increased to 80-90% within the last few decades, whereas 5-year overall survival for pediatric T-ALL patients is inferior with 70-80% (Karrman & Johansson, 2017). Monitoring of T-ALL patients by minimal residual disease (MRD) analysis plays an important role for evaluating the effect of treatment and the risk of relapse (Schrappe et al., 2011). T-ALL relapses usually occur within the first two years after initial diagnosis and are associated with chemotherapy resistance and poor outcome (Fielding et al., 2006). Most frequently T-ALL recurrences are located in the BM (57.3%) or CNS (20.9%) (Lato et al., 2021).

Standard of care therapy for T-ALL patients includes a risk-based chemotherapy with a variety of multidrug regimens over a period of 2-3 years. Cranial radiation therapy prevents CNS relapse in high-

risk settings (Fattizzo, Rosa, Giannotta, Baldini, & Fracchiolla, 2020; Raetz & Teachey, 2016). Dexamethasone has shown to reduce relapse rates at the cost of increased infectious toxicity (Lato et al., 2021). Nelarabine (an antimetabolite causing inhibition of DNA synthesis) was originally used for relapsed/refractory T-ALL and is currently also applied in cases of high-risk patients to reduce the risk of CNS relapse and improve the outcome (Berg et al., 2005; Dunsmore et al., 2020). Hematopoietic stem cell transplantation (HSCT) is considered for patients with persistent MRD or relapse (Raetz & Teachey, 2016).

Acute and long-term chemotherapy related toxicity and the development of secondary malignancies present a serious issue in pediatric cancers (Durinck et al., 2015). Despite intensified chemotherapy protocols around 20% of pediatric T-ALL patients relapse and pass away due to disease progression (Belver & Ferrando, 2016). The survival rate for relapsed T-ALL is reported at around 25% (Teachey & O'Connor, 2020). Consequently, new therapy options are urgently needed preeminently in cases of refractory or relapsed T-ALL (Lato et al., 2021).

4.2. Cancer immunology

T cells can recognize tumor specific antigens by their T-cell receptor (TCR), such detection enabling elimination of tumorous cells (Thaxton & Li, 2014). However, pediatric T-ALL has been labelled a low immunogenic disease with few somatic mutations and therefore few tumor specific antigens (TSA) (Karrman & Johansson, 2017). The analysis of mutations in a wide spectrum of malignancies underlines that the mutational burden of ALL is low, especially compared to other tumor entities including melanoma and various lung cancers (Alexandrov et al., 2013). Current data suggests that both mutations in the coding genome and the non-coding genome may contribute to tumor immunogenicity (Laumont et al., 2018). Consequently, the assumption that T-ALL is a non-immunogenic disease will have to be reevaluated in the future.

The expression of co-inhibitory and co-stimulatory surface molecules, also known as immune checkpoints (IC) (Figure 1), results in an anti-, or pro-inflammatory modulation of the immune response. In healthy individuals those mechanisms play an essential role for self-tolerance and prevention of autoimmune reactions against endogenous tissue (Pardoll, 2012). However, these mechanisms can be used by malignant cells to escape both the innate and adaptive immune system (Jiménez-Morales, Aranda-Uribe, Pérez-Amado, Ramírez-Bello, & Hidalgo-Miranda, 2021). The overexpression of co-inhibitory as well as the downregulation of co-stimulatory IC on the surface of tumor cells can lead to T-cell anergy and decreased T-cell response against the malignant cells (Pardoll, 2012).

Continuous presentation of tumor cells bearing a weakly immunogenic TSA can lead to chronic activation and T-cell dysfunction (Jiang, Li, & Zhu, 2015). Those dysfunctional T cells are termed exhausted and are characterized by the expression of surface molecules (exhaustion markers) on the T-cell surface, e.g., programmed cell death Protein 1 (PD-1) and cytotoxic T-lymphocyte-associated antigen 4 (CTLA-4). Further molecules such as T-cell immunoglobulin and mucin-domain containing-3 (TIM-3), lymphocyte-activation gene 3 (LAG-3) and T-cell immunoreceptor with Ig and ITIM domains (TIGIT) have been associated with T-cell exhaustion (Pauken & Wherry, 2015; Zarour, 2016). Exhausted T cells fail to control tumor growth and tumors can progress despite the presence of tumor-infiltrating lymphocytes (TIL) and TSA-specific cytotoxic T cells. Exhausted T cells show decreased proliferation and cytokine production as well as inhibition of the cytotoxic capacity of T cells (Zarour, 2016). By blocking the co-inhibitory IC PD-1 the process of T-cell exhaustion itself was found to be reversible leading to durable or no tumor response, the latter being denoted as “terminally exhausted” (Miller et al., 2019).

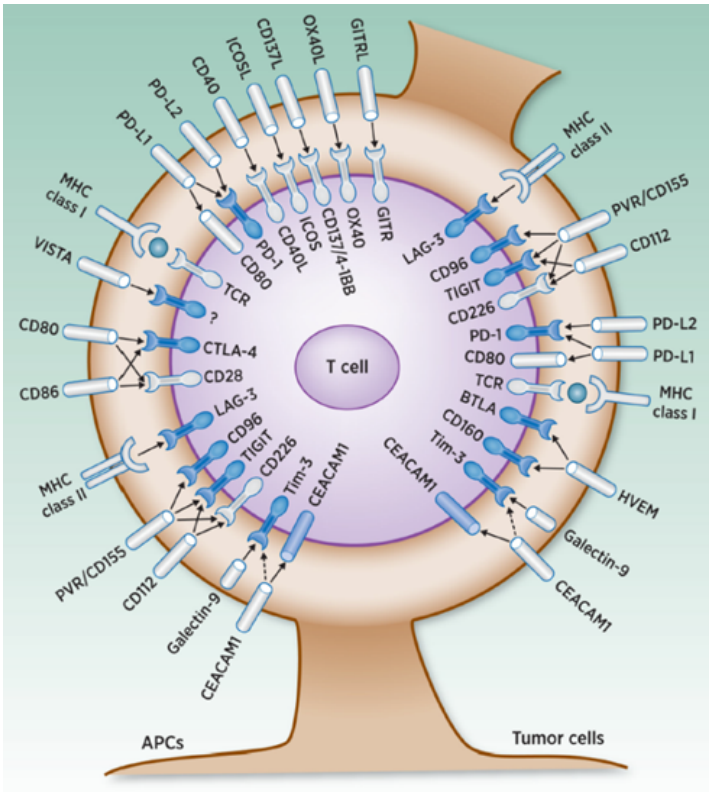

Figure 1: Co-stimulatory andCo-stimulatory and co-inhibitory molecules and their responsive ligands on the surface of T cells, tumor cells and antigen presenting cells (APC) ((Zarour, 2016): Surface molecules on T cells have either stimulatory effects (white symbols) or inhibitory effects (blue symbols).

4.3. Cancer immunotherapy

Alternative treatment strategies directly target the host immune system and not the cancer itself and therefore present an opportunity to avoid chemotherapy related off-target side effects and long-term toxicity. Within the group of immunotherapeutic approaches modalities that amplify existing antitumor immunity (e.g., checkpoint inhibition) are distinguished from synthetic immunotherapies that initiate an immune response to tumor-expressed targets (e.g., chimeric antigen receptor T cells, CAR T cells) (Majzner, Heitzeneder, & Mackall, 2017). Developing specific targeted therapies with limited side effects and off-target-organ toxicity shows the great potential of new immunotherapies.

The application of immune checkpoint inhibitors (CPI) represents one possible immunotherapeutic approach for the treatment of diverse malignancies. CPI are antibodies that antagonize/agonize co-inhibitory/co-stimulatory IC leading to enhanced endogenous antitumor activity. Depending on the expression of different IC molecules on the tumor-cell surface there is a large variety of potential target structures for CPI-mediated immunotherapeutic approaches (Pardoll, 2012).
Feucht et al. could already show that leukemic cells in the BM of pediatric BCP-ALL patients display a different checkpoint profile than physiological precursor cells of healthy BM donors. The T-cell mediated immune response could be amplified via the blockade of PD-1 in vitro. The treatment of a pediatric patient suffering from a refractory BCP-ALL with Pembrolizumab (PD-1 CPI) in combination with the bispecific T-cell engager (BiTE) Blinatumomab enhanced tumor regression in vivo without significant side effects (Feucht et al., 2016).
Boekstegers et al. documented the clinic response of a 9-year-old girl with refractory T-ALL to the anti PD-1 CPI Pembrolizumab. After relapsing the patient was treated with intensified chemotherapy. Due to refractory disease Pembrolizumab was applied in a single dose 12 months post allogenic stem cell transplantation. After reaching a donor chimerism of 100% two weeks after CPI treatment the patient showed symptoms of grade IV graft-versus-host disease (GvHD) which resulted in the decease of the patient 50 days after Pembrolizumab application (Boekstegers et al., 2017).

Another immunotherapeutic approach are CAR T cells that have already been successfully used for the treatment of B cell malignancies and were approved by the FDA (Hong, Clubb, & Chen, 2020; Maude et al., 2014). Meta-analysis of studies and clinical trials represent the potential of anti-CD19 CAR T cells (as paradigm of CAR T-cell therapy) including the reduction of the tumor burden in adult and pediatric BCP-ALL patients. Antigen loss and relapsed CD19- B-cell leukemia after CD19-specific antitumor therapy was one of the arising problems (Majzner et al., 2017). Documented side effects included severe cytokine response and neurotoxicity (Curran et al., 2019). Targeting solid tumors via CAR T cells presents challenges currently under investigation in several trials (Wang, Wu, Liu, & Han, 2017).

While pediatric T-ALL in general presents with a wide range of genetic alterations, 50-60% of T-ALL patients show activating mutations of the NOTCH1 gene (Liu et al., 2017; Weng et al., 2004). Targeting the NOTCH1-Myc pathway via small molecules gamma secretase inhibitors (GSI) and antibodies could present an alternative treatment option (Sanchez-Martin & Ferrando, 2017). However, Agnusdei et al. could show that heterogenous mechanism lead to resistance to NOTCH1-targetted therapy in T-ALL xenografts (Agnusdei et al., 2020). Overcoming the resistance to sensitize T-ALL blasts for targeted therapy against the NOTCH1 receptor is under investigation. Further genetic targets are being investigated in clinical trials such as CDK4/6, PI3K/Akt/mTOR, BCL-2, CD5 and CD38 (Lato et al., 2021).

5. Aim and Objective of this study

Initial data suggests a potential of immunotherapy in pediatric T-cell acute lymphoblastic leukemia (T-ALL). While anti-CD19 chimeric antigen receptor T cells (CAR T cells) have set the stage for synthetic immunotherapy of B-cell acute lymphoblastic leukemia (BCP-ALL), it remains unclear whether immunotherapy could present a valid therapy option in pediatric T-ALL patients.

Currently, there is no systematic characterization of T-cell populations in the bone marrow (BM) of pediatric T-ALL patients. The primary objective of this project is the description of immune checkpoint (IC) expression as well as differentiation markers on leukemic blasts (physiological T-cell progenitors in cases of healthy bone marrow donors) and bone marrow T cells (bmT cells) via:

1) Flow cytometry
2) RNA-sequencing
3) ATAC-sequencing

A total of 72 BM samples are analyzed in this project:

1) 24 samples from pediatric T-ALL patients from the Hauner children´s hospital
2) 34 samples from pediatric T-ALL patients from the CoALL study (CoALL 07-03: NCT00343369; CoALL 08-09: NCT01228331)
3) 14 samples from healthy bone marrow donors (healthy BM donors) as a reference

The following differential analyzes are of interest:

1) T-ALL patient samples (initial diagnosis) vs. healthy BM donor samples
2) Samples of T-ALL patients without future relapse vs. T-ALL patients with future relapse (initial diagnosis)
3) T-ALL patient samples (initial diagnosis) vs. relapsed T-ALL patient samples

The first aim of this project is to analyze, whether bmT cells are altered by the presence of T-ALL. Next, we want to investigate whether receptor-ligand pairs are expressed by T-ALL and bmT cells that might lead to specific interaction between these two cell types. Finally, we aim to describe changes in the T-cell phenotype and particularly of IC expression in bmT cells of T-ALL patients compared to healthy BM donors to identify possible targets for immunotherapeutic approaches.

6. Materials

6.1. Equipment and software

Equipment/software	Name, Manufacturer
Cell counting auxiliaries	Cell Counting Chamber Neubauer, Chamber Depth 0.1 mm, Paul Marienfeld, Lauda-Königshofen, Germany
Centrifuges	Mini Centrifuge Fresco 17, Heraeus, Hanau, Germany
	Centrifuge 5810R, Eppendorf, Hamburg, Germany
Cooling units	Cooler (4 °C) Comfort No Frost, Liebherr, Biberach an der Riß, Germany
	Freezer (-20 °C) Premium No Frost, Liebherr, Biberach an der Riß, Germany
	Freezer (-86 °C) HERAfreeze HFC Series, Heraeus, Hanau, Germany
	Thermo Scientific Cryo 200 liquid nitrogen dewar, Thermo Fisher Scientific, Waltham, Massachusetts, USA
Flow cytometer	BD FACSAria III, BD, Franklin Lakes, New Jersey, USA
	BD LSRFortessa Cell Analyzer, BD, Franklin Lakes, New Jersey, USA
Heat block	Eppendorf ThermoMixer comfort, Eppendorf, Hamburg, Germany
Incubator	HERAcell 240, 150i CO_2 Incubator, Thermo Fisher, Waltham, Massachusetts, USA
Laminar flow hood	HERAsafe, Thermo Fisher, Waltham, Massachusetts, USA
Cleaner Box	UVC/T-M-AR, DNA-/RNA UV-cleaner box, Biosan, Riga, Latvia
Vortexer	Vortex Genie 3, IKA-Werke, Staufen, Germany
Microscope	Leica DM IL, Leica Microsysteme, Wetzlar, Germany
Agilent 2100 Bioanalyzer	Agilent Technologies, Santa Clara, California, USA
Pipettes (manual)	2,5 µl, 20 µl, 200 µl, 1000 µl Eppendorf Research, Eppendorf, Hamburg, Germany
Software	BD FACSDiva 8.0.1, BD Biosciences, Franklin Lakes, New Jersey, USA
	FlowJo 10.0.7r2, Ashland, Oregon, USA
	GraphPad PRISM 7.0, La Jolla, California, USA
	Microsoft Office 2010, Redmond, Washington, USA
	2100 Bioanalyzer Expert, Agilent Technologies, Santa Clara, California, USA
	DNASTAR – Lasergene, DNASTAR, Madison, Wisconsin, USA
Sequencer	NextSeq500 & NextSeq550, Illumina, San Diego, California, USA
Thermocycler	peqSTAR 96 Universal Gradient, Isogen, Utrecht, Netherlands
Vacuum pump	Vakuumsytem BVC 21 NT, Vacuubrand, Wertheim, Germany
Water bath	3043, Köttermann, Uetze/Hänigsen, Germany

Freezing container	Nalgene Mr. Frosty, Thermo Fisher Scientific, Waltham, USA
Pipettes (electrical)	Easypet 3, Easypet Original, Eppendorf, Hamburg, Germany
Scale	R 200 D, Sartorius AG, Göttingen, Germany

6.2. Solutions, media, and sera for cell culture

Solution/ Medium/Serum	Order number	Manufacturer
Compensation beads	552843	BD Biosciences, San Diego, California, USA
Fetal Bovine Serum	F0804	Sigma-Aldrich CHEMIE, Steinheim, Germany
FIX & PERM™ Cell Permeabilization Kit	GAS004	Life Technologies, Frederick, Maryland, USA
L-Glutamine 200 mM	K 0283	Biochrom, Berlin, Germany
Penicillin/Streptomycin	15140-122	Gibco, Life Technologies, Darmstadt, Germany
Trypan blue	15250-061	Gibco, Life Technologies, Darmstadt, Germany
Tween 20	11332465001	Sigma-Aldrich, St.Louis, Missouri, USA
VLE RPMI 1640 Medium	F1415	Biochrom, Berlin, Germany
Nonidet P40 Substitute	11332473001	Sigma-Aldrich, St.Louis, Missouri, USA
PBS	14190-250	Invitrogen, Carlsbad, California, USA
FoxP3 Staining Kit	130-093-142	Miltenyi Biotec, Bergisch Gladbach, Germany
Quick-RNA™ Microprep	R1051	Zymo, Irvine, California, USA
Human BD Fc Block™	564220	Becton, Dickinson and Company (BD), Franklin Lakes, New Jersey, USA
DNAse I	18047-019	Invitrogen, Carlsbad, California, USA
Agilent RNA 6000 Pico Kit	5067-1513	Agilent Technologies, Santa Clara, California, USA
Bioanalyzer High Sensitivity DNA Analysis Kit	5067-4626	Agilent Technologies, Santa Clara, California, USA
Digitonin	G9441	Promega, Fitchburg, Wisconsin, USA
Illumina NextSeq 500 Mid	FC-404-2001	Illumina, San Diego, California, USA
Nextera DNA Library Kit	FC-121-1030	Illumina, San Diego, California, USA
RNAse free Tubes	20170-038	VWR International, Radnor, Pennsylvania, USA
DNA Clean & Concentrator™ -5	D4014	Zymo, Irvine, California, USA
DMSO	4720.4	Carl Roth, Karlsruhe, Germany
NEBNext® Multiplex Oligos for Illumina® (Dual Index Primers Set 1)	E7600S	New England Biolabs, Ipswich, Massachusetts, USA
NEBNext® Ultra™ II Directional RNA Library Prep Kit for Illumina	E7765S	New England Biolabs, Ipswich, Massachusetts, USA
NEBNext® Poly(A) mRNA Magnetic Isolation Module	E7490S	New England Biolabs, Ipswich, Massachusetts, USA

6.3. Consumables

Consumable	Order number	Name, Manufacturer
Cannula	851.638.235	Safety-Multifly-Needle, Sarstedt, Nümbrecht, Germany
Cell culture dish	664 160	Cellstar Greiner Labortechnik, Kremsmünster, Austria
Cell culture flasks with ventilation caps	83.3910.002, 83.3911.002, 83.3912.002	T25, T75, T175, Sarstedt, Nümbrecht, Germany
Compresses	18507	Gauze Compresses 10 x 10 cm, Nobamed Paul Danz, Wetter, Germany
Cover slips	C10143263NR1	Menzel-Gläser 20 x 20 mm, Gerhard Menzel, Braunschweig, Germany
FACS buffers and solutions	340345, 340346, 342003	FACS clean/rinse/flow, Becton, Dickinson and Company (BD), Franklin Lakes, New Jersey, USA
Freezing tubes	72.379	Cryo Pure Gefäß 1.8 ml, Sarstedt, Nümbrecht, Germany
Pasteur pipettes	747720	Glass Pasteur Pipettes 230 mm, Brand, Wertheim, Germany
Pipette tips	70.1130.217, 70.760.213, 70.760.212, 70.762.211	0.1-2.5 µl, 10 µl, 20 µl, 100 µl, 2-200 µl, 1000 µl, Sarstedt, Nümbrecht, Germany
Reaction vessels	62.554.502	15 ml, Sarstedt, Nümbrecht, Germany
	4440100	50 ml, Orange Scientific, Braine-l'Alleud, Belgium
	72.690.550	1.5 ml, Sarstedt, Nümbrecht, Germany
	72.737	Multiply-Pro 0,2ml Biosphere, Sarstedt, Nümbrecht, Germany
Round bottom tubes with cell strainer snap cap	352235	5 ml Polystyrene Round Bottom Tube, Falcon, Corning Science, Taumaulipas, Mexico
Safety gloves	9209817	Vaso Nitril Blue, B. Braun Melsungen, Melsungen, Germany
Serological pipettes	86.1685.001, 86.1253.001, 86.1254.001	5 ml, 10 ml, 25ml Serological Pipette, Sarstedt, Nümbrecht, Germany
Skin disinfectant	975512, 306650	Sterilium Classic Pure, Sterilium Virugard, Hartmann, Heidenheim, Germany
Surface disinfectant	CLN-1006.5000	Ethanol 80 % MEK/Bitrex, CLN, Niederhummel, Germany
RNAse AWAY	A998.4	Molecular bioproducts

6.4. Antibodies

Fluoro-chrome	Antigen	Clone	Order number	Manufacturer
7-AAD	Viability dye		420403	Biolegend, San Diego, California, USA
AF488	CD160	BY55	53-1609-41	eBioscience/ Thermo Fisher Scientific, Waltham, Massachusetts, USA
AF647	FOXP3	259D/C7	356103	Becton, Dickinson and Company (BD), Franklin Lakes, New Jersey, USA
APC	2B4	C1.7	329511	Biolegend, San Diego, California, USA
APC	VISTA	730804	FAB71261A	R&D Systems, Minneapolis, Minnesota, USA
APC	HVEM	122	318808	Biolegend, San Diego, California, USA
APC	CD86	IT2.2	305411	Biolegend, San Diego, California, USA
APC	CD27	M-T271	561400	Becton, Dickinson and Company (BD), Franklin Lakes, New Jersey, USA
APC	CTLA-4	BNI3	555855	Becton, Dickinson and Company (BD), Franklin Lakes, New Jersey, USA
APC	MUC1	5E5	/	By MTA from university of Copenhagen
APC	CD56	NCAM16.2	341027	Becton, Dickinson and Company (BD), Franklin Lakes, New Jersey, USA
APC	CD25	M-A251	356110	Biolegend, San Diego, California, USA
APC	CD8	SK1	345775	Becton, Dickinson and Company (BD), Franklin Lakes, New Jersey, USA
APC-eFluor780	CD7	eBio124-1D1	47-0079-42	eBioscience/ Thermo Fisher Scientific, Waltham, Massachusetts, USA
BB515	CD40	5C3	565258	Becton, Dickinson and Company (BD), Franklin Lakes, New Jersey, USA
BB515	TIM-3	7D3	565568	Becton, Dickinson and Company (BD), Franklin Lakes, New Jersey, USA
BUV395	CD4	L200	564107	Becton, Dickinson and Company (BD), Franklin Lakes, New Jersey, USA
BUV496	CD8	RPA-T8	564805	Becton, Dickinson and Company (BD), Franklin Lakes, New Jersey, USA
BUV737	CD3	UCHT1	564308	Becton, Dickinson and Company (BD), Franklin Lakes, New Jersey, USA
BV421	PD-1	EH12.2H7	329919	Biolegend, San Diego, California, USA
BV421	TIM-3	F38-2E2	345007	Biolegend, San Diego, California, USA
BV421	BTLA	MIH26	344511	Biolegend, San Diego, California, USA
BV421	CD137	4B4-1	309819	Biolegend, San Diego, California, USA
BV421	CD80	2D10	305221	Biolegend, San Diego, California, USA
BV421	PD-L1	29E.2A3	329714	Biolegend, San Diego, California, USA
BV421	CD39	A1	328214	Biolegend, San Diego, California, USA
BV421	GITR	108-17	371208	Biolegend, San Diego, California, USA
BV421	TIGIT	A15153G	372709	Biolegend, San Diego, California, USA

BV421	OX40	Ber-ACT35	350013	Biolegend, San Diego, California, USA
BV650	CD62L	DREG-56	563808	Becton, Dickinson and Company (BD), Franklin Lakes, New Jersey, USA
BV650	PD-1	EH12.2H7	329949	Biolegend, San Diego, California, USA
BV650	CD28	CD28.2	302945	Biolegend, San Diego, California, USA
BV650	TCR γ/δ	B1	564156	Becton, Dickinson and Company (BD), Franklin Lakes, New Jersey, USA
BV650	CD33	WM53	303429	Biolegend, San Diego, California, USA
BV785	CD3	Oct-03	317330	Biolegend, San Diego, California, USA
BV786	CD45	HI30 (RUO)	563716	Becton, Dickinson and Company (BD), Franklin Lakes, New Jersey, USA
FITC	CTLA-4	14D3	11-1529-41	eBioscience/ Thermo Fisher Scientific, Waltham, Massachusetts, USA
FITC	CD57	HCD57	322306	Biolegend, San Diego, California, USA
FITC	CD28	CD28.2	302906	Biolegend, San Diego, California, USA
FITC	CD56	NCAM 16.2	345811	Miltenyi Biotec, Bergisch Gladbach, Germany
FITC	CD73	AD2	344016	Biolegend, San Diego, California, USA
FITC	ICOS	C398.4A	313505	Biolegend, San Diego, California, USA
FITC	TRBC1	Jovi1	LS-C134140-120	Biozol, Eching, Germany
PE	LAG-3	11C3C65	369306	Biolegend, San Diego, California, USA
PE	TIGIT	MBSA43	12-9500-42	eBioscience/ Thermo Fisher Scientific, Waltham, Massachusetts, USA
PE	PD-L1	29E.2A3	329705	Biolegend, San Diego, California, USA
PE	OX-40	Ber-ACT35	350003	Biolegend, San Diego, California, USA
PE	CD70	113-16	355103	Biolegend, San Diego, California, USA
PE	CD112	TX31	337410	Biolegend, San Diego, California, USA
PE	CD25		356104 (100 356103 (25	Biolegend, San Diego, California, USA
PE	MUC	5E10	/	By MTA from university of Copenhagen
PE	CD127	HIL-7R-M21	557938	Becton, Dickinson and Company (BD), Franklin Lakes, New Jersey, USA
PE	TCR α/β	IP26	306707	Biolegend, San Diego, California, USA
PE	CD56	REA196	130-100-653	Miltenyi Biotec, Bergisch Gladbach, Germany
PE/Cy7	CD45RO	UCHL1	304230	Biolegend, San Diego, California, USA
PE/Cy7	CD57	HNK-1	359623	Biolegend, San Diego, California, USA
PE/Cy7	CD70	113-16	355111	Biolegend, San Diego, California, USA
PE/Cy7	TCR α/β	IP26	306719	Biolegend, San Diego, California, USA
PEVio770	CD19	LT19	130-096-641	Miltenyi Biotec, Bergisch Gladbach, Germany

VioBlue	CD45	5B1	130-092-880	Miltenyi Biotec, Bergisch Gladbach, Germany
Viobright FITC	CD4	REA623	130-109-457	Miltenyi Biotec, Bergisch Gladbach, Germany
Viobright FITC	CD4	REA623	130-113-229	Miltenyi Biotec, Bergisch Gladbach, Germany

6.5. Isotype controls

Fluorochrome	Isotype control	Order number	Company
APC	Mouse IgG1, k	400121	Biolegend, San Diego, California, USA
APC	Mouse IgG2a k	552893	Becton, Dickinson and Company (BD), Franklin Lakes, New Jersey, USA
BV421	Mouse IgG2b, k	562748	Becton, Dickinson and Company (BD), Franklin Lakes, New Jersey, USA
BV421	Mouse IgG1, k	400158	Biolegend, San Diego, California, USA
FITC	Mouse IgG1, k	130-098-105	Miltenyi Biotec, Bergisch Gladbach, Germany
FITC	Mouse IgG1, k	400109	Biolegend, San Diego, California, USA
PE	Mouse IgG1, k	400113	Biolegend, San Diego, California, USA
PE-Cy7	Mouse IgG1, k	400125	Biolegend, San Diego, California, USA
PerCP Cy5.5	Mouse IgG1, k	400149	Biolegend, San Diego, California, USA
BV786	Mouse IgG1, k	563330	Becton, Dickinson and Company (BD), Franklin Lakes, New Jersey, USA
PE	Mouse IgG1, k	400113	Biolegend, San Diego, California, USA
BB515	Mouse, IgG1, k	564416	Becton, Dickinson and Company (BD), Franklin Lakes, New Jersey, USA

7. Methods

The project included the measurement of bone marrow (BM) samples of pediatric patients with T-cell acute lymphoblastic leukemia (T-ALL) and those of healthy bone marrow donors (healthy BM donors). The T cells are referred to as bone marrow T cells (bmT cells) due to their location in the tumor microenvironment (TME) BM. The nomenclature T-cell progenitors (TCP) describes leukemic T-cell progenitors (leukemic T-ALL blasts, LTCP) as well as physiological TCP. If a statement refers to leukemic T-ALL blasts or physiological TCP it is described as such.

7.1. Sample selection

7.1.1. BM samples of the Hauner children´s hospital

25 samples of pediatric T-ALL patients were selected from the biobank (HaunerHematologyBiobank) of the Hauner children's hospital (HCH). The following criteria were used for sample filtering: (1) date of diagnosis, (2) age at time of initial diagnosis, (3) gender, (4) therapy status (naïve or post treatment), (5) follow-up, (6) initial count of white blood cells (WBC) and (7) blast frequency in the BM. Only therapy naïve samples were included in the analysis. Sample selection and analysis was performed according to the guidelines of the HaunerHematologyBiobank (Projekt Nummer: 17-163, Ethikkomission der LMU, München). To put observations made in T-ALL patients into context, 17 BM samples of healthy BM donors (3-16 years) from the HCH were processed and measured. Patient and donor samples were anonymized and subsequently labelled according to their utilization in this project:

1) samples of patients without relapse, initial diagnosis (n=16, B001 – B016)
2) primary samples of relapse patients, initial diagnosis (n=5; B301-B305)
3) relapse samples (first relapse: n=3, B401, B402, B405; second relapse: n=1; B502)
4) healthy BM donors (B101-B117)

T-ALL patient B001 was excluded from analysis due to therapy prior to BM puncture. Healthy BM donor samples B104-B106 were excluded from analysis due to technical issues in flow cytometric measurement.

7.1.2. T-ALL BM samples provided by the Cooperative acute lymphoblastic leukemia study

35 samples of pediatric T-ALL patients at first diagnosis were received for measurement from the Cooperative acute lymphoblastic leukemia study (CoALL study) center in Hamburg, Germany. Patients were treated according to the CoALL 07-03 or CoALL 08-09 protocol. In terms of the CoALL 07-03 study

the samples were collected from the 1st of September 2003 until the 31st of August 2015. The CoALL 08-09 study was initiated on the 1st of October 2010 and terminated on the 30th of September 2016. Samples were stored at -80°C in Hamburg. Since one patient sample was not found 34 T-ALL samples from the CoALL study were measured. Patient samples were received after anonymization and subsequently labelled B601-B634. 21/34 patients were therapy naïve, 7/34 received chemotherapy prior to BM puncture and for 6/34 patients the therapy status at initial diagnosis was unknown.

An overview of the characteristics of healthy BM donors and T-ALL patients of the HCH and COALL study are presented in Table 1. Table 2 shows the labelling of measured HCH samples of relapsed patients. The clinical data of the CoALL patients is presented in Table 3. The data was updated on the 3rd of July 2018.

	Healthy BM donors	**HCH patients**	**COALL patients**
Number of patients	14	20	34
Number of samples	14	24	34
Age at initial diagnosis, mean (range)	10.3y (1.7-19.1y)	9.9y (3.8-15.6y)	8.5y (3-17y)
Therapy status			
Therapy naive	-	24	21
Treated	-	-	7
Unknown status	-	-	6
Gender, n (%)			
Male	7 (50)	17 (85)	30 (88.2)
Female	7 (50)	3 (15)	4 (11.8)
Future relapse	-	5 (25)	6 (17.6)
Time to relapse, median (range)	-	2.2y (0.3-8.5y)	1.5y (0.6-4.7y)
Exitus letalis, n (%)	-	7 (35)	5 (14.7)
Monitoring period, mean (range)	-	3.6y (0.1-12.1Y)	6.2y (0.8-12.0y)

Table 1: Characteristics (1st column) of healthy BM donors (2nd column) of the Hauner children´s hospital, pediatric T-ALL patients of the Hauner children´s hospital (3rd column) and pediatric T-ALL patients of the CoALL study (4th column): High variation of the HCH and CoALL cohort could be due to alternative sample selection criteria including the measurement of treated T-ALL patients and patients with unknown therapy status on the side of the CoALL cohort. The CoALL cohort only consisted of samples at initial diagnosis, whereas HCH samples were partly sequential. *y = years, HCH = Hauner children´s hospital.*

Relapsed patient	Initial diagnosis	1st relapse	2nd relapse
Patient 1	B301	B401	
Patient 2	B302	B402	B502
Patient 3	B303		
Patient 4	B304		
Patient 5	B305	B405	

Table 2: Measured samples of relapsed T-ALL patients of Hauner children´s hospital: B301-B305 label samples at initial diagnosis of patient 1-5. B401, B402 and B405 label samples of the 1st relapse of patient 1, 2 and 5. B502 labels the sample of the second relapse of patient 2.

	blast frequency in the BM [%] at iDx	WBC [10^3/µl] at iDx	A) therapy naive B) Cortison C) Chemotherapy	response on day 29	gender	age at initial diagnosis [y]	death	CD7 expression on blasts [%] at iDx	CD34 expression on blasts [%] at iDx
B601	76	7	A	CCR	M	3	No/ N/A	36	0
B602	87	69.2	N/A	CCR	M	16	yes	93	0
B603	99	29.2	A	CCR	M	12	No/ N/A	95	0
B604	96	23.3	A	CCR	M	4	No/ N/A	89	1
B605	86	14.4	N/A	CCR	M	8	No/ N/A	79	2
B606	87	30	A	CCR	M	4	No/ N/A	80	0
B607	100	11.6	B	CCR	M	7	No/ N/A	95	0
B608	99	365.1	A	CCR	M	9	No/ N/A	94	88
B609	61	423	B+C	CCR	M	9	No/ N/A	89	4
B610	70	54	A	CCR	M	4	No/ N/A	95	0
B611	73	32	A	CCR	M	4	No/ N/A	70	0
B612	85	10.8	A	CCR	M	9	No/ N/A	92	N/A
B613	96	67.5	A	CCR	M	5	No/ N/A	98	6
B614	94	55	N/A	CCR	M	13	No/ N/A	55	44
B615	92	38.2	A	CCR	F	2	No/ N/A	89	0
B616	98	105.3	A	CCR	M	5	No/ N/A	64	81
B617	57	29.3	A	CCR	M	8	yes	65	N/A
B618	89	27.8	N/A	CCR	M	16	No/ N/A	63	4
B619	99	224	A	CCR	M	11	No/ N/A	89	0
B620	75	49.96	A	CCR	M	10	No/ N/A	90	14
B621	N/A	351	A	LR	M	9	No/ N/A	88	0
B622	97	16.9	N/A	CCR	M	14	No/ N/A	75	14
B623	91	172.8	N/A	CCR	F	1	No/ N/A	84	1
B624	N/A	242.9	A	CCR	M	11	No/ N/A	96	0
B625	45	17.2	B	CCR	M	2	No/ N/A	60	34
B626	61	283	B	CCR	M	17	yes	90	0
B627	91	107	A	LR	M	5	No/ N/A	97	0
B628	98	533	A	LR	M	15	No/ N/A	97	78
B629	97	99	A	LR	M	9	yes	99	78
B630	63	12.6	A	LR	F	3	No/ N/A	71	28
B631	53	12.8	A	CCR	F	13	No/ N/A	99	0
B632	85	524	B	CCR	M	12	No/ N/A	99	4
B633	85	141	B	CCR	M	2	No/ N/A	99	0
B634	82	19.7	C	CCR	M	17	yes	100	1

Table 3: Relevant clinical data of CoALL patients B601-B634 (initial diagnosis and the clinical course): 21/34 samples were collected prior to treatment. 7/34 patients received chemotherapy prior to BM puncture. For 6/34 there is no information available regarding therapy status. One sample could not be found and is not included. Patient B610 was excluded from analysis due to poor sample quality and low cell count. *iDx = initial diagnosis, WBC = White blood cell, N/A = not available, CCR = complete cytogenic remission, LR = late responder, M = male, F = Female.*

7.2. Cell culture methods

7.2.1. Cell culture

Cells were cultivated in an incubator at 37°C and 5% CO_2 in water steam saturated atmosphere. All cell culture related processes were performed under sterile bench conditions.

7.2.2. Thawing of cells

Sample thawing from liquid nitrogen was performed after transport on dry ice. The thawing process took place under sterile bench conditions in the S1 area. Samples were thawed by agitating them for about 2min in a 37°C water bath. 1.8ml of sample volume was added to 13.2ml of 37°C RPMI medium (+10%FCS+1%Glutamin+1%Penicillin/Streptomycin) and DNAseI (100 U/ml). Living cells were counted in a Neubauer counting chamber using trypan blue to exclude dead cells. After 10min of centrifugation at 300g at room temperature (RT) the supernatant was aspirated, and the remaining cell pellet resuspended in PBS+1% FCS.

In cases of insufficient resuspension of the cell pellet after centrifugation due to cell lysis the pellet was exposed to a higher DNAseI concentration (200U/ml) and incubated for 15min at 37°C in an incubator. After cell counting and centrifugation for 4min at 400g the cell pellet was resuspended in PBS+1% FCS.

7.3. Immunological methods

7.3.1. Antibody titration

The volume of an antigen specific antibody was determined via titration for an optimal discrimination between positive and negative. To that end, the antibody volume recommended by the manufacturer (e. g. 2,5µl in 50µl) was used aside of three reduced volumes (e. g. 1,0µl, 0,5µl and 0,25µl in 50µl) and an unstained control. The volume yielding the best result was used consistently in all patient sample measurements.

7.3.2. Sample staining with fluorochrome labelled antibodies for flow cytometric analysis of BM samples

Sample staining was performed in an unsterile environment. All samples excluding B002-B011 and B101-B110 were subjected to the Human BD Fc Block™ to prevent unspecific binding of the antibodies to surface immunoglobulin G (IgG) receptors on the cells. Samples were divided into different tubes

for staining a multitude of markers. A backbone panel was used for categorization of different BM populations (to differentiate healthy bmT cells from TCP) (Figure 2A+B). The staining with fluorochrome labelled antibodies was performed in a total volume of 50µl: 25µl of cell suspension (containing 1-10x10^5 cells) were added to 25µl of the antibody mix containing 12 fluorochrome labelled antibodies in previously determined concentrations (see subchapter 7.3.1).
Four to six immune checkpoints (IC) were analyzed in combination with the backbone panel. As changes in marker selection were made during the project, not all markers were stained for all samples; for some markers the antigen fluorochromes were changed during sample measurements. Figure 2C shows an overview of the antigens measured including the used fluorochromes. An isotype control (mostly IgG1) was measured for the detection of unspecific binding of the respective fluorochrome. A fluorescence minus four (FMF) was stained for all HCH samples to detect issues regarding the compensation (not performed in cases of CoALL samples). An unstained sample was measured for all samples to control auto fluorescence.

After addition of the antibodies, the cell suspension mixture was incubated for 20min in the dark at RT. Cells were washed with 900µl PBS+1% FCS and the supernatant removed. The stained cells were resuspended in 450µl PBS+1% FCS and stored in the dark at a 4°C for up to 4 hours. Prior to flow cytometric analysis the samples were strained through a 35µm filter. Staining of the intracellular antigens CTLA-4 and PD-L1 was performed after staining of extracellular antigens as mentioned above. Subsequently, cells were fixed, permeabilized and stained intracellularly using the Fix and Perm kit by ThermoFisher using a volume of 50µl + 50µl for fixation and 50µl + flow cytometry antibodies for permeabilization and staining. The intracellular staining of the FoxP3 transcription factor was performed according to Miltenyi Biotecs´ FoxP3 staining Kit. All samples were resuspended in PBS+1% FCS, stored in the dark at 4°C for up to four hours and strained through a 35µm filter prior to measurement.

Prior to the measurement of the stained BM samples the voltages of the lasers of the LSRFortessa Cell Analyzer were automatically determined by the CST beads check.

A

7AAD live/dead
BUV737 CD3
BUV395 CD4
BUV496 CD8
BV786 CD45
APC-eFluor780 CD7
PE/Cy7 CD45Ro
BV650 CD62L

B

7AAD live/dead
BUV737 CD3
BUV395 CD4
BUV496 CD8
BV786 CD45
APC-eFluor780 CD7

C

Antigen	HCH 1	HCH 2	CoALL
2B4	APC	APC	APC
BTLA	BV421	BV421	
CD112	PE	PE	PE
CD127		PE	PE
CD137	BV421		
CD160	AF488	AF488	
CD25	PE	APC	APC
CD27	APC	APC	APC
CD28	FITC	FITC	BV650
CD39	BV421	BV421	BV421
CD40	BB515	BB515	
CD56	FITC	APC	
CD57	FITC	FITC	PE/Cy7
CD70	PE	PE	PE/Cy7
CD73	FITC	FITC	
CD80	BV421		
CD86	APC	APC	
CTLA-4	APC	APC	
CTLA-4	FITC		
FoxP3	AF647		
GITR		BV421	
HVEM	APC	APC	
ICOS		FITC	FITC
LAG-3	PE	PE	PE
MUC1 5E10	PE		
MUC1 5E5	APC		
OX40	PE	PE	BV421
PD-1	BV421	BV421	BV650
PD-L1	BV421	BV421	
PD-L1	PE	BV421	
TCRα/β		PE	PE/Cy7
TCRγ/δ			BV650
TIGIT	PE	PE	BV421
TIM-3	BV421	BV421	BB515
TRBC1		FITC	FITC
VISTA	APC		

intracellularly stained

Figure 2: Structure and antibody composition of flow cytometric panels: A) Backbone markers for B002-B016, B301-B305, B401, B402, B405, B502 and B101-B117. **B)** Backbone markers for patients B601-B634. **C)** Measured antigens including respective fluorochrome used for samples measurement. HCH 1 describes patient samples B001-B011 and healthy BM donor samples B101-B110; HCH 2 describes patient samples B012-B016, B301-B305, B401-B405, B502 and healthy BM donor samples B111-B117, CoALL describes CoALL samples B601-B634. Markers CTLA-4 and PD-L1 were stained extracellularly and intracellularly (Fix and Perm kit by ThermoFisher); therefore, those antigens are listed twice in the table. FoxP3 was stained intracellularly using the Miltenyi Biotecs´ FoxP3 staining Kit. *HCH = Hauner children´s hospital.*

7.3.3. Automated bead compensation

A compensation for the 12 fluorochromes used was performed every 2-4 months in order to take continuous changes of baseline voltages into account. 12 tubes containing each one specific fluorochrome coupled to an antibody were incubated with positive (BD™ CompBeads Anti-Mouse Ig, κ particles) and negative (BD™ CompBeads Negative Control) beads for all fluorochromes and dead peripheral blood mononuclear cells (PBMC) for the viability dye 7-AAD. Additionally, one tube containing negative beads and no fluorochrome labelled antibodies (negative control) and one tube containing positive beads, antibodies of all fluorochromes and dead cells with 7-AAD live/dead stain were prepared. All the tubes contained a total volume of 50µl (antibody + beads/cells or both + PBS+1% FCS). The samples were incubated for 20min in the dark at RT, washed once with PBS+1% FCS and resuspended in PBS+1% FCS. The spectral overlap of the fluorochromes was measured at the LSRFortessa Cell Analyzer and a compensation matrix was automatically generated by the BD FACSDiva 8.0.1 software according to BD LSRFortessa Cell Analyzer User´s Guide. The voltage of some channels had to be adapted to generate a valid compensation (e. g. the BUV496 voltage had to be reduced to 420mV to reduce spill-over in the BUV395 channel to about 20%). The compensation matrix was used to generate an experiment template that was used for multiple sample measurements.

7.4. Sorting of BM populations at the BD FACSAria III

Four BM populations were sorted in 1.5ml tubes containing 100% FCS at 4°C to maximize viability of recovered cells. Cells were stained with a solution of seven or eight fluorochrome labelled antibodies: 7AAD live/dead, BV785 CD3, VioBright FITC CD4, APC CD8, APC-eFluor780 CD7, VioBlue CD45, PE CD56, BV650 CD33, PEVio770 CD19. The samples of pediatric T-ALL were measured at the BD FACSAria III depending on the expression of CD3, CD45, CD4 and CD8 on the surface of leukemic blasts (Figure 3). Cell sorting was performed by the flow cytometry core facility of the Kubus research center (Prof. Dr. Christoph Klein). Repeatedly T-ALL BM samples were sorted according to alternative gating strategies including gates as CD3 vs. CD45 and CD4 vs. CD8 within the living cells to differentiate between the following populations: CD4+ bmT cells, CD8+ bmT cells, CD7+ TCP and natural killer cells (NK cells). Healthy BM samples were equally sorted. For BM donors B110-B117 the following physiological precursor populations were sorted (in addition to CD8+ bmT cells) as a reference to leukemic blast populations of different leukemia entities (T-ALL, BCP-ALL and AML): CD19+ B-cell precursors, CD7+ LTCP and CD19-CD7- myeloid precursors (Figure 3).

A post-sort analysis was performed in approximately 40% of the measurements depending on the number of sorted cells (mostly leukemic blasts of T-ALL patients and TCP, CD4+ and CD8+ bmT cells of healthy BM donors). The post-sort was done to ensure sample purity higher than 95% of the sorted

populations (Figure 4). Compensation matrices for the eight-color panel were generated every three months according to the manufacturers' specifications. The sorted BM populations were subsequently used for further experiments including chromatin transposition and RNA/DNA isolation.

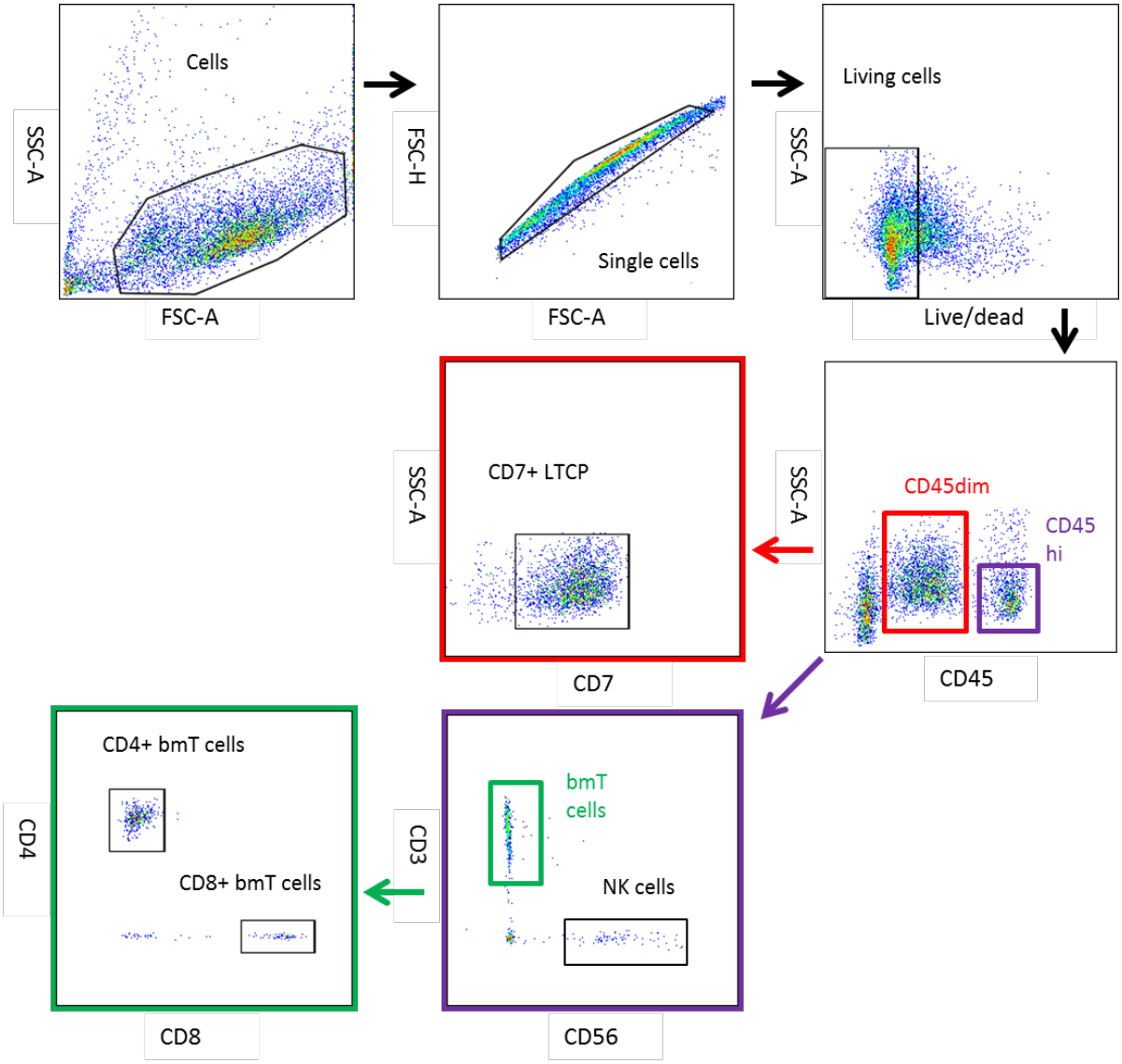

Figure 3: Representative gating strategy for sorting of sample B004: Events were gated for cells (SSC-A vs. FSC-A), duplets (FSC-H vs. FSC-A) and dead cells (SSC-A vs. 7AAD) were excluded. Subsequently, CD45hi cells and CD45dim cells were differentiated (SSC-A vs. CD45); the latter population was analyzed for CD7+ LTCP (SSC-A vs. CD7). CD45hi cells were divided into bmT cells and NK cells (CD3 vs. CD56) and CD3+ bmT cells were classified into CD4+ bmT cells and CD8+ bmT cells (CD4 vs. CD8). The number of CD8+ bmT cells was comparatively low due to the loss of CD8+ bmT cells in the live/dead gate in this particular case. For healthy BM donors B111-B117 the following four BM populations were sorted: CD8+ bmT- cells, CD19+ B-cell precursors, CD7+ TCP and CD19- CD7- myeloid precursors (not shown). *LTCP = leukemic T-cell progenitors, NK cells = natural killer cells, TCP = T-cell progenitors.*

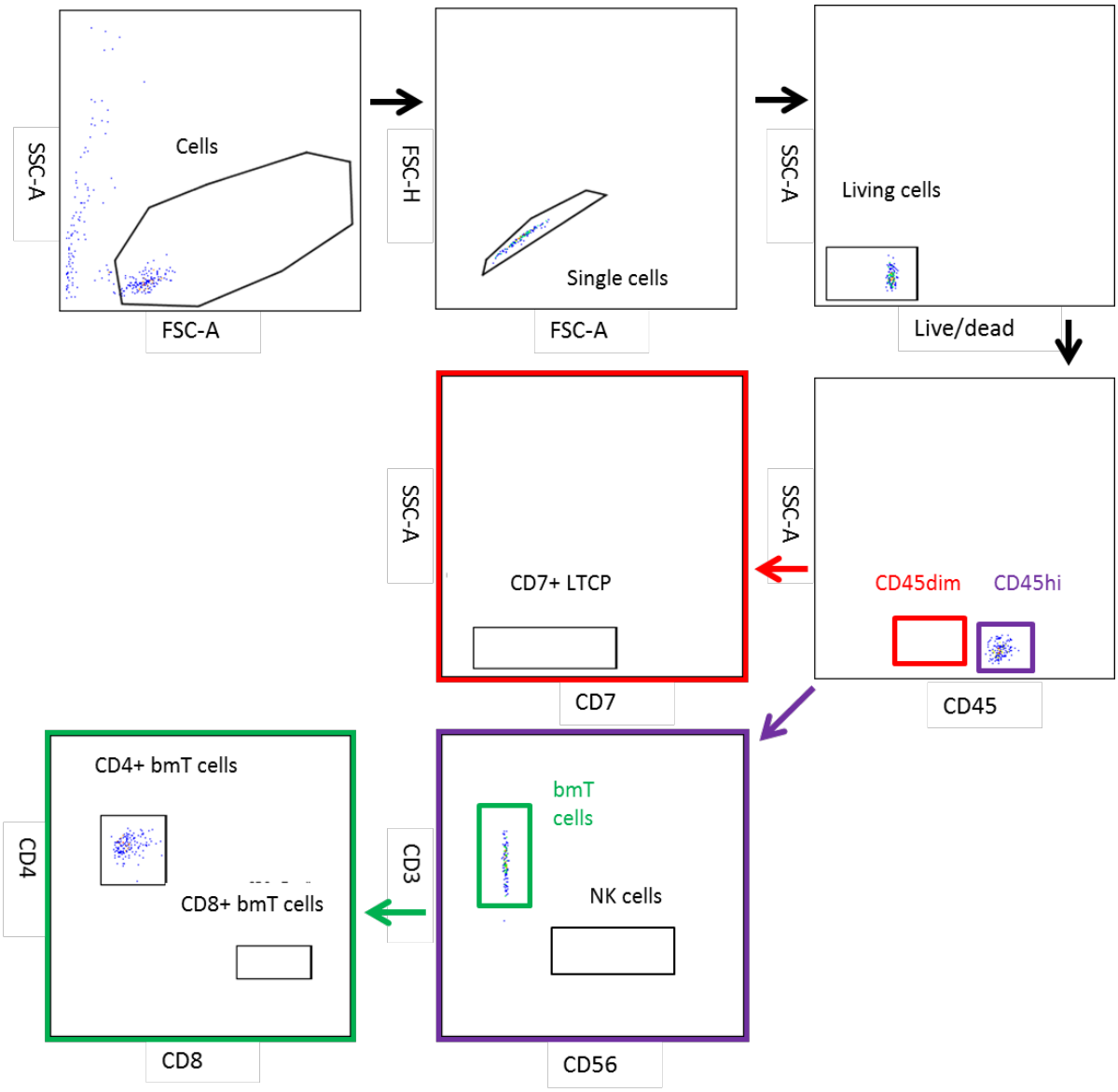

Figure 4: Representative post-sort for CD4+ bmT cells of patient sample B009 with high purity: post-sort analysis was performed in 100% FCS (note events on the left in SSC-A vs. FSC-A plot). All measured events lay within the CD4+ bmT-cell gate; gates for other sorted populations (CD8+ bmT cells, NK cells and CD7+ LTCP were event free. *LTCP = leukemic T-cell progenitors, NK cells = natural killer cells.*

7.5. Flow cytometric data analysis

7.5.1. General gating strategy

Flow cytometry data generated using the BD LSRFortessa Cell Analyzer (Fortessa III special order) was analyzed via FlowJo10.0.7r2. The CoALL samples were heterogeneous regarding cell count and partially showed reduced cell viability (Figure 5A-C). This was independent of the therapy status at the time of BM puncture. Unintentionally, samples B609-B612 were not stained for CD45. However, discrimination between T-ALL blasts and CD4+ and CD8+ bmT cells could still be performed for samples

B609, B611 and B612. Patient B610 was excluded from analysis due to low cell count and cell viability (Figure 5D).

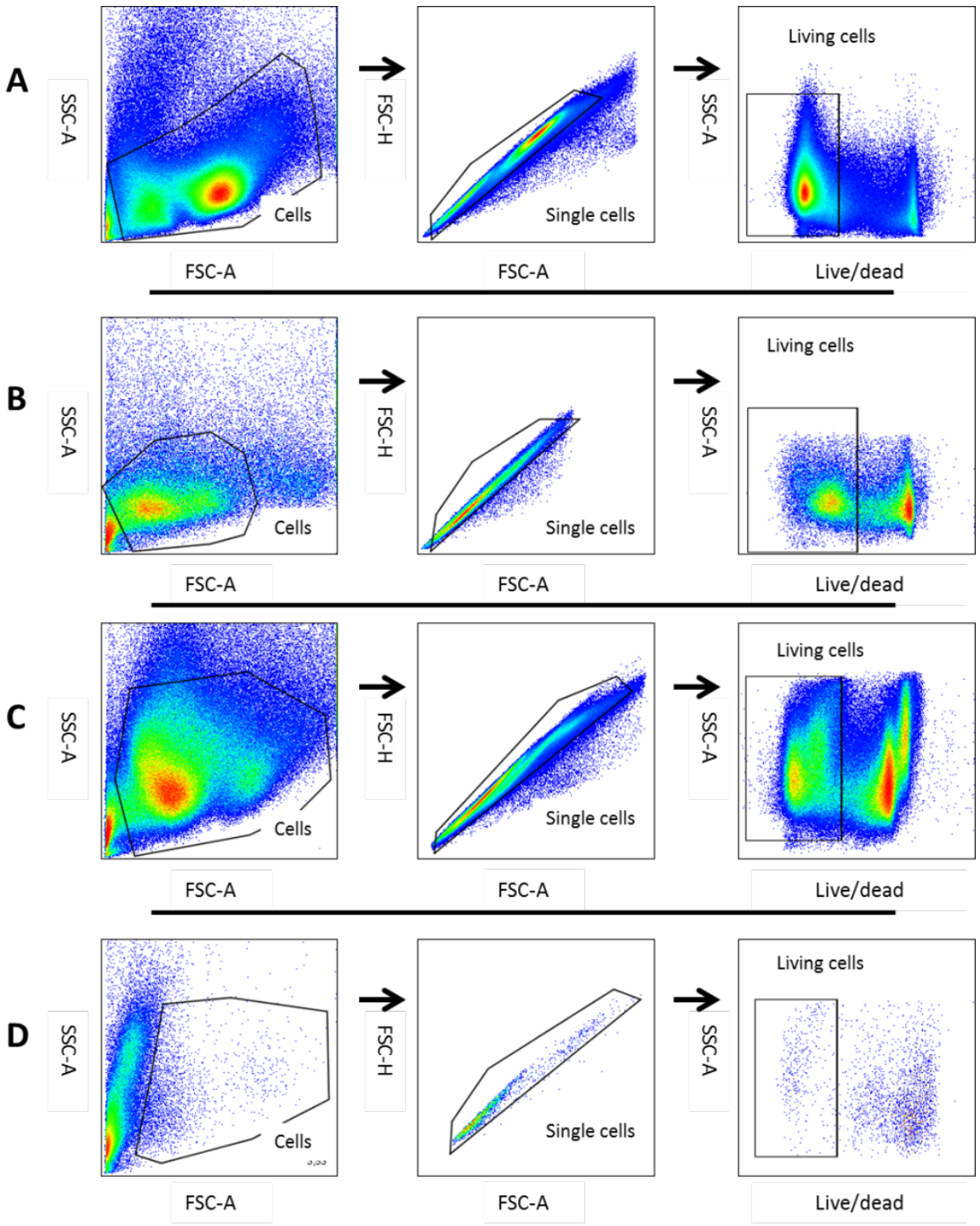

Figure 5: General FlowJo gating strategy for four CoALL samples illustrating different sample viability: SSC-A vs. FSC-A: selection of cells by size and granularity; FSC-A vs. FSC-H: excluding duplets; SSC-A vs. live/dead: selection of living cells. Samples **A), B)** and **C**) could be evaluated while the fourth example **D)** showed few viable cells and was excluded from evaluation.

Two general gating strategies were employed to differentiate between bmT cells and LTCP/TCP. Subsequently, for most cases of T-ALL samples (44/58) and all the healthy BM donors (14/14) the living cells could be differentiated into bmT cells (CD3hiCD45hi) and TCP (CD3loCD45dim) in the CD3 vs. CD45 plot. Within the bmT-cell population CD4+ and CD8+ bmT cells were identified for further analysis. Within the CD3loCD45dim population gating on CD7+ LTCP in cases of T-ALL was performed (Figure 6). To compare surface marker expression on CD7+ LTCP to TCP of healthy BM donors, the gate within the CD45loCD3dim population was set for CD7+ TCP. It was assumed this would be the closest biological pendant in healthy BM donors.

Due to high expression of CD3 and CD45 on 14/58 patient sample´s LTCP, CD4 vs. CD8 plotting was performed on living cells. This gate could be used to define both CD4+ and CD8+ bmT cells and TCP: While physiological TCP of healthy BM donors either expressed CD4 or CD8, LTCP showed atypical expression patterns of those markers. To increase the purity of CD4+ bmT cells, CD8+ bmT cells and LTCP additional CD3 vs. CD45 gating was performed. Within the LTCP gate the CD7+ LTCP were selected (Figure 7).

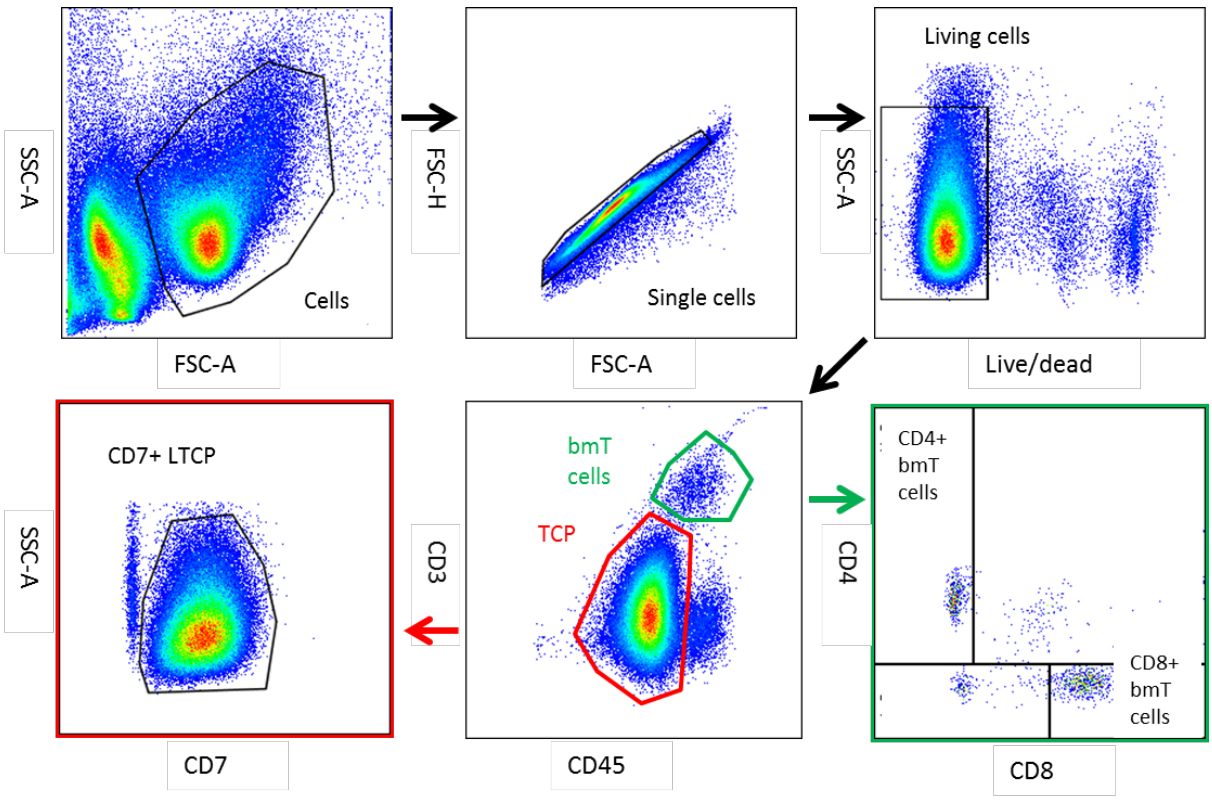

Figure 6: Representative FlowJo gating strategy for T-ALL patient B002: SSC-A vs. FSC-A: selection of cells by size and granularity; FSC-A vs. FSC-H: excluding duplets; SSC-A vs. live/dead: selection of living cells; CD3 vs. CD45: gating for bmT cells (CD3hiCD45hi) and LTCP (CD3loCD45dim); CD4 vs. CD8: differentiation of CD4+ and CD8+ bmT cells; SSC-A vs. CD7: gating on CD7+ LTCP. *TCP = T-cell progenitors, LTCP = leukemic T-cell progenitors.*

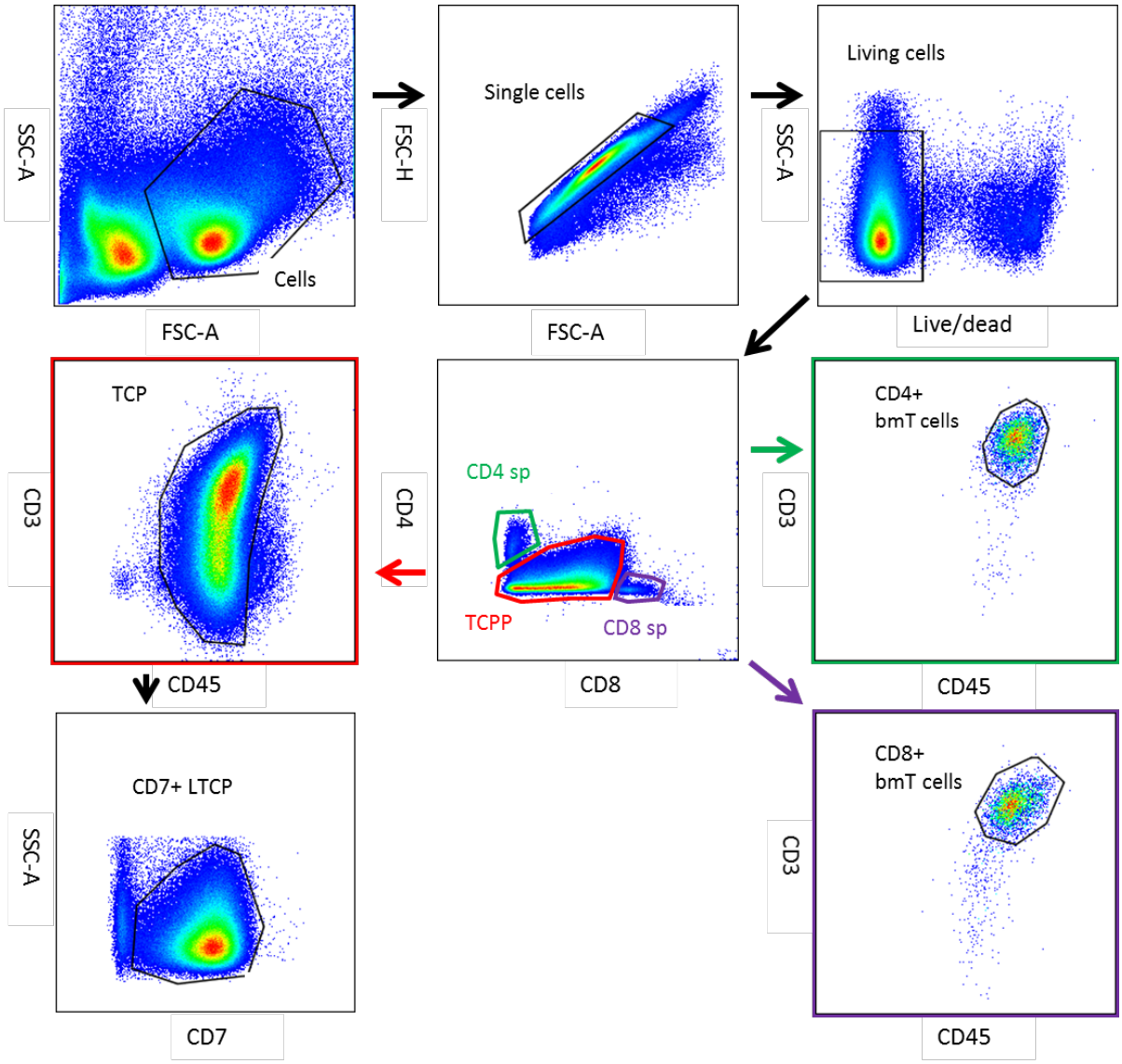

Figure 7: Representative alternative FlowJo gating strategy for T-ALL patient B006: Events were gated for cells (SSC-A vs. FSC-A), duplets (FSC-H vs. FSC-A) and dead cells (SSC-A vs. 7AAD) were excluded. Gating on CD4sp and CD8sp and characterization of a TCPP was performed in the CD4 vs. CD8 plot. CD4+ and CD8+ bmT cells and LTCP were selected in the CD3 vs. CD45 plot. For LTCP the gate was set on the CD7+ LTCP within the LTCP gate. *sp = single positive, TCPP = T-cell progenitor pre-gate, TCP = T-cell progenitors, LTCP = leukemic T-cell progenitors.*

Since the alternative gating prevented the definition of the population "bmT cells" as a whole (CD3hiCD45hi) the evaluation was limited on CD4+ and CD8+ bmT cells for all T-ALL patients and healthy BM donors. No CD4:CD8 ratio was determined.

Repeatedly, low cell count of CD4+ or CD8+ bmT cells prohibited reasonable gating. Whether to include the percentages in the final evaluation or not was decided individually depending on cell count within the gate, number of positive cells, positivity of the isotype control and marker specific gating experience. As a rule evaluation was performed if:

1. > 10 cells positive in stained sample + negative isotype control
2. > 10 cells positive in stained sample + clearly positive population

In few cases evaluation of CD4+ and CD8+ bmT cells was not possible due to low cell count or LTCP contamination (overlapping bmT-cell and LTCP population).

The populations of CD4+ bmT cells, CD8+ bmT cells and the CD7+ LTCP or physiological CD7+ TCP were analyzed regarding the expression of multiple surface molecules and intracellular antigens (FoxP3, PD-L1 and CTLA4). Four maturation stages of TCP and bmT cells were evaluated via CD45Ro and CD62L: naïve/stem cell-like memory bmT cells ($T_{N/SCM}$, CD45RO-CD62L+), central memory bmT cells (T_{CM}, CD45RO+CD62L+), effector memory bmT cells (T_{EM}, CD45RO+CD62L-) and effector bmT cells (T_{EFF}, CD45RO-CD62L-) (Figure 8A+B). The expression of single surface molecules was quantified. CD25 vs. CD127 was used on CD4+ bmT cells for definition of regulatory T cells (T_{regs}) for patients B012-B016, B301-B305, B401, B402, B405 and B501 as well as healthy BM donors B111-B117 (Figure 8C).

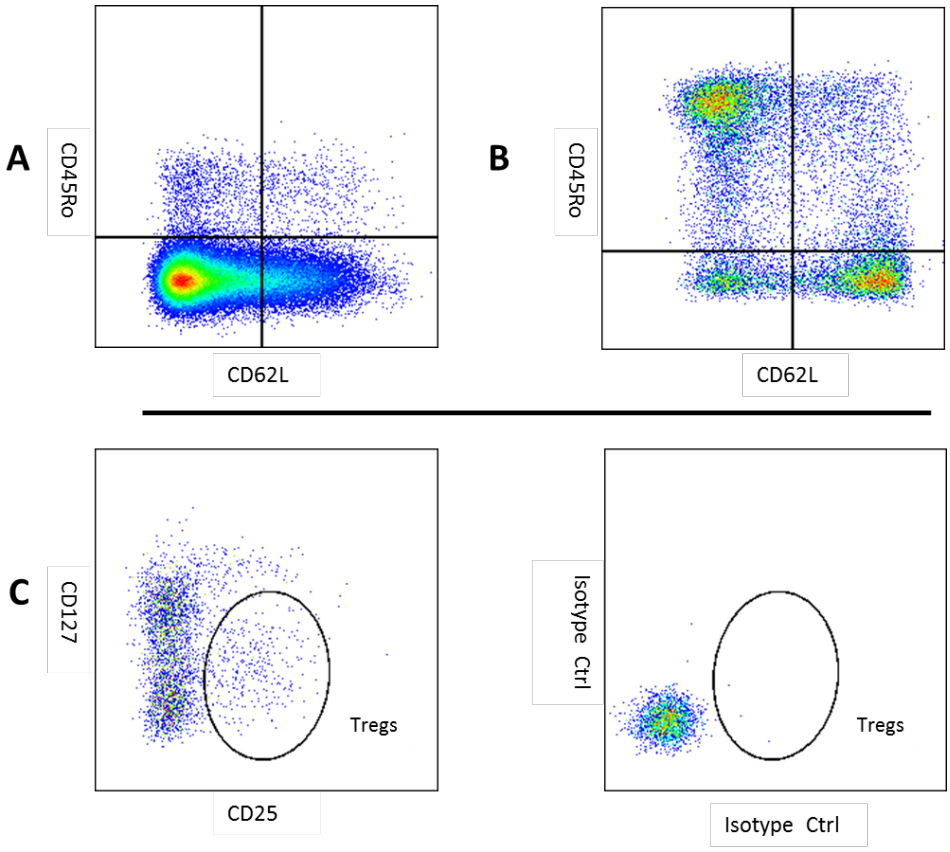

Figure 8: Representative FlowJo gating strategy for maturation stages of patient B013 and T_{regs} of patient B016: Four maturation stages of TCP **(A)** and bmT cells **(B)** were differentiated via CD45Ro and CD62L: naïve/stem cell-like memory bmT cells ($T_{N/SCM}$, CD45RO-CD62L+), central memory bmT cells (T_{CM}, CD45RO+CD62L+), effector memory bmT cells (T_{EM}, CD45RO+CD62L-) and effector bmT cells (T_{EFF}, CD45RO-CD62L-). **C)** T_{regs} were characterized as CD4+CD127lowCD25high; the isotype control was used as a reference. *TCP = T-cell progenitors, T_{regs} = regulatory T cells, Isotype Ctrl = isotype control.*

7.5.2. Quantification of surface marker expression

In general, gating was performed based on the appearance of the population/s, cell count and the unstained sample as an alternative control as well as gating experience for the individual IC. Figure 9 illustrates the principles used to ensure consistent and objective gating: If possible, gating was performed according to defined populations and the isotype control sample was used to guarantee specific gating (Figure 9A). Some immune checkpoints did not show a defined positive population. In cases of two clear populations the gate was set near the negative population or in between the two populations depending on the marker (Figure 9B+C). Again, the isotype control was employed to ensure specific gating (Figure 9D). FMF and unstained were used as a secondary control. Visualizations like zebra plot and density plot were used for more accurate gating.

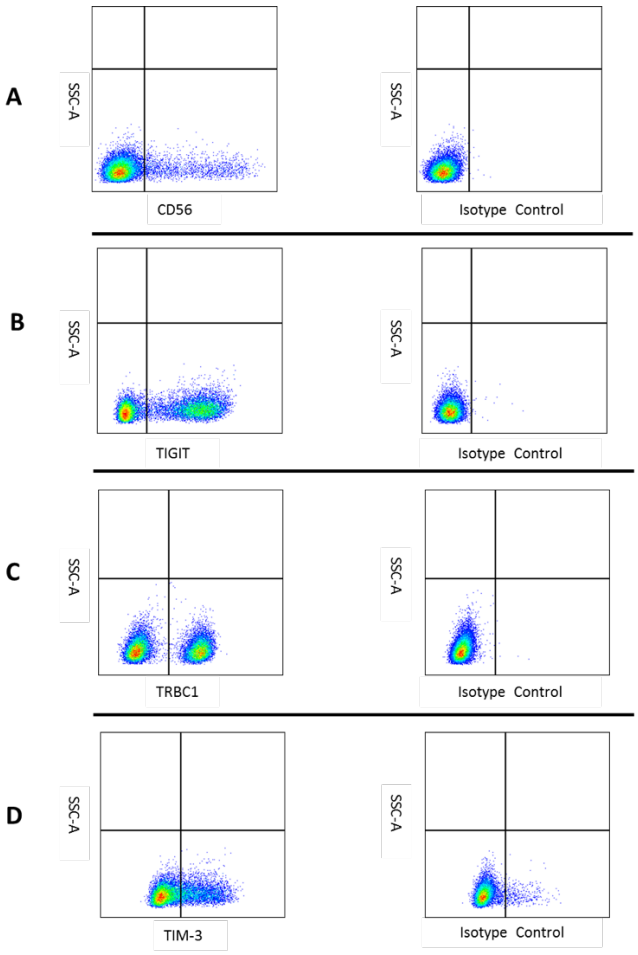

Figure 9: Representative FlowJo gating strategy for different immune checkpoints by the example of patient B013: A) Gating according to stained population with negative isotype control. **B)** Gating in case of two populations according to stained. **C)** Gating in case of two population in between two populations. **D)** Population shift with gating according to stained sample (subtract percentages of isotype control).

After the data was exported from FlowJo into text files, the percentage of positive events in the isotype control was substracted from the stained sample to ensure that only specifically stained cells were taken into account in the analysis.

7.5.3. CoALL specific evaluation strategy

The evaluation of the CoALL samples was performed according to several rules: The CD4+ and CD8+ bmT cells were excluded from analysis if:

1. < 50 cells per population
2. > 50 cells per population, but:
    a. Less than 10 cells positive for the immunomodulatory molecule and/or
    b. Positive isotype control
3. Risk of contamination with leukemic blasts

The leukemic blasts were excluded from evaluation if:

1. Unusual expression patterns of CD7/CD4/CD8 and
2. Unusual expression of surface markers (especially TCR, TRBC1)

7.6. RNA isolation

The ribonucleic acid (RNA) isolation of the sorted BM populations was performed according to the Quick-RNA™ Microprep Kit from Zymo Research. BM populations (TCP, CD4+ bmT cells, CD8+ bmT cells and NK cells) were sorted in 100% FCS at 4°C and stored on ice for up to 4 hours. Subsequently, they were pelleted at 500g for 5min. The supernatant was aspirated, and the cells resuspended in lysis buffer before storing at -20°C. RNA isolation was performed within 7 days, and RNA was transferred to -80°C. Alternatively, RNA isolation was performed after the sorted cells had been stored at -80°C for more than 7 days in Lysis Buffer. On-column DNA digestion was performed to reduce DNA contamination of RNA samples prior to sequencing as recommended by the manufacturer.

7.6.1. Quality control of RNA samples

The quality of isolated RNA was analyzed using the Agilent RNA 6000 Pico Kit and the Agilent Bioanalyzer 2100 according to the Agilent RNA 6000 Pico Kit Quick Start Guide. 1µl of the 15 µl isolated RNA was used for analysis. Samples generated from more than 100.000 cells were first diluted in nuclease free water at a ratio of 1:10 to avoid overloading. Quality assessment was based on the RNA integrity number (RIN), the height of the 28S peak and the amount of micro-RNA. For the RIN-value the cutoff was set at 7 (Figure 10). RNA concentrations were too low to measure by Qubit.

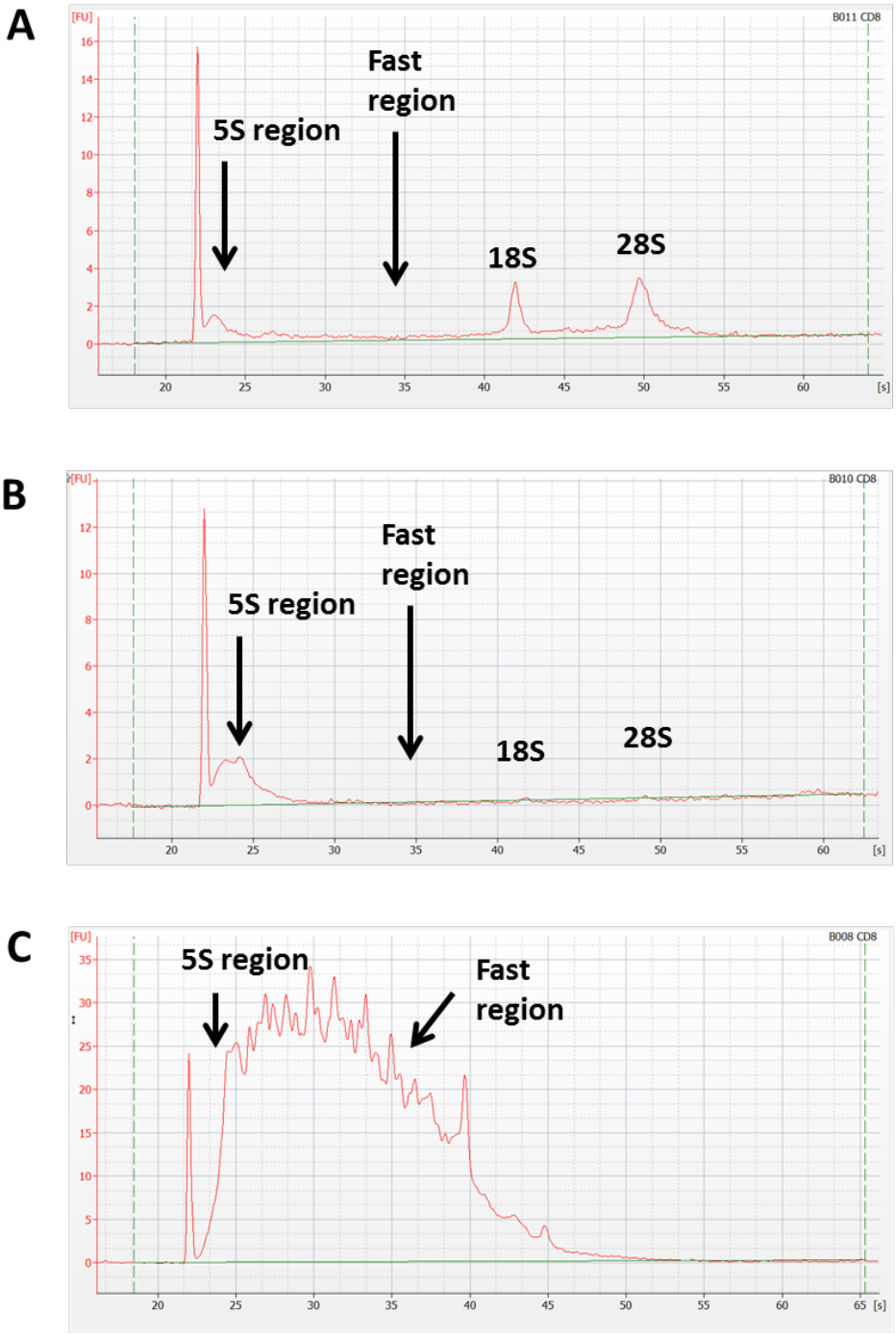

Figure 10: Representative electropherograms of CD8+ bmT cells of different quality: The cells were analyzed using the Agilent 6000 Pico Kit and the Agilent Bioanalyzer 2100. **A)** B011: good samples quality (RIN=8.2, 3.6ng total RNA), curve in Fast region near zero line (no degraded RNA), 28S peak higher than 18S peak, sample used for RNA-sequencing. **B)** B010: bad quality (RIN=1.7, 1.8ng), low amount of mRNA (18S and 28S peak only hardly noticeable), micro-RNA in 5S region (RNA isolation was performed for ~1600 cells). **C)** B008: bad quality (RIN=2.7, 68ng), high amount of degraded RNA (Fast region), no mRNA (no visible 18S and 28S peak). *RIN = RNA integrity number.*

7.6.2. RNA-sequencing

RNA library preparation was performed according to the NEBNext® Ultra™ II Directional RNA Library Prep Kit for Illumina in combination with the NEBNext Poly(A) mRNA Magnetic Isolation Module. In brief the following protocol was followed:

- Sample RNA (up to 100ng as available) was used as input material
- Washed Oligo dT Beads were mixed with input RNA 1:1 (total 100µl)
- The RNA-Bead mix was denatured at 65°C for 4min and subsequently washed, eluted, rebound, rewashed and then eluted and fragmented by 15min at 94°C
- Fragmented mRNA was subsequently used for first strand cDNA synthesis, then second strand synthesis
- End Prep of cDNA Library was followed by Adaptor Ligation (100-fold dilution of adapters)
- Finally, adapter ligated cDNA library was enriched by 14 cycles of PCR using NEB primers for multiplexed sequencing.

Analysis of RNA-Seq libraries was performed by DNA high sensitivity chip on the Bioanalyzer 2100. Pooling of 24 libraries for sequencing on a NextSeq500 high output 150 cycles kit was performed according to average library size and library concentration.
Pooled libraries were diluted and loaded on the NextSeq500 as described in the documentation of Illumina using paired end sequencing with 2 x 75 bp reads.

The CD8+ bmT-cell population showed the most promising effects in the flow cytometric analysis and was sequenced first. Table 4 shows the characteristics of healthy BM donors and pediatric HCH T-ALL patients. As healthy BM donors have been analyzed both by another MD student in the lab (Paula Rothämel) and me, healthy BM donor RNA-Seq data was used as reference in both projects to have more reference samples. Differential analysis as documented here was derived following the standard RNA-Seq pipeline of the DNASTAR Lasergene Arrayexpress.
RNA-Seq Analysis focused on the question whether differences between healthy BM donors and T-ALL patients could be seen and if so, whether (a) the molecules changed by flow cytometry analysis could be confirmed as differentially expressed, and (b) whether other molecules could be found to be differentially expressed.
The gene expression data was subjected to multiple testing correction and then filtered using the following criteria:

1) RPKM≥2 T-ALL patients and RPKM≥2 healthy BM donors
2) Fold change ≥2 in either group
3) Statistics: $p<0.05$ (false discovery rate)

The filtered genes were researched and categorized by known function in CD8+ T cells. Genes with estimated relevance were colored in the volcano plots in subchapter 8.7. Genes that showed significant differences in flow cytometric analysis were also compared to their location in the volcano plots.

	healthy BM donors	HCH T-ALL patients
All samples, n	14	12
Initial diagnosis NFR	-	9
Initial diagnosis FR	-	2
Relapse	-	1
Age, mean (range)	8.5y (1.7-13.0y)	11,5y (5.0-15.2y)
Gender, n (%)		
Male	7 (50)	10 (83.3)
Female	7 (50)	2 (16.7)

Table 4: Characteristics of healthy BM donors and pediatric T-ALL patients from the Hauner children´s hospital used for RNA-sequencing: 12 patient RNA samples (9 samples of initial diagnosis NFR, 2 samples of initial diagnosis FR, 1 sample of relapse) were sequenced (mean age: 11.5y). 14 RNA samples of healthy BM donors were used as a reference (mean age: 8.5y). *HCH = Hauner children´s hospital, NFR = no future relapse, FR = future relapse, y = years.*

7.7. DNA isolation

If sufficient leukemic blasts could be sorted, about 50% of leukemic T-ALL blasts were frozen in 200µl PBS. Frozen material will be used for DNA isolation and further down-stream analysis. However, this was not within the scope of this project at the time of submission of this document.

7.8. Chromatin transposition

ATAC-sequencing was performed according to the "Supplementary Protocol 1 – Omni-ATAC – An improved and broadly applicable ATAC-seq" published in Nature Methods 2017 by the Howard Chang Lab. This method has been tested in our lab previously and yielded data of comparable quality to the original Omni-ATAC protocol. Minor adaptions were undertaken (10.000 – 15.000 cells were used in a total transposition volume of 10µl).

After sorting at the BD FACSAria III $9x10^3$ to $15x10^3$ cells were used for ATAC-sequencing when there was at least a total of $18x10^3$ cells sorted of one population ($9x10^3$ was the minimum amount of cells used for RNA isolation to ensure reliably RNA-library preparation). After the dilution of the cells in 100-200µl of RSB I buffer (1M Tris-HCl pH 7.4, 10mM + 5M NaCl, 10mM + 1M $MgCl_2$, 3mM + sterile water) the cells were centrifuged at 5min at 500g at 4°C. The supernatant was removed completely, and the cells were resuspended in 50µl RSB II buffer (97.5% RSB I buffer + 1% Tween 10% + 1% NP40 10% + 0.5% Digitonin 2%). After three minutes of incubation on ice 100µl RSB III buffer (99% RSB I + 1% Tween 10%) were added to the solution. The mix was then centrifuged 10min at 500g at 4°C. The supernatant

was aspirated completely before adding the transposition mix (70% 2X TD buffer + 6.25% Tn5 enzyme + 22.25% PBS + 0.5% Digitonin 2% + 1% Tween 10%). The PCR tubes were incubated in a heating block for 30min at 37°C at 1000RPM. After DNA isolation was performed according to the Zymo Clean and Concentrator kit, DNA was eluted in 23µl nuclease free water. Transposed DNA fragments were amplified before sample storage by 9 cycles of PCR. To that end, 1µl of primer Ad1.0 and 1µl of an index primer (Ad2.1 – Ad2.24) were added to 25µl of the NEB Next ultra 2x mastermix (primer sequences are documented in Supplementary Table 1, https://www.ncbi.nlm.nih.gov/pmc/articles/PMC3959825/). All eluted DNA was added, and the PCR was performed at the peqSTAR 96 Universal Gradient as follows:

1. 1 cycle of 72°C for 5min, 98°C for 30sec
2. 9 cycles of 98°C for 10sec, 63°C for 30sec, 72°C for 1min

The samples were stored at -20°C until library preparation was performed, which did consist mainly in reducing high molecular weight DNA from libraries to enrich for small DNA fragments which had been transposed by the transposase and marked open chromatin.

7.9. Statistics

All statistical tests were performed by GraphPad PRISM 7.0. Statistical significance was evaluated via the Mann-Whitney-U-test (non-parametric test). Asterisks (*) were added to the figures to describe the level of significance of p values: <0.05 (*), <0.01 (**), <0.001 (***) and <0.0001 (****). No statistical tests were performed if one of the compared groups contained three or less values (e.g., initial diagnosis vs. relapse: n=2-3).

7.9.1. Multiple testing correction

Multiple testing corrections were performed using the *Original FDR method of Benjamini and Hochberg* (Ferreira, 2007). P values were analyzed and corrected for CD4+/CD8+ bmT cells and TCP including the comparisons of T-ALL vs. healthy BM donors and no future relapse vs. future relapse. Since no statistical testing was performed for the comparison initial diagnosis vs. relapse due to a low sample number no multiple testing correction was done. Kaplan Meier estimates were not corrected since there was only one significant marker for each of the BM populations of interest. The uncorrected and corrected p values are presented in each subchapter. All p values are uncorrected (including asterisks in figures) if not mentioned otherwise.

7.9.2. Kaplan-Meier plots

Kaplan-Meier estimates were evaluated via Log-rank test. The cut-off was evaluated using the mean expression level of a respective marker on a respective BM population of all T-ALL patients in the comparison of interest. The cut-off was then used for the categorization of two or more groups. Clusting of the K-means on SPSS was performed in cooperation with the statistic department but did not show to be expedient in case of the projects´ cohorts.

8. Results

8.1. Focus of the project

The focus of the project was the comparison of bone marrow T-cell populations of pediatric T-ALL patients with those of healthy bone marrow donors (healthy BM donors). Moreover, we investigated whether the T-cell phenotype carries prognostic relevance (future relapse vs. no future relapse) and whether differences exist between primary T-ALL and relapsed T-ALL (initial diagnosis vs. relapse). The samples from the Hauner children´s hospital (HCH) (healthy BM donors as well as pediatric T-ALL patients at initial diagnosis) and the Cooperative Acute Lymphoblastic Leukemia study (CoALL study) center (pediatric T-ALL patients at initial diagnosis) were evaluated separately due to different sample processing. An integration of both data sets (CoALL study center T-ALL samples and HCH T-ALL samples) was only performed for selected markers (see subchapter 8.4.3).

Expression levels of co-inhibitory and co-stimulatory molecules were analyzed on the following BM populations:

1) CD4+ bone marrow T cells (bmT cells)
2) CD8+ bmT cells
3) T-cell progenitors (TCP) or leukemic T-ALL blasts

The subsequent chapters 8.2-8.3 deal with flow cytometric findings from the HCH samples (detection cohort). In cases where graphs originate from the flow cytometry data of the CoALL samples (validation cohort), reference is made in the respective caption. Two samples were measured within the HCH and the CoALL cohort. In those cases, only HCH results were considered for statistical testing. The data presented in chapter 8.4 includes collected data of the HCH and CoALL cohort which were joined for selected graphs as mentioned above. For examining the role of immunomodulatory markers as prognostic factors, Kaplan Meier estimates were assessed showing the relapse free survival (RFS); respective p-values were calculated via Log-rank test. An analysis of the interaction of leukemic blasts and T cells is topic of chapter 8.5. The findings on RNA level of the sorted CD8+ T-cell populations are presented in chapter 8.7. Statistical testing of the flow cytometric data was performed using the Mann-Whitney-U-test.

8.2. Flow cytometric analysis: pediatric T-ALL patients vs. healthy BM donors

8.2.1. Flow cytometric analysis of physiological populations in the BM of pediatric T-ALL patients of the Hauner children´s hospital and healthy BM donors

In this subsection the focus is on phenotypic differences of CD4+ and CD8+ bmT cells in primary T-ALL samples and those of healthy BM donors. TCP describes T-cell progenitors of healthy BM donors and leukemic T-ALL blasts of pediatric T-ALL patients whereas leukemic T-ALL blasts only describes pathological TCP of the pediatric T-ALL patients.

8.2.1.1. Limited evaluation of CD3hiCD45hi bmT cells due to T-ALL blast contamination

Leukemic T-ALL blasts showed high expression of CD3 and/or CD45 on the surface in some cases (subchapter 7.5.1). The application of an alternative gating strategy was used for a more reliable differentiation between CD4+ and CD8+ bmT cells and leukemic T-ALL blasts in cases of high CD3 and/or CD45 expression and to avoid blast contamination within the bmT-cell gate (Figure 7). As a result, the bmT-cell population (CD3hiCD45hi cells) as a whole was not evaluated regarding the following characteristics:

1. Ratio of CD4+ vs. CD8+ bmT cells (CD4:CD8 ratio)
2. Ratio of CD3+ cells amongst all living cells
3. Expression of immunomodulatory molecules on the population “bmT cells”

All results of flow cytometric data on side of bmT cells refer to the CD4+ and CD8+ bmT-cell population. The CD4:CD8 ratio was not estimated due to repetitively low numbers of bmT cells.

8.2.1.2. CD4+ and CD8+ bmT cells of pediatric T-ALL patients of the Hauner children´s hospital show increased frequency of late maturation stages over those of healthy BM donors

The CD4+ and CD8+ bmT-cell populations were analyzed regarding CD45RO and CD62L surface expression and characterized regarding the distribution of four maturation stages: naïve/stem cell-like memory T cells ($T_{N/SCM}$, CD45RO-CD62L+), central memory T cells (T_{CM}, CD45RO+CD62L+), effector memory T cells (T_{EM}, CD45RO+CD62L-) and effector T cells (T_{EFF}, CD45RO-CD62L-). More matured maturation stages of CD4+ and CD8+ bmT cells were enriched in pediatric T-ALL patients in comparison to healthy BM donors. Pediatric T-ALL patients had significantly less CD4+ $T_{N/SCM}$ (24.6 % vs. 41.2 %, mean values T-ALL patients vs. healthy BM donors, p=0.0030) and CD8+ $T_{N/SCM}$ (24.91 % vs. 35.8 %, p=0.0422) than healthy BM donors. T-ALL patients showed increased effector memory frequency

within the CD4+ (36.0 % vs. 23.5 %, p=0.0154) and the same trend in CD8+ bmT cells (38.6 % vs. 34.9 %, p=0.6979) (Figure 11).

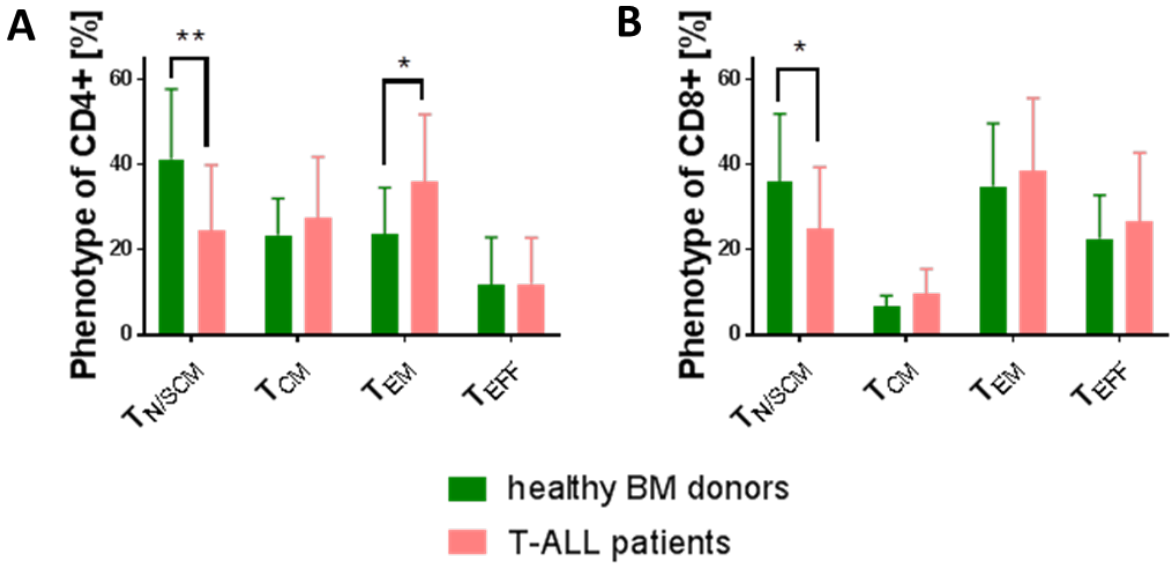

Figure 11: Mean distribution of maturation stages of CD4+ and CD8+ bmT cells in pediatric T-ALL patients of the Hauner children´s hospital at initial diagnosis (n=19-20) and healthy BM donors (n=14): The CD4+ and CD8+ bmT-cell populations were analyzed regarding the CD45RO and CD62L surface expression and then characterized regarding the mean distribution of four maturation stages: $T_{N/SCM}$ (CD45RO-CD62L+), T_{CM} (CD45RO+CD62L+), T_{EM} (CD45RO+CD62L-) and T_{EFF} (CD45RO-CD62L-). **A)** T-ALL patients showed a significantly decreased frequency of $T_{N/SCM}$ (p=0.0030) and increased frequency of T_{EM} (p=0.0154) within the CD4+ bmT-cell population. **B)** T-ALL patients showed a significantly lower frequency of $T_{N/SCM}$ (p=0.0422) within the CD8+ T-cell population. *$T_{N/SCM}$ = naïve/stem cell-like memory T cells, T_{CM} = central memory T cells, T_{EM} = effector memory T cells, T_{EFF} = effector T cells.*

8.2.1.3. Overexpression of co-inhibitory and co-stimulatory molecules on bmT cells of T-ALL patients of the Hauner children´s hospital compared to healthy BM donors

The CD4+ and CD8+ bmT-cell population of pediatric T-ALL patients and healthy BM donors were analyzed regarding the expression of co-inhibitory and co-stimulatory molecules.

8.2.1.3.1. Overexpression of co-inhibitory and co-stimulatory molecules on CD4+ bmT cells

The comparison of HCH T-ALL patients at initial diagnosis with healthy BM donors showed a significant upregulation of co-inhibitory markers on patients´ CD4+ bmT cells: 2B4 (7.5 % vs. 1.3 %, p=0.0119), TIM-3 (7.0 % vs. 1.5 %, p=0.0025), CD57 (8.6 % vs. 2.7 %, p=0.0139). The same trend – though not significant (ns) - with regards to an overexpression on T-ALL patient CD4+ bmT cells, could be observed for other co-inhibitory molecules (LAG-3, CD39, PD-L1, PD-1 and TIGIT). CD28 (94.5 % vs. 98.9 %,

p=0.0035) and CD27 (81.5 % vs. 91.9 %, p=0.0018) expression was reduced in pediatric T-ALL patients. ICOS, OX40 and GITR (ns) were overexpressed on CD4+ bmT cells of T-ALL patients, albeit not significantly.

Figure 12 presents an overview of the markers of interest on CD4+ bmT cells showing the results of HCH T-ALL patients and healthy BM donors at initial diagnosis. Figure 13 and Figure 14 constitute a more detailed visualization of results using the same data set as Figure 12 (Figure 13: co-inhibitory molecules; Figure 14: co-stimulatory molecules).

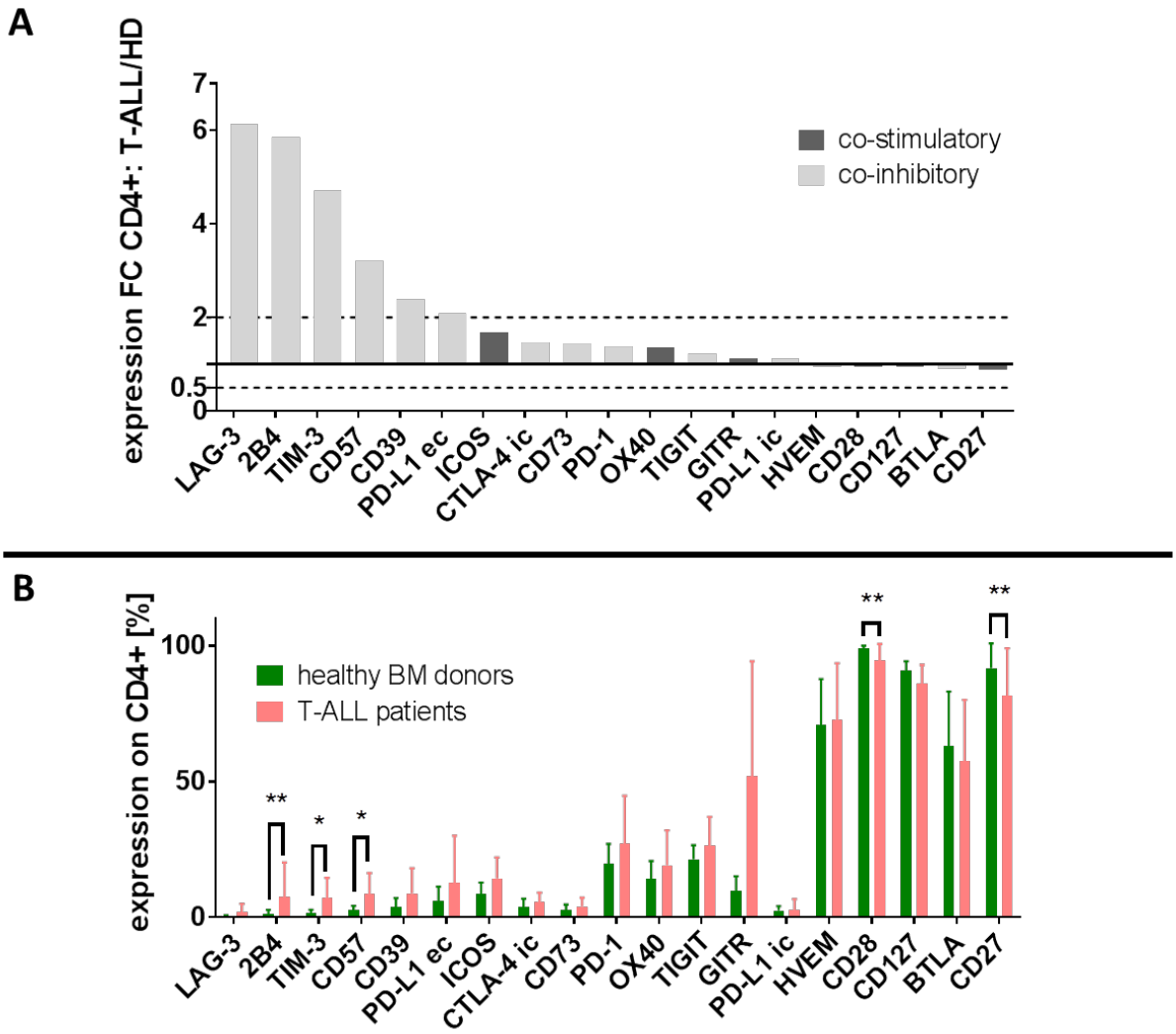

Figure 12: Overexpression of co-inhibitory and co-stimulatory molecules on CD4+ bmT cells of pediatric T-ALL patients of the Hauner children´s hospital at initial diagnosis (n=9-20) compared to healthy BM donors (n=7-14): A) Expression fold change on CD4+ bmT cells: mean expression T-ALL patients/mean expression HD. Co-inhibitory markers were overexpressed on CD4+ bmT cells of T-ALL patients (LAG-3, 2B4, TIM-3, CD57, CD39, PD-L1 ec, PD-1, TIGIT). **B)** The absolute expression level of immunomodulatory molecules on CD4+ bmT cells was arranged according to Figure 12A. An upregulation of co-inhibitory markers 2B4 (p=0.0119), TIM-3 (p=0.0025), CD57 (p=0.0139), and a downregulation of CD28 (p=0.0035) and CD27 (p=0.0018) could be observed on patients' CD4+ bmT cells. Markers with expression levels <1% of all CD4+ T cells in both cohorts were excluded from analysis due to high fold changes without evident biological relevance. CTLA-4 ic and PD-L1 ic were stained intracellularly. *FC = fold change, HD = healthy BM/bone marrow donors, ec = extracellular, ic = intracellular.*

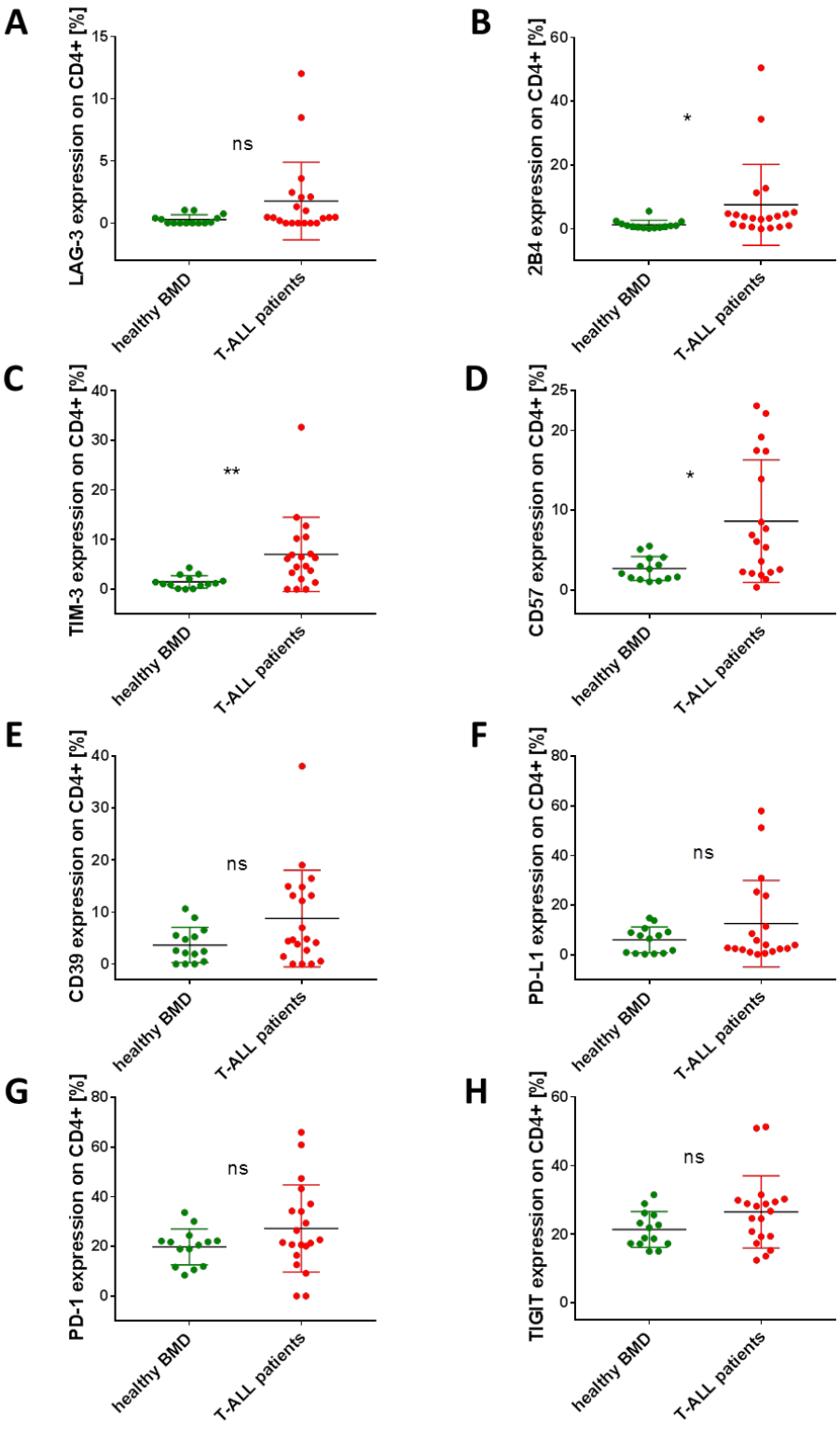

Figure 13: Overexpression of co-inhibitory molecules on CD4+ bmT cells of pediatric T-ALL patients of the Hauner children´s hospital at initial diagnosis (n=18-20) compared to healthy BM donors (n=14): The graphs are based on the same data set as Figure 12. A significant upregulation of co-inhibitory markers **B)** 2B4 (p=0.0139), **C)** TIM-3 (p=0.0025) and **D)** CD57 (p=0.0119) on CD4+ bmT cells of pediatric T-ALL patients compared to healthy BM donors could be observed. **A)** LAG-3 (ns), **E)** CD39 (ns), **F)** PDL1 (ns), **G)** PD-1 (ns) and **H)** TIGIT (ns) showed similar tendencies towards overexpression on CD4+ bmT cells of pediatric T-ALL patients (ns). *healthy BMD = healthy BM/bone marrow donors, ns = not significant.*

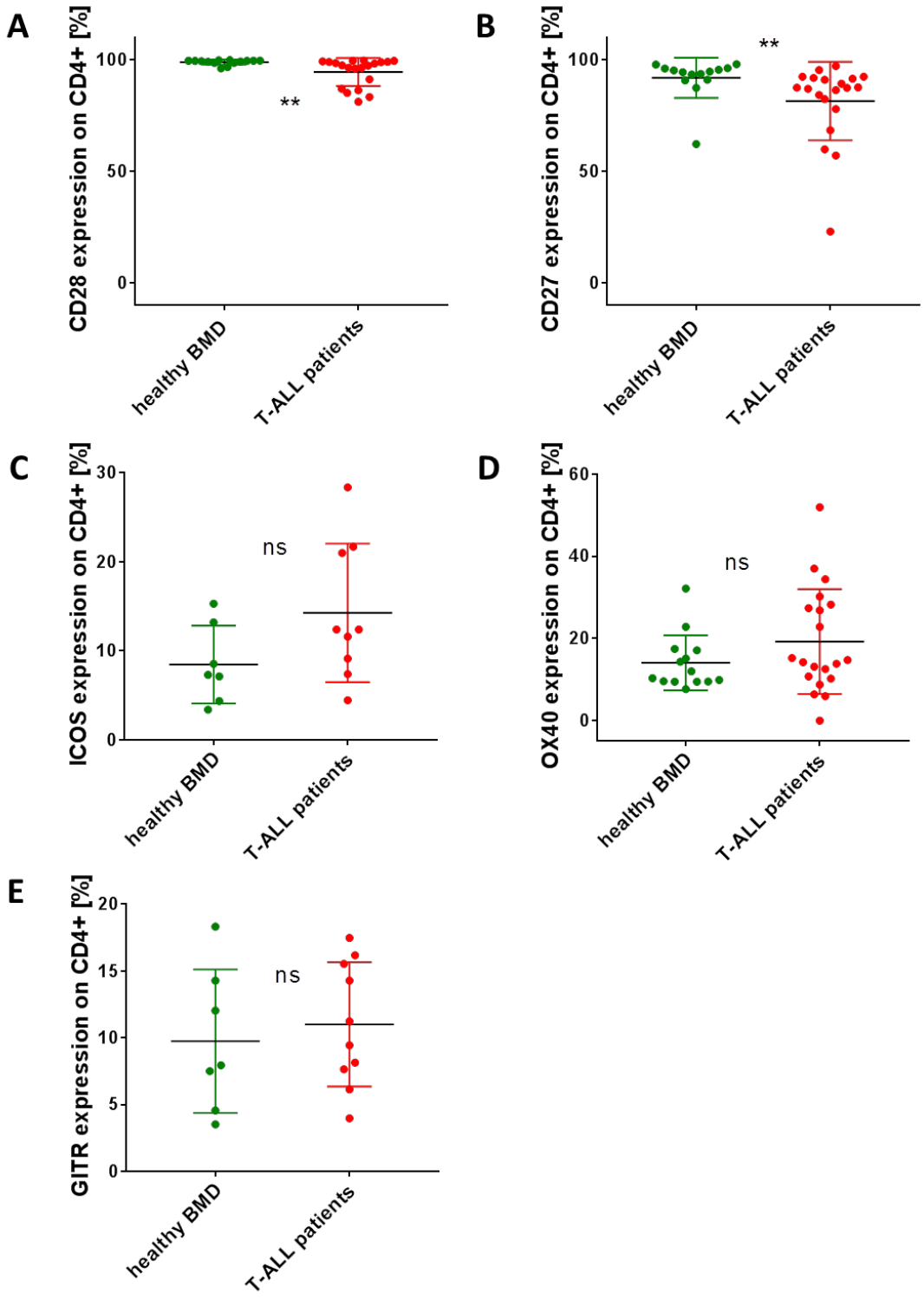

Figure 14: Differential expression of co-stimulatory molecules on CD4+ bmT cells of pediatric T-ALL patients of the Hauner children´s hospital at initial diagnosis (n=9-20) compared to healthy BM donors (n=7-14): The graphs emerged from the same data set as Figure 12. A significant downregulation of co-stimulatory markers **A)** CD28 (p=0.0035) and **B)** CD27 (p=0.0018) on CD4+ bmT cells of pediatric T-ALL patients compared to healthy BM donors could be observed. A trend towards upregulation of co-stimulatory markers **C)** ICOS (ns), **D)** OX40 (ns) and **E)** GITR (ns) on CD4+ bmT cells of pediatric T-ALL patients compared to healthy BM donors could be observed. *healthy BMD = healthy BM/bone marrow donors, ns = not significant.*

8.2.1.3.2. Overexpression of co-inhibitory and co-stimulatory molecules on CD8+ T cells

Similar to CD4+ bmT cells, an increased expression of co-inhibitory markers was observed on CD8+ bmT cells of pediatric T-ALL patients compared to healthy BM donors: LAG3 (6.0 % vs. 1.3 %, p=0.0165), TIM-3 (10.7 % vs. 2.5 %, p=0.0012), CD57 (31.2 vs. 14.2 %, p=0.0600), 2B4 (54.7 % vs. 40.0 %, p=0.1122) and TIGIT (48.9 % vs. 41.0 %, p=0.3037). Intracellularly stained co-inhibitory marker CTLA-4 was significantly increased in CD8+ bmT cells of T-ALL patients in comparison to the healthy control (1.5 % vs. 0.3 %, p=0.0276). The co-stimulatory molecule ICOS was significantly increased on patients CD8+ bmT cells (5.4 % vs. 2.0 %, p=0.0033). The co-inhibitory molecule CD73 was significantly lower expressed on T-ALL patient´s CD8+ bmT cells compared to the healthy control (29.9 % vs. 42.8 %, p=0.0361).

Figure 15 presents an overview of markers of interest on/in CD8+ bmT cells comparing healthy HCH T-ALL patients at initial diagnosis to healthy BM donors. Figure 16 and Figure 17 constitute a more detailed representation of relevant results using the same data set as Figure 15 (Figure 16: co-inhibitory molecules; Figure 17: other significant markers).

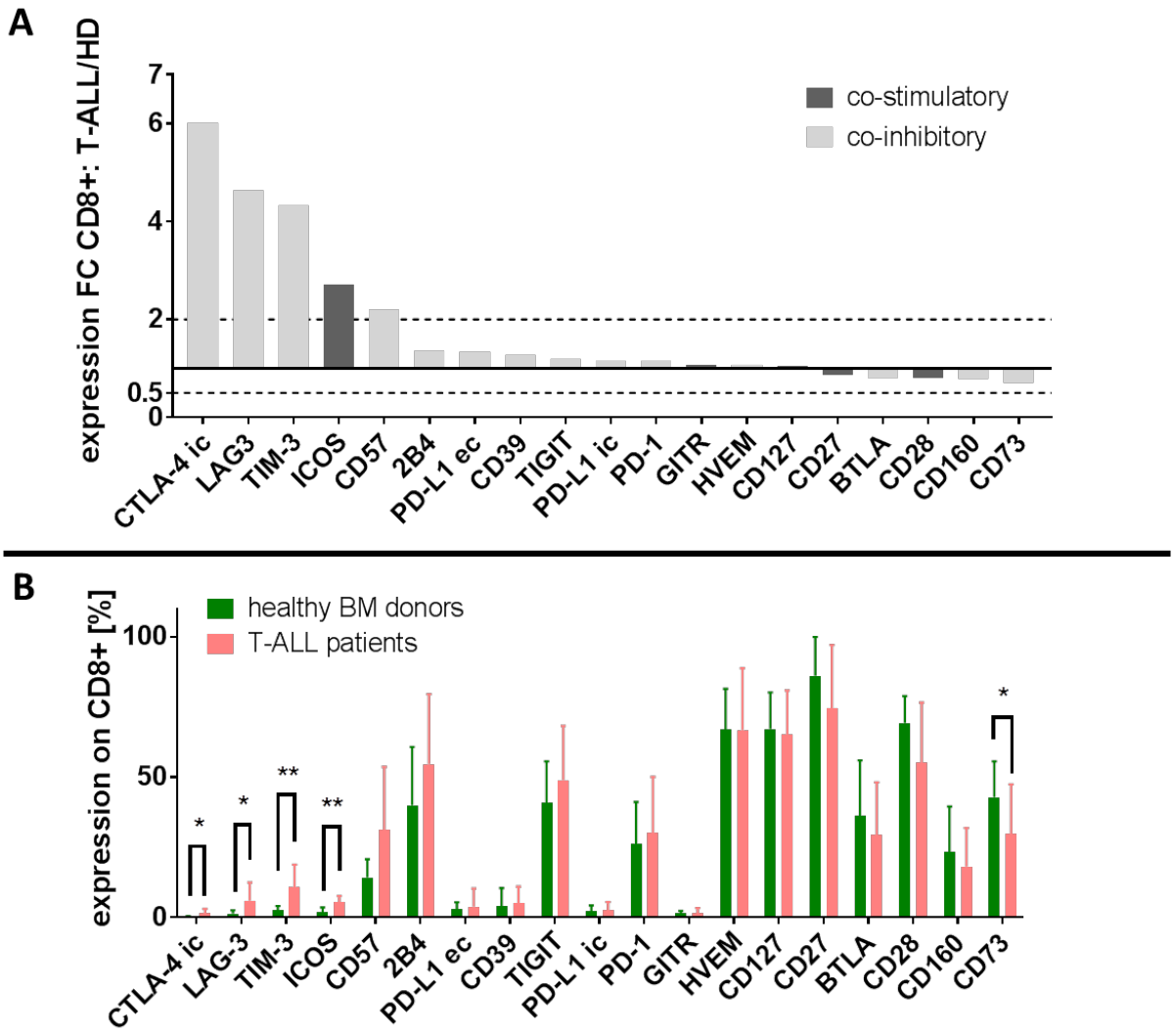

Figure 15: Overexpression of co-inhibitory and co-stimulatory molecules on CD8+ bmT cells of pediatric T-ALL patients of the Hauner children´s hospital at initial diagnosis (n=9-20) compared to healthy BM donors (7-14): A) Expression fold change on CD8+ bmT cells: mean expression T-ALL patients/mean expression HD. Co-inhibitory markers were overexpressed on CD4+ bmT cells of pediatric T-ALL patients (CTLA-4, LAG-3, TIM-3, CD57, 2B4, PD-L1 ec). **B)** The absolute expression of immunomodulatory molecules on CD8+ bmT cells was arranged according to Figure 15A. A significant upregulation of co-inhibitory markers CTLA-4 ic (p=0.0276), LAG-3 (p=0.0165), TIM-3 (p=0.0012) could be observed on patients CD8+ bmT cells. CD73 expression was significantly reduced on CD8+ bmT cells of T-ALL patients (p=0.0361). The co-stimulatory molecule ICOS was significantly overexpressed on CD8+ bmT cells of pediatric T-ALL patients compared to the healthy control (p=0.0033). Markers with expression levels <1% of all CD8+ T cells in both cohorts were excluded from analysis due to high fold changes without evident biological relevance. CTLA-4 ic and PD-L1 ic were stained intracellularly. *FC = fold change, HD = healthy BM/bone marrow donors, ec = extracellular, ic = intracellular.*

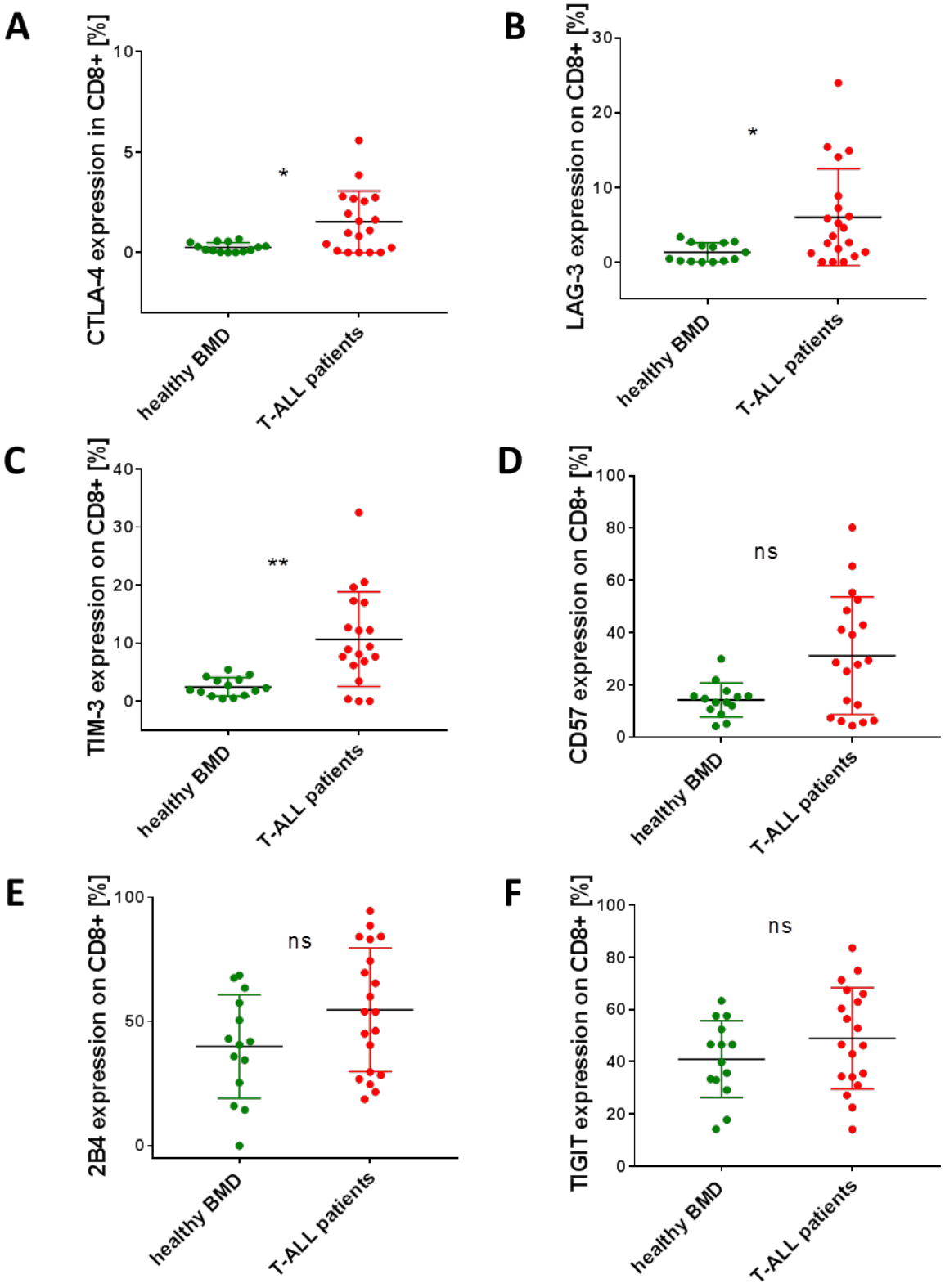

Figure 16: Overexpression of co-inhibitory molecules on CD8+ bmT cells of pediatric T-ALL patients of the Hauner children´s hospital at initial diagnosis (n=18-20) compared to healthy BM donors (n=14): The graphs emerged from the same data set as Figure 15. A significant upregulation of co-inhibitory markers **A)** CTLA-4 ic (p=0.0276), **B)** LAG-3 (p=0.0165) and **C)** TIM-3 (p=0.0012) on CD8+ bmT cells of pediatric T-ALL patients compared to healthy BM donors could be observed. **D)** CD57 (ns), **E)** 2B4 (ns) and **F)** TIGIT (ns) showed a similar trend towards overexpression on CD8+ bmT cells of pediatric T-ALL patients but were not significant. CTLA-4 was stained intracellularly. *healthy BMD = healthy BM/bone marrow donors, ns = not significant.*

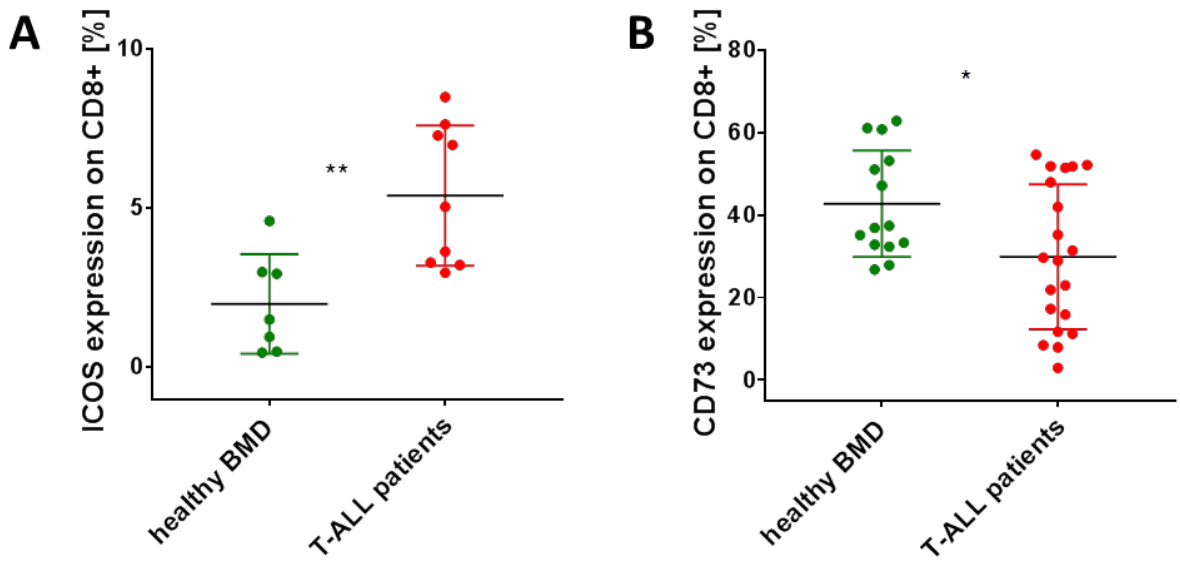

Figure 17: Overexpression of co-stimulatory molecules ICOS and downregulation of co-inhibitory molecules CD73 on CD8+ bmT cells of pediatric T-ALL patients of the Hauner children´s hospital at initial diagnosis (n=9-20) compared to healthy BM donors (n=7-14): The graph emerged from the same data set as Figure 15. **A)** A significant upregulation of co-stimulatory marker ICOS on CD8+ bmT cells of pediatric T-ALL patients compared to healthy BM donors could be observed (p=0.0033). **B)** The co-inhibitory marker CD73 was significantly decreased on patients' CD8+ bmT cells compared to the heathy control (p=0.0361). *healthy BMD = healthy BM/bone marrow donor.*

8.2.1.4. Frequency of regulatory T cells in the BM of pediatric T-ALL patients with future relapse compared to healthy BM donors

A trend towards a reduced T_{regs} frequency in the BM of pediatric T-ALL patients without future relapse at initial diagnosis (n=5) was observed when comparing to healthy BM donors (n=7) (10.4 % vs. 11.4 %, ns) (Figure 18A). Pediatric T- ALL patients with future relapse (n=5) showed a significantly decreased T_{regs} frequency at initial diagnosis compared to healthy BM donors (n=5) (7.1 % vs. 11.4 %, p=0.0303) (Figure 18A). Differential expression between no future relapse and future relapse T-ALL patients at initial diagnosis was not significant (10.4 % vs. 7.1 %). A further trend towards downregulation could be observed for the 2^{nd} relapse (n=1) compared to initial diagnosis (n=10) and 1^{st} relapse (n=3). Due to low patient numbers no statistical testing was performed for the comparison of initial diagnosis and $1^{st}/2^{nd}$ relapse (Figure 18B).

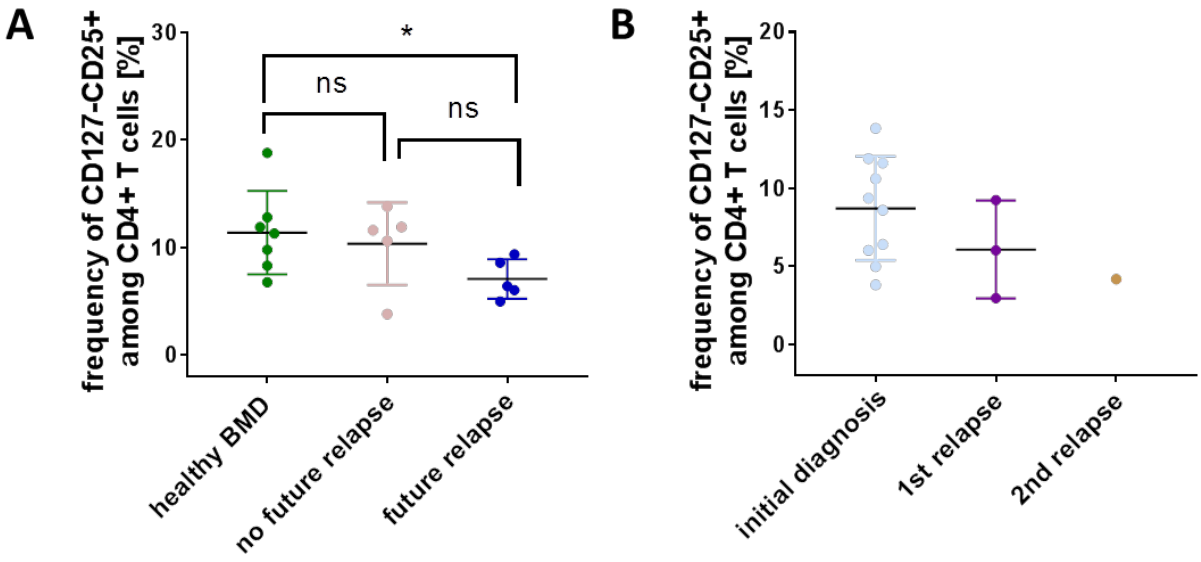

Figure 18: Frequency of regulatory T cells in pediatric T-ALL patients of the Hauner children´s hospital and healthy BM donors (n=7): The T_{regs} population was characterized as CD127-CD25+ cells within the CD4+ bmT-cell population. **A)** No future relapse T-ALL patients at initial diagnosis (n=5) showed a trend towards a decreased T_{regs} frequency compared to healthy BM donors (n=7) (ns). A significant downregulation of the T_{regs} frequency in the BM of pediatric T-ALL patients with future relapse (n=5) was observed compared to healthy BM donors (n=7) (p=0.0303). T- ALL patients with future relapse (n=5) showed a trend towards decreased T_{regs} frequencies compared to patients without future relapse (n=5) (ns). **B)** A further trend towards downregulation could be observed for the 2nd relapse (n=1) compared to initial diagnosis (n=10) and 1st relapse (n=3). No statistics were performed for B) due to samples number ≤3 for two of the three groups. *T_{regs} = regulatory T cells, healthy BMD = healthy BM/bone marrow donors, ns = not significant.*

8.2.2. Flow cytometric analysis of physiological and leukemic T-cell progenitors in the BM of pediatric T-ALL patients of the Hauner children´s hospital and healthy BM donors

8.2.2.1. Intermediate maturation phenotype, CD4 and CD8 expression and high CD7+ expression of leukemic blasts compared to physiological T-cell progenitors

As CD7 was expressed on all T-ALL blast populations, this marker was used to gate for either physiological TCP in healthy BM donors or leukemic blasts in T-ALL patients (Figure 19A+B). Moreover, physiological T-cell maturation markers were applied on malignant TCP: naïve/stem cell-like memory T cells ($T_{N/SCM}$, CD45RO-CD62L+), central memory T cells (T_{CM}, CD45RO+CD62L+), effector memory T cells (T_{EM}, CD45RO+CD62L-) and effector T cells (T_{EFF}, CD45RO-CD62L-). Leukemic blasts showed significantly higher frequencies of intermediate maturation stages T_{CM} (52.8 % vs. 3.1 %, p<0.0001) and T_{EM} (23.3 % vs. 5.1 %, p=0.0167) and significantly lower frequencies of $T_{N/SCM}$ (11.9 % vs. 27.2 %, p=0.0003) and T_{EFF} (12.0 % vs. 64.4 %, p<0.0001) maturation stages (Figure 19C) compared to TCP of healthy BM donors.

For further characterization of TCP blasts, CD4 and CD8 expression was analyzed (Figure 19D): T-ALL patients showed a significantly higher frequency of CD4+CD8- (10.0 % vs. 1.8 %, p=0.0394) TCP and

significantly less CD4-CD8+ (25.7 % vs. 26.2 %, p=0.0255) phenotype. Differences regarding the frequency of CD4+CD8+ (17.7 % vs. 0.4 %, p=0.3319) and CD4-CD8- (46.7 % vs. 71.6 %, p=0.3293) TCP were not significant.

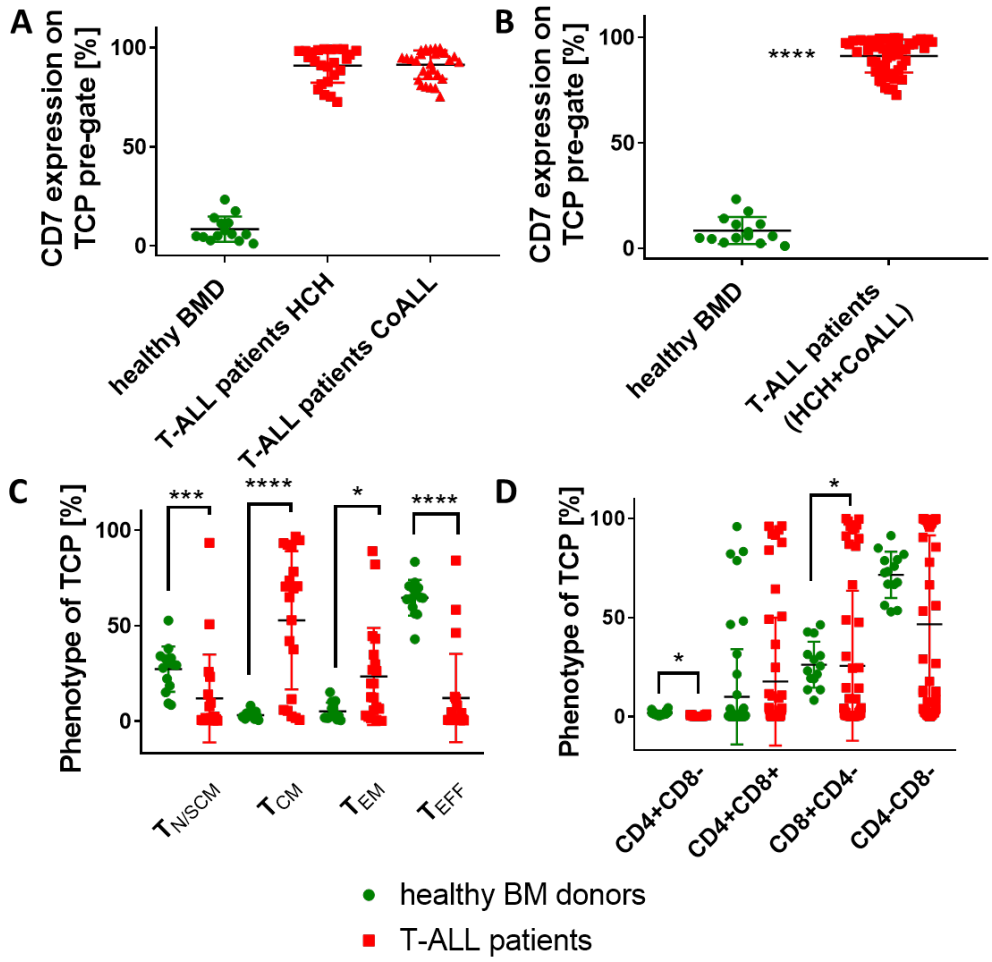

Figure 19: Increased frequency of CD7+ TCP in T-ALL patients with altered TCP phenotype by CD4, CD8, CD45RO and CD62L expression compared to healthy BM donors: presentation of pediatric T-ALL patients of the Hauner children´s hospital (n=24) and CoALL study (n=29) and physiological TCP precursors of healthy BM donors (n=14). A), B) and D) include the integration of HCH and CoALL data. **A)** Cells within the TCP pre-gate of pediatric T-ALL patients showed higher CD7 expression compared to the healthy control (n=14). This applied to HCH T-ALL patients (n=24) and CoALL T-ALL patients (n=29). No statistical testing was performed. **B)** After integration of all measured T-ALL patients (n=53), a significantly higher CD7 expression could be detected on cells of the TCP pre-gate compared to healthy donors (n=14) (p<0.0001). B) shows the same data as A). **C)** The frequency of maturation stages of TCP in healthy BM donors and pediatric T-ALL patients of the HCH was analyzed using CD45RO and CD62L surface expression. The characterization was performed regarding four maturation stages: $T_{N/SCM}$ (CD45RO-CD62L+), T_{CM} (CD45RO+CD62L+), T_{EM} (CD45RO+CD62L-) and T_{EFF} (CD45RO-CD62L-). Precursors of pediatric T-ALL patients showed significantly higher percentages of T_{CM} (p<0.0001) and T_{EM} (p=0.0167) and lower rates of $T_{N/SCM}$ (p=0.0003) and T_{EFF} (p<0.0001) maturation. **D)** T-ALL patients of the HCH and CoALL cohort showed significantly higher percentages of CD4+CD8- (p=0.0394) TCP and significantly less CD4-CD8+ (p=0.0255) TCP. Differences regarding the frequency of CD4+CD8+ and CD4-CD8- TCP were not significant. *HCH = Hauner children´s hospital, healthy BMD = healthy BM/bone marrow donors, TCP = T-cell progenitors, $T_{N/SCM}$ = naïve/stem cell-like memory T cells, T_{CM} = central memory T cells, T_{EM} = effector memory T cells, T_{EFF} = effector T cells.*

8.2.2.2. Upregulation of co-stimulatory molecules and downregulation of co-inhibitory molecules on T-cell progenitors of pediatric T-ALL patients

We analyzed expression of co-stimulatory molecules on malignant TCP and observed a striking upregulation of co-stimulatory markers while co-inhibitory markers were downregulated in comparison to healthy BM donors. Figure 20 presents an overview of co-stimulatory and co-inhibitory markers that were measured on TCP of healthy BM donors and on leukemic blasts of pediatric T-ALL patients. Figure 21, Figure 22, Figure 44, Figure 23 and Figure 24 constitute a more detailed visualization of relevant results using the same data set as Figure 20.

A significant upregulation of co-stimulatory markers was observed for CD127 (20.0 % vs. 8.4 %, p=0.001) and OX40 (11.1 % vs. 3.5 %, p=0.0049). Other co-stimulatory molecules showed a similar trend without reaching significance: CD70 (13.4 % vs. 0.5 %, p=0.1266), ICOS (47.5 % vs. 2.0 %, p=0.1142) and CD28 (50.0 % vs. 3.7 %, p=0.5167). Data regarding the CD28 expression on TCP of the HCH and the CoALL cohort were integrated and evaluated in a joined analysis (67.9 % vs. 3.7%, p=0.0003) (Figure 22). Co-stimulatory markers CD27 (16.0 % vs. 18.4 %, p=0.0388) and GITR (1.7 % vs. 18.1 %, p=0.0001) were significantly higher expressed on healthy TCP compared to expression on leukemic T-ALL blasts of pediatric patients (Figure 21 & Figure 44: co-stimulatory molecules).

A variety of co-inhibitory molecules were downregulated on TCP of pediatric T-ALL patients. This included the markers HVEM (23.2 % vs. 54.0 %, p=0.0005), 2B4 (26.6 % vs. 93.7 %, p<0.0001), BTLA (0.7 % vs. 3.2 %, p=0.0041), CD39 (1.0 % vs. 10.4 %, p<0.0001), CD57 (2.6 % vs. 29.2 %, p<0.0001), TIM-3 (4.1 % vs. 53.5 %, p<0.0001), TIGIT (0.6 % vs. 78.6 %, p<0.0001) and CD160 (0.6 % vs. 75.3 %, p<0.0001) (Figure 23: co-inhibitory molecules). CD112 was upregulated (>50%) on TCP of 6 out of 19 pediatric T-ALL patients (31.9 % vs. 3.5 %, p=0.5268) and showed a bimodal distribution (Figure 24).

Table 5 presents an overview of the expression levels of different co-stimulatory molecules including CD28, CD27, OX40, CD70, ICOS and CD127. Different ranges of percentages were defined and translated in a coloring code for better visualization to illustrate that all malignant TCP populations express at least one co-stimulatory molecule. ICOS and CD127 were only measured for 14/24 samples due to changes in the antibody selection for sample measurements. The table shows that in 19/24 of the samples leukemic T-ALL blasts were strongly positive for at least one of the markers (cut-off: 50%): 9/24 samples were strongly positive for one marker, 8/24 for two markers and 2/24 for three markers. 5/24 samples showed no expression level above the selected cut-off. The CoALL data was not integrated in this table.

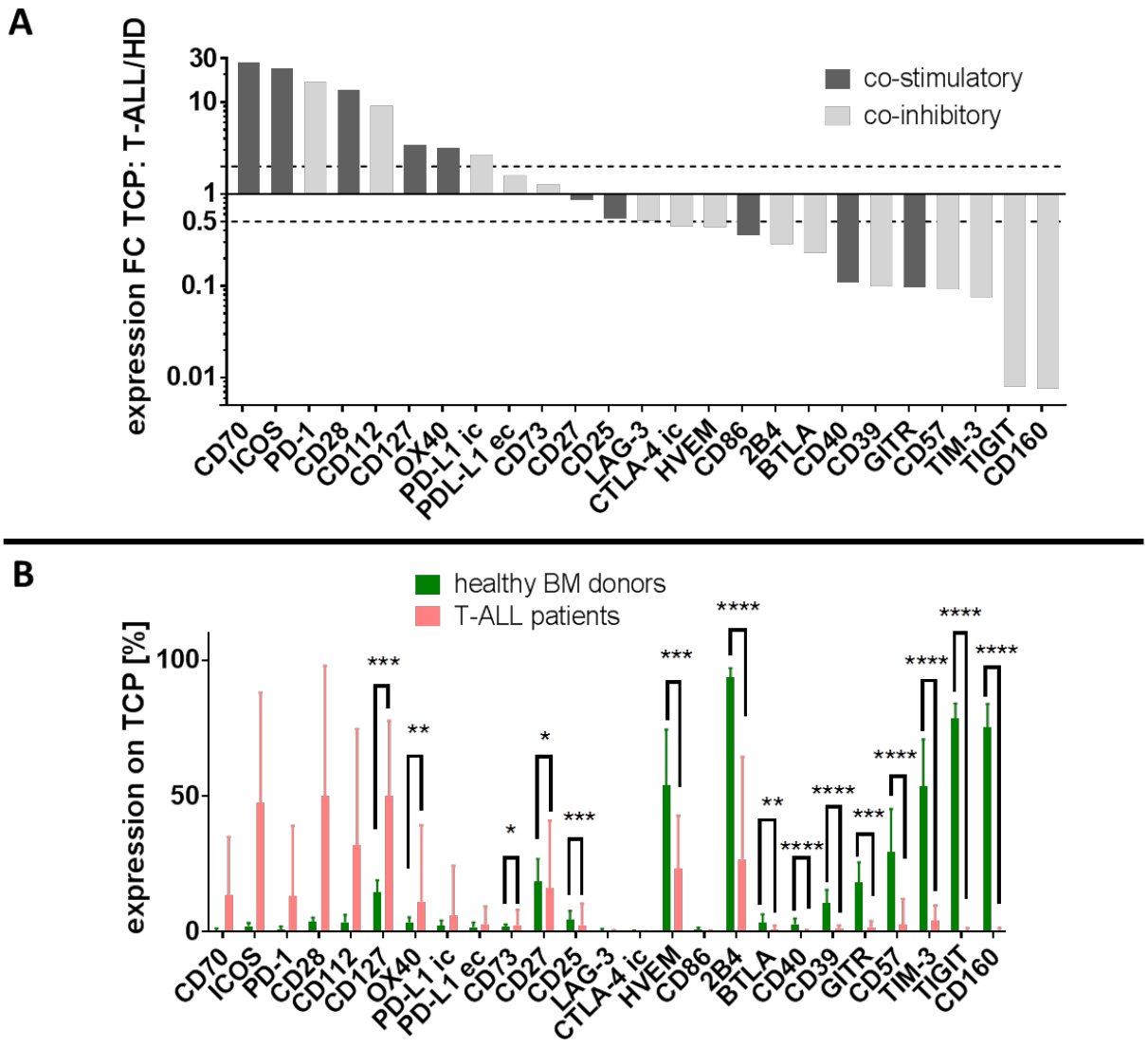

Figure 20: Upregulation of co-stimulatory and downregulation of co-inhibitory molecules on T-cell progenitors in the BM of pediatric T-ALL patients of the Hauner children´s hospital at initial diagnosis (n=9-20) and healthy BM donors (n=7-14): A) Expression fold change on TCP: mean expression T-ALL patients/mean expression HD. **B)** The absolute expression of immune modulatory molecules on TCP was arranged according to A. A significant upregulation on T-ALL blasts in contrast to healthy TCP could be observed for co-stimulatory markers CD127 (p=0.001) and OX40 (p=0.0049). CD112 and the co-stimulatory markers CD70 (ns), ICOS (ns), CD28 (ns) showed a trend towards overexpression on T-ALL TCP without reaching significance due to a high deviation of individual expression levels. Co-stimulatory markers CD27 (p=0.0388), CD25 (p=0.0001), CD40 (p<0.0001) and GITR (p=0.0001) were significantly higher expressed on healthy TCP than on leukemic blasts of pediatric T-ALL patients. Co-inhibitory markers were downregulated on TCP of pediatric T-ALL patients compared to healthy BM donors: HVEM (p=0.0005), 2B4 (p<0.0001), BTLA (p=0.0041), CD39 (p<0.0001), CD57 (p<0.0001), TIM-3 (p<0.0001), TIGIT (p<0.0001) and CD160 (p<0.0001). The co-inhibitory molecule CD73 was significantly overexpressed on T-ALL blasts compared to physiological TCP of healthy BM donors (p=0.0199). CTLA-4 ic and PD-L1 ic were stained intracellularly. *FC = fold change, TCP = T-cell progenitors, HD = healthy BM/bone marrow donors, ec = extracellular, ic = intracellular.*

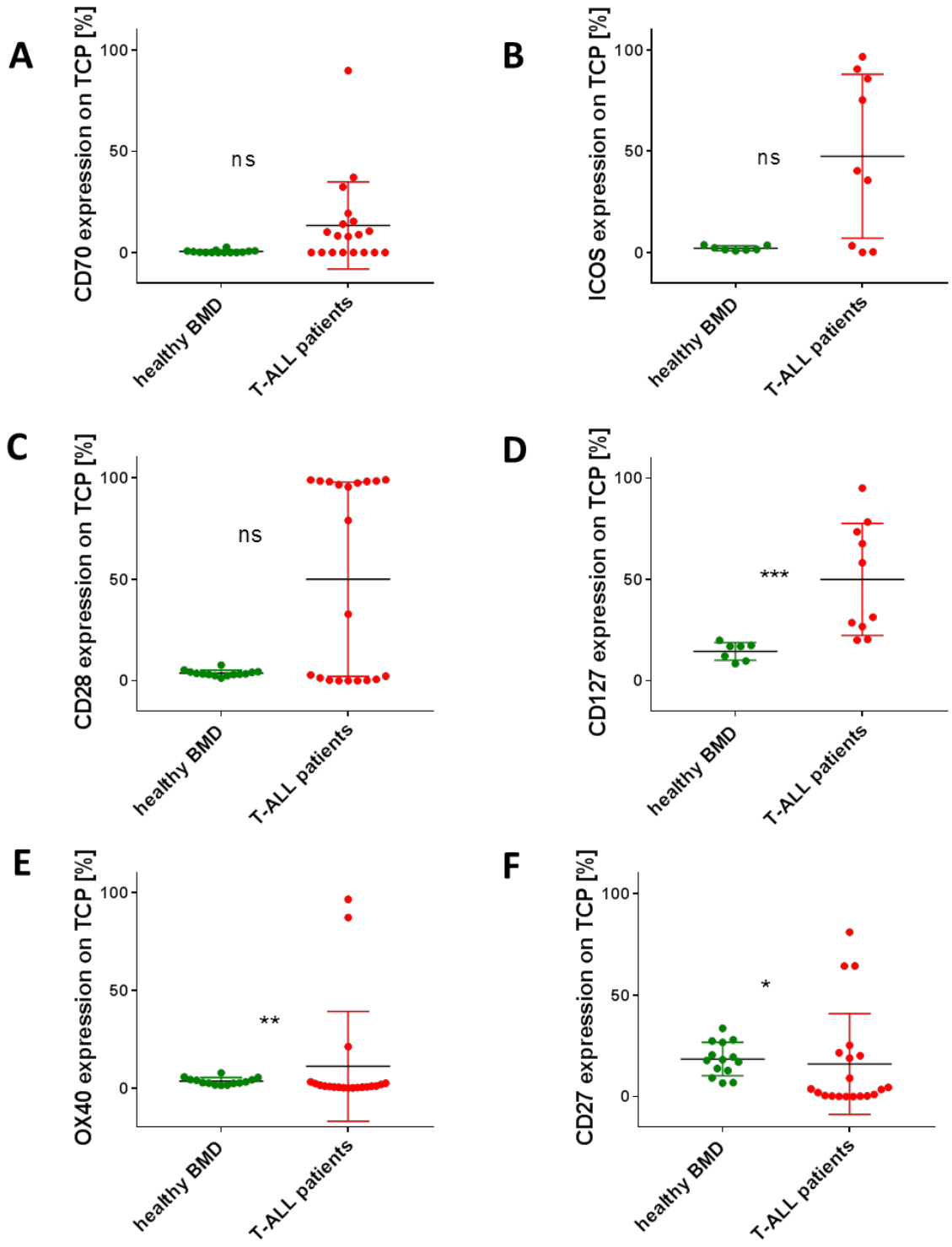

Figure 21: Upregulation of co-stimulatory molecules on T-cell progenitors of pediatric T-ALL patients at initial diagnosis (n=9-20) in comparison to healthy BM donors (n=7-14): The graph emerged from the same data set as Figure 20. A significant upregulation was observed for **F)** CD127 (p=0.001) and **E)** OX40 (p=0.0049). **A)** CD28 (ns), **C)** ICOS (ns) and **D)** CD70 (ns) were higher expressed on TCP of T-ALL patients but not significantly. **B)** Although CD27 was slightly overexpressed in healthy TCP (p=0.0388), three out of 20 T-ALL patients showed a CD27 expression level >50% on TCP. For that reason, CD27 was included in this figure. *TCP = T-cell progenitors, healthy BMD = healthy BM/bone marrow donors, ns = not significant.*

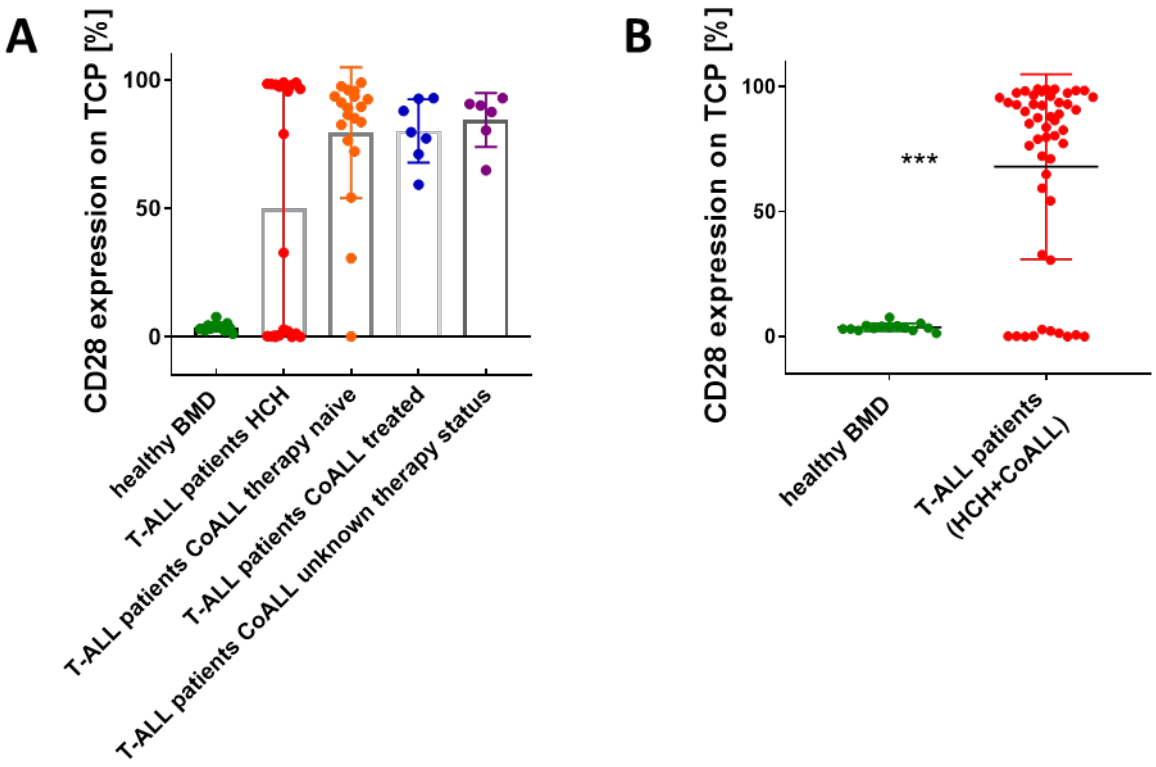

Figure 22: CD28 expression on T-cell progenitors of pediatric T-ALL patients and healthy BM donors (n=14): Data regarding T-ALL patients of the HCH hospital (n=20) and the CoALL study (therapy naïve: n=19, treated: n=7, therapy status unknown: n=6) was analyzed. The data regarding healthy BM donors and HCH T-ALL patients emerged from the same data set as Figure 20. **A)** T-ALL patients of the HCH showed CD28 expression levels >50% on leukemic blasts in 38 out of 50 cases. Within the CoALL cohort 17/19 therapy naïve patients, 7/7 treated patients and 6/6 patients with unknown therapy status showed expression levels >50%. **B)** After integration of the data (HCH and CoALL cohort) statistical testing confirmed a significant overexpression of CD28 on the TCP of pediatric T-ALL patients compared to the healthy control (p=0.0003). Two patient samples were measured in both cohorts. For integrated analysis the CoALL expression level was put aside. *HCH = Hauner children´s hospital, TCP = T-cell progenitors, healthy BMD = healthy BM/bone marrow donors.*

	CD28	CD27	OX40	CD70	ICOS	CD127	n of markers with expression levels > 50 %
B002	98,1	19,0	0,0	0,0			1
B003	2,9	64,4	0,7	8,2			1
B004	99,0	1,0	0,2	0,0			1
B005	97,4	4,5	0,4	0,0			1
B006	99,1	21,6	87,4	19,3			2
B007	95,6	20,1	2,4	0,0			1
B008	32,8	3,8	96,7	10,6			1
B009	96,6	1,9	0,1	0,0			1
B010	98,2	64,4	1,8	10,1			2
B011	2,3	0,2	21,2	15,4			0
B012	0,0	0,3	1,0	32,4	90,5	78,3	2
B013	0,6	0,5	0,5	89,9	35,6	58,2	2
B014	0,2	0,0	2,2	37,1	0,2	28,7	0
B015	0,0	0,2	0,6	7,9	75,3	73,5	2
B016	0,0	3,5	0,0	8,8	0,0	20,4	0
B301	98,5	0,0	0,3	0,0	85,7	67,6	3
B302	79,0	0,1	0,9	14,1	3,2	26,8	1
B303	98,5	81,1	0,9	0,0	40,3	31,4	2
B304	1,4	25,3	1,4			20,0	0
B305	0,3	9,1	3,1	0,0	96,6	95,1	2
B401	94,9	0,6	0,2	0,0	0,4	14,9	1
B402	52,8	64,7	0,2	17,8	14,1	37,4	2
B405	93,4	4,4	0,6	0,7	92,4	55,5	3
B502	5,7	14,0	0,1	2,0	2,3	16,8	0

Expression > 80%
Expression > 50%
Expression > 20%
Expression > 5%
Expression > 2%
Expression < 2%

sample at initial diagnosis, no future relapse
sample at initial diagnosis, future relapse
sample at time of relapse (1st/2nd)
markers not measured for this sample

Table 5: Expression of co-stimulatory molecules on leukemic T-ALL blasts of pediatric T-ALL patients at initial diagnosis (n=20) and 1st (n=3) and 2nd (n=1) relapse: The table emerged from the same data set as Figure 20. The first column shows the respective patient samples. Columns two to eight represent the expression levels of checkpoint molecules in [%] (from left to right: CD28, CD27, OX40, CD70, ICOS and CD127). The presented samples were taken at initial diagnosis (no future relapse or future relapse) and at time of 1st (4XX) or 2nd (5XX) relapse. For better visualization, expression levels were color coded (see legend). Column 8 shows the sum of co-stimulatory markers for a respective patient that was expressed higher than the elected cut-off 50%: 9/24 samples were strongly positive for one marker, 8/24 for two markers and 2/24 for three markers. 5/24 samples contained leukemic blasts that did not express any of the depicted markers at more than 50%. Some markers were only measured for part of the samples due to changes in the antibody selection used for sample measurement. No statements were made regarding the not measured checkpoints for those samples (marked grey).

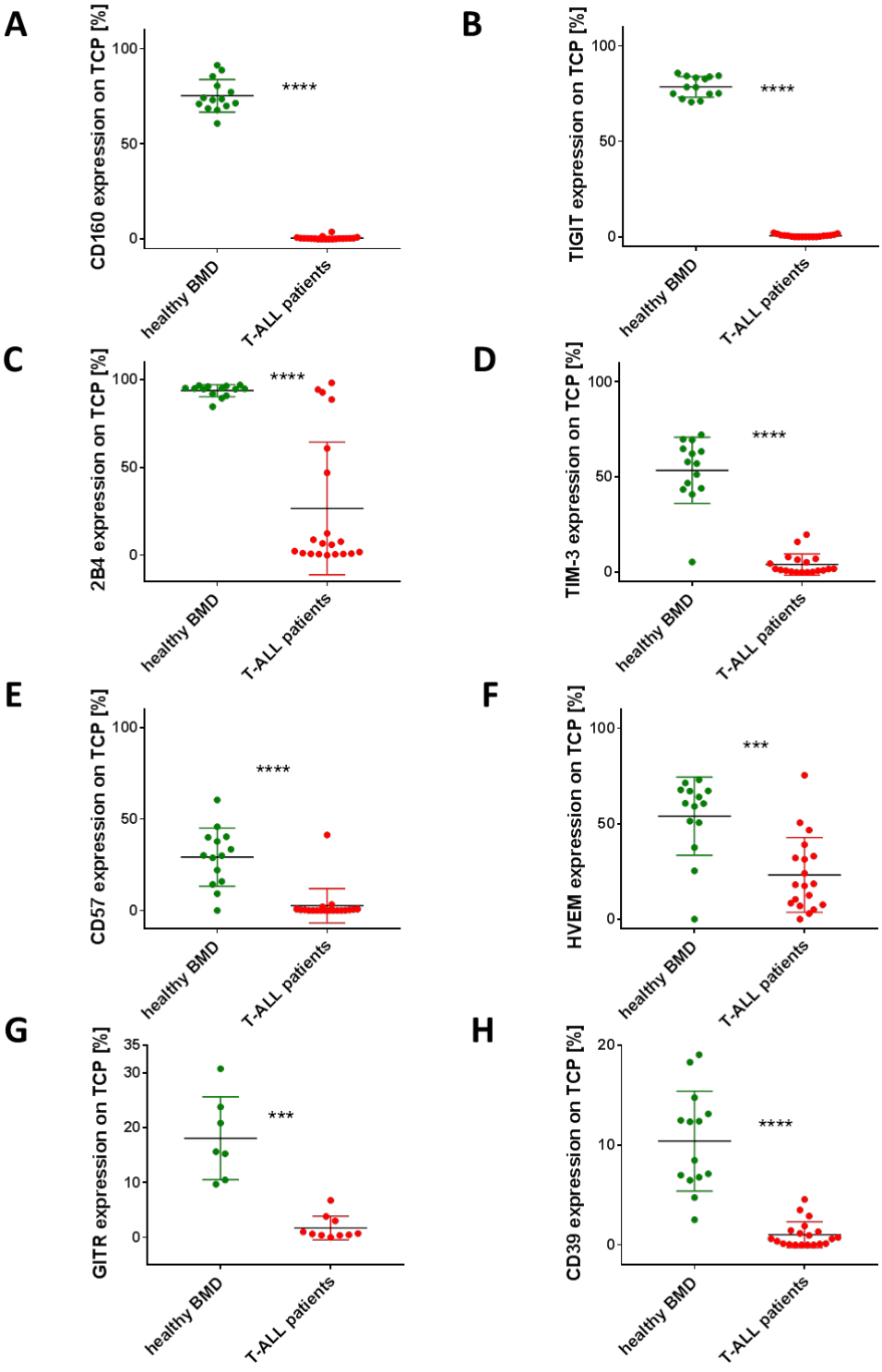

Figure 23: Downregulation of co-inhibitory markers on T-cell progenitors of pediatric T-ALL patients (n=20) compared to healthy BM donors (n=14): The graph emerged from the same data set as Figure 20. **A)** CD160 ($p<0.0001$), **B)** TIGIT ($p<0.000$), **C)** 2B4 ($p<0.0001$), **D)** TIM-3 ($p<0.0001$), **E)** CD57 ($p<0.0001$), **F)** HVEM ($p=0.0005$), **G)** GITR ($p=0.0001$) and **H)** CD39 ($p<0.0001$) were significantly downregulated on TCP of pediatric T-ALL patients compared to the healthy control. *TCP = T-cell progenitors, healthy BMD = healthy BM/bone marrow donor.*

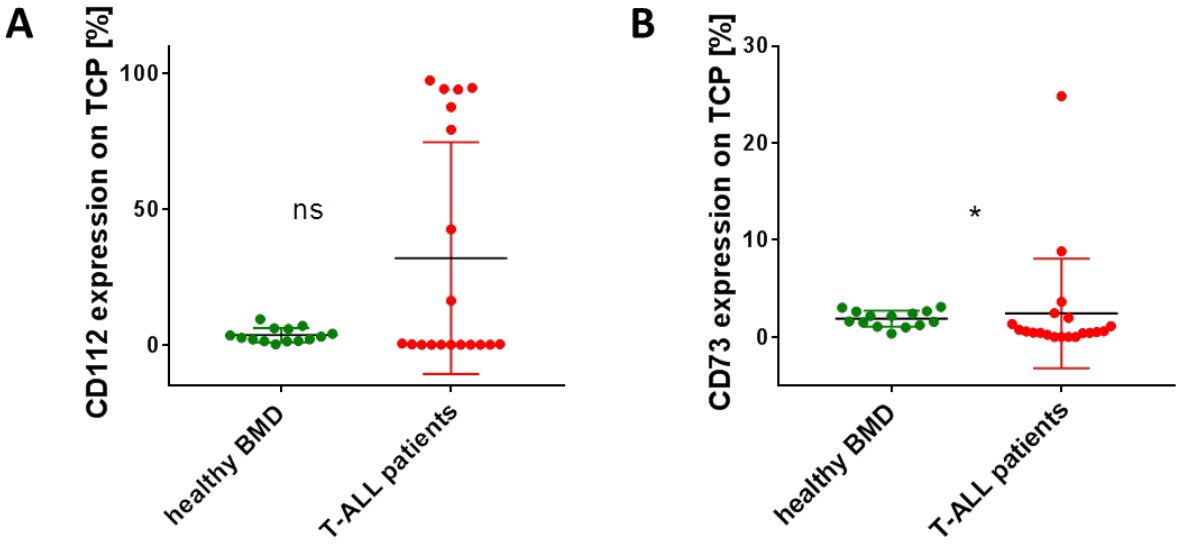

Figure 24: Upregulation of other markers on T-cell progenitors of pediatric T-ALL patients compared to healthy BM donors: The graph emerged from the same data set as Figure 20. **A)** CD112 was higher expressed on T-ALL TCP compared to healthy BM donors (ns). **B)** The upregulation of the co-inhibitory marker CD73 was significantly increased on T-ALL patient´s TCP (p=0.0199). *TCP = T-cell progenitors, healthy BMD = healthy BM/bone marrow donor, ns = not significant.*

8.2.2.3. TRBC1 is not expressed on T-ALL leukemic blasts

TRBC1 has been described as a potential target for synthetic immunotherapy as some T-cell malignancies express homogenous TRBC1 (https://www.ncbi.nlm.nih.gov/pubmed/29131157). As this question has not been addressed in pediatric T-ALL, we analyzed both TCRα/β and TRBC1 surface expression on our cohort. For both healthy and leukemic TCP we could not detect any relevant expression of either TCRα/β or TRBC1 by flow cytometry (Figure 25A+B). Only five samples showed homogenous TCRα/β expression and of those, only two samples expressed about TRBC1 in about 30% of leukemic TCPs (Figure 25C).

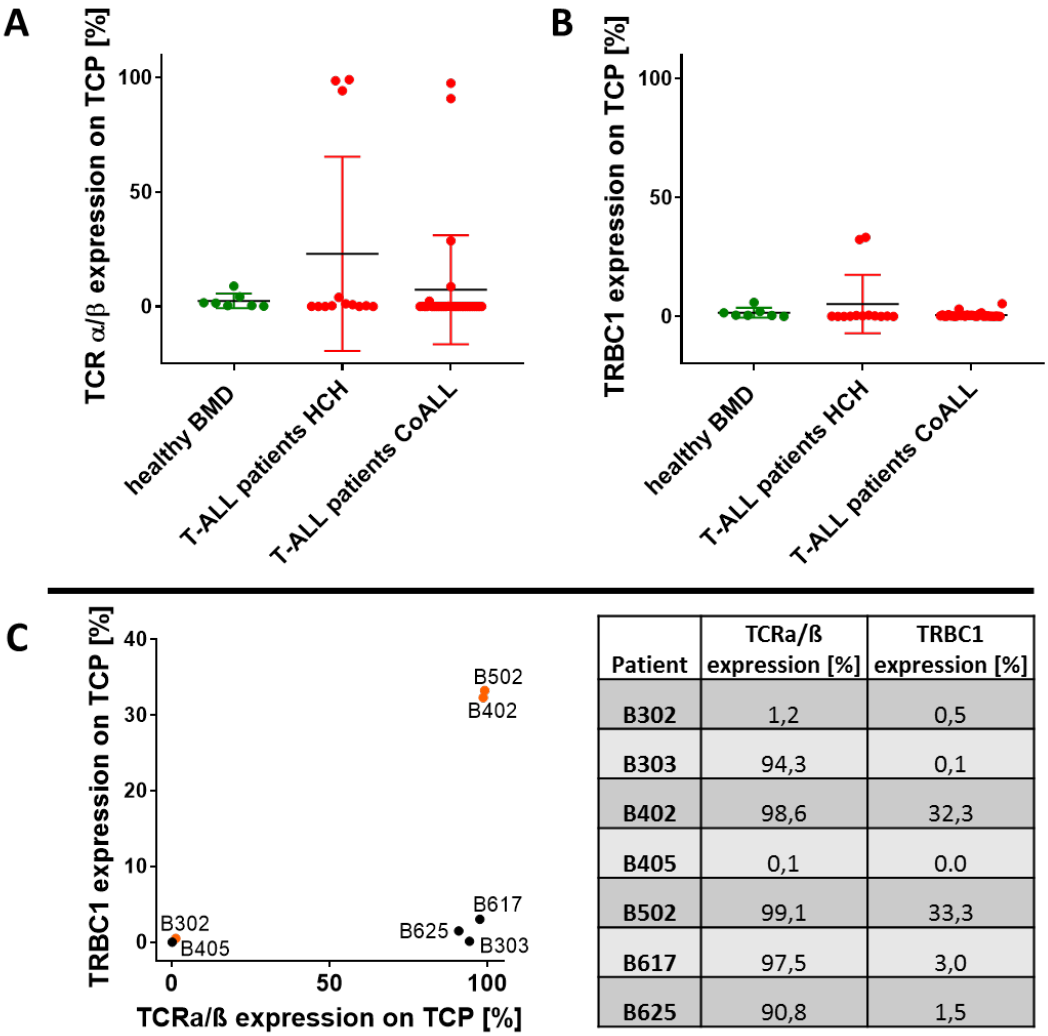

Patient	TCRa/ß expression [%]	TRBC1 expression [%]
B302	1,2	0,5
B303	94,3	0,1
B402	98,6	32,3
B405	0,1	0.0
B502	99,1	33,3
B617	97,5	3,0
B625	90,8	1,5

Figure 25: TRBC1 and TCRα/β expression on T-cell progenitors of pediatric T-ALL patients from the Hauner children´s hospital (n=9) and the CoALL study (n=31) and healthy BM donors (n=7): A) TCRα/β was not expressed on TCP of healthy BM donors (mean: 2.5 %). TCRα/β expression on TCP of pediatric T-ALL patients was negative except from five cases with an expression level higher than 5% (mean HCH: 23.0 %; mean CoALL: 7.4 %). **B)** TRBC1 was not expressed on healthy BM donors (mean: 1.5 %) and T-ALL patients (mean HCH: 5.2 %; mean CoALL: 0.5 %). Due to the low count of cases with a clearly positive TCP population for TRBC1 or TCRα/β, no statistical analysis was performed. **C)** 37 T-ALL patients expressed no TCRα/β, 40 patients no TRBC1 (B405 representative for majority of pediatric T-ALL patients). However, some patients showed TCRα/β expression. At initial diagnosis, B302 expressed no TCRα/β and no TRBC1. At the time of the 1st (B402) and 2nd (B502) relapse, TCRα/β expression was at 98.6% (1st relapse) and 99.1% (2nd relapse), TRBC1 expression at 32.3% (1st relapse) and 33.3% (2nd relapse). B625, B617 and B303 showed TCRα/β expression levels above 90% on the surface but no TRBC1 expression. *HCH = Hauner children´s hospital, TCP = T-cell progenitors, healthy BMD = healthy BM/bone marrow donors.*

All p values of the previous chapters are uncorrected. Multiple testing correction was performed according to the Original FDR method of Benjamini and Hochberg (subchapter 7.9.1). Figure 26 shows an overview of uncorrected p values and corrected p values (q values) for the BM populations CD4+ bmT cells, CD8+ bmT cells and TCP of T-ALL patients and healthy BM donors. P values of the CoALL study were not corrected.

A

Antigen	p value	q value
PD-1	0.2142	0.3392
2B4	0.0119	0.0528
LAG-3	0.081	0.208
CD57	0.0139	0.0528
TIM-3	0.0025	0.0222
TIGIT	0.1139	0.208
ICOS	0.1077	0.208
BTLA	0.4605	0.5528
HVEM	0.529	0.5528
CD28	0.0035	0.0222
GITR	0.5528	0.5528
CD27	0.0018	0.0222
OX40	0.2783	0.4067
PD-L1 ec	0.5056	0.5528
CD73	0.4177	0.5528
CD39	0.1132	0.208
CD127	0.1088	0.208
PDL-1 ic	0.4769	0.5528
CTLA-4 ic	0.1204	0.208

B

Antigen	p value	q value
CD160	0.3362	0.5371
PD-1	0.6165	0.7809
2B4	0.1122	0.2588
LAG-3	0.0165	0.1045
CD57	0.06	0.19
TIM-3	0.0012	0.0228
TIGIT	0.3037	0.5371
ICOS	0.0033	0.0314
BTLA	0.3392	0.5371
HVEM	0.5056	0.739
CD28	0.1226	0.2588
GITR	0.6142	0.7809
CD27	0.0969	0.2588
PD-L1 ec	0.7807	0.8241
CD73	0.0361	0.1372
CD39	0.7602	0.8241
CD127	0.7396	0.8241
PDL-1 ic	0.9356	0.9356
CTLA-4 ic	0.0276	0.1311

C

Antigen	p value	q value
CD160	0.0001	0.0003
PD-1	0.1315	0.1644
2B4	0.0001	0.0003
LAG-3	0.3785	0.4114
CD57	0.0001	0.0003
TIM-3	0.0001	0.0003
TIGIT	0.0001	0.0003
ICOS	0.1142	0.1586
BTLA	0.0041	0.0085
HVEM	0.0005	0.0011
CD112	0.5268	0.5268
CD28	0.5167	0.5268
GITR	0.0001	0.0003
CD27	0.0388	0.0647
OX40	0.0049	0.0094
CD40	0.0001	0.0003
PD-L1 ec	0.0882	0.1297
CD86	0.0725	0.1133
CD70	0.1266	0.1644
CD73	0.0199	0.0355
CD39	0.0001	0.0003
CD25	0.0001	0.0003
CD127	0.0001	0.0003
PDL-1 ic	0.2993	0.3401
CTLA-4 ic	0.1398	0.1664

Figure 26: Corrected (q values) and uncorrected p values for analysis of CD4+ bmT cells (A), CD8+ bmT cells (B) and T-cell progenitors (C) in pediatric T-ALL patients compared to healthy BM donors. Multiple testing correction was performed by using the Original FDR method of Benjamini and Hochberg**.** P values of the CoALL study were not corrected.

8.3. Flow cytometric analysis: T-ALL at initial diagnosis vs. T-ALL at time of relapse

To analyze changes in both bmT cell and leukemic TCP phenotype in the course of T-ALL relapse, we compared flow cytometry data from primary and relapse time points of T-ALL patients. Due to n≤3 for the relapse group, no statistical analysis was performed for this subchapter. The following figures focus on giving an overview of the expression FC and absolute expression levels of a variety of immune modulatory molecules on/in CD4+ bmT cells (Figure 27), CD8+ bmT cells (Figure 28) and leukemic T-ALL blasts (Figure 29).

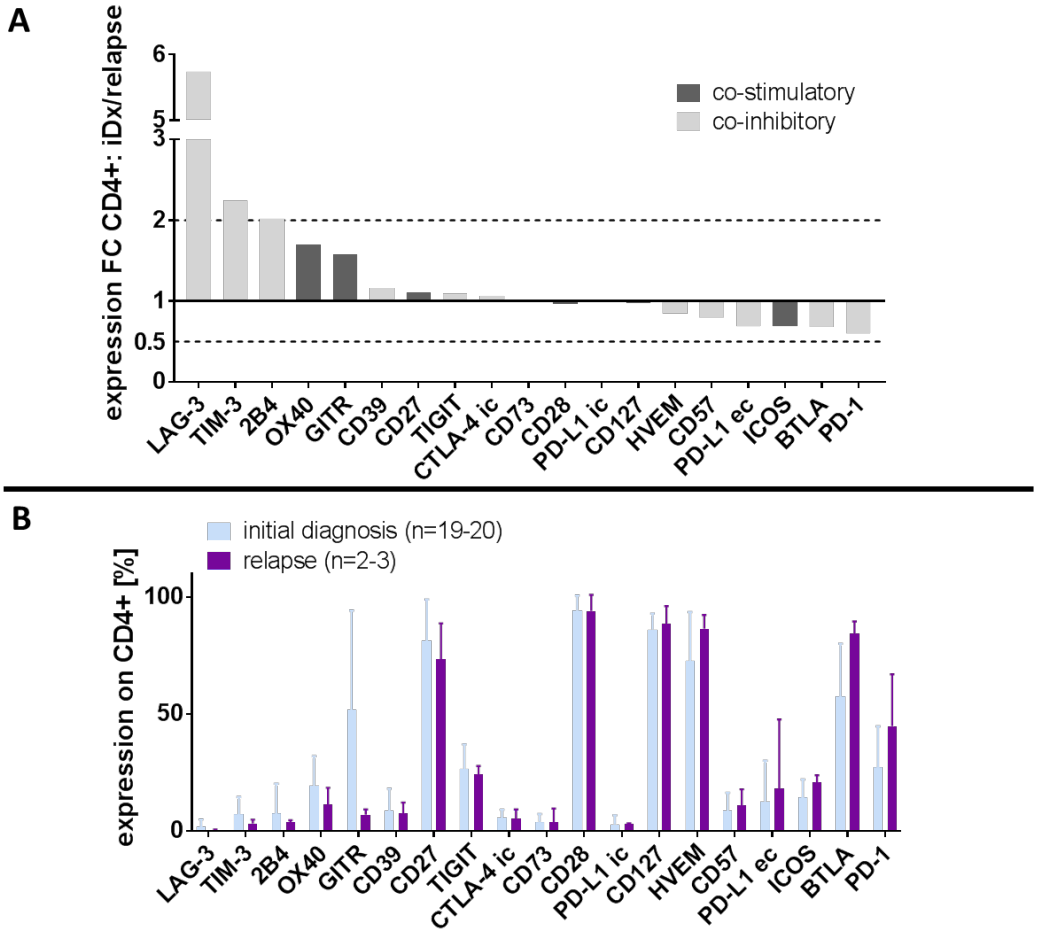

Figure 27: Expression of co-stimulatory and co-inhibitory molecules on CD4+ bmT cells in the BM of T-ALL patients at initial diagnosis (n=9-20) and relapse (n=2-3): A) Expression fold change on CD4+ bmT cells: mean expression at initial diagnosis/mean expression at relapse. **B)** The absolute expression levels of immune modulatory molecules on CD4+ bmT cells were arranged according to A. Markers with an absolute expression level <1% of CD4+ bmT cells in both groups were excluded from analysis due to high fold changes without evident biological relevance. CTLA-4 ic and PD-L1 ic were stained intracellularly. *No statistical tests were performed between the two groups due to the low number of relapse samples (n=2-3). iDx = initial diagnosis, ec = extracellular, ic = intracellular.*

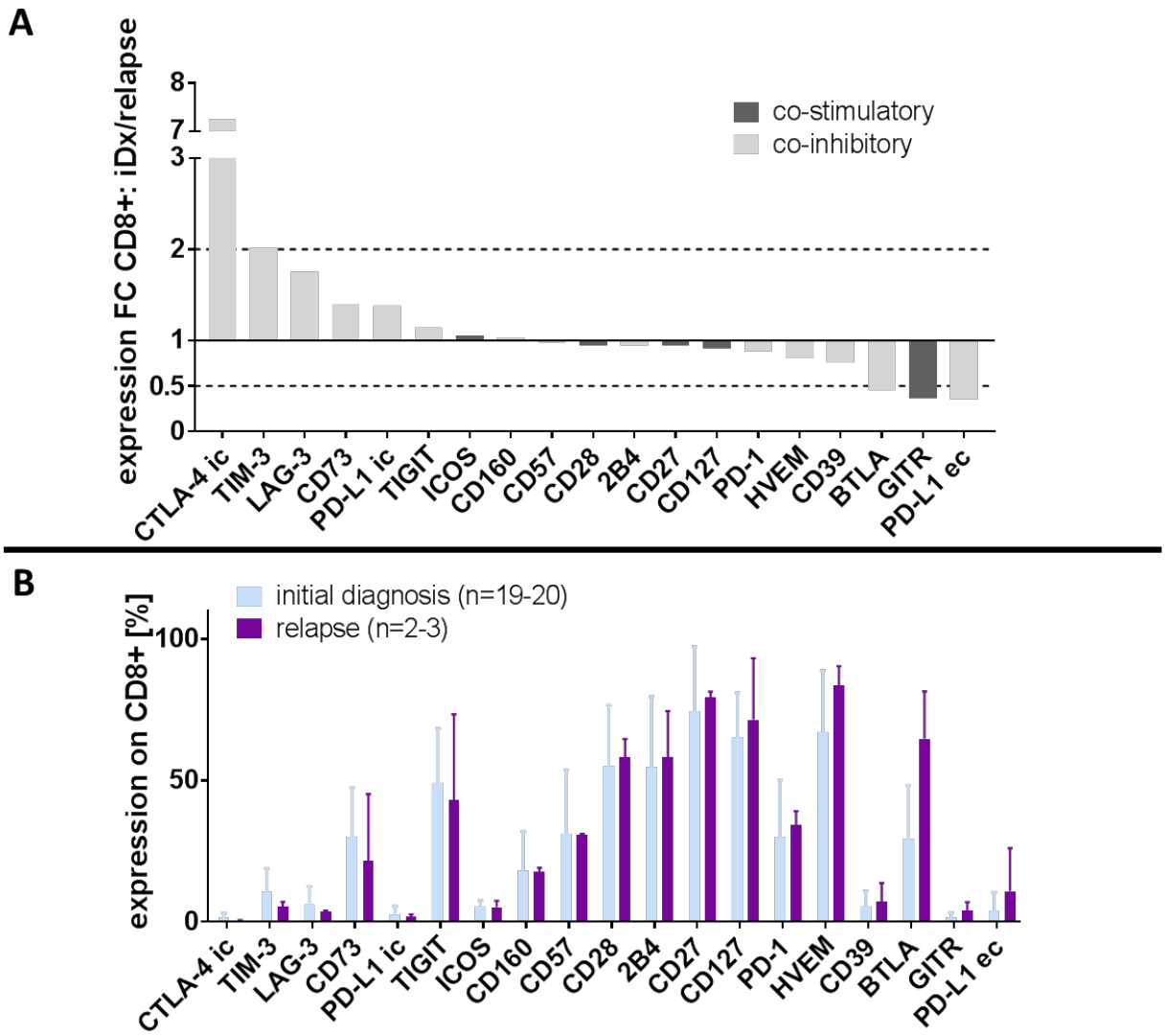

Figure 28: Expression of co-stimulatory and co-inhibitory molecules on CD8+ bmT cells in the BM of T-ALL patients at initial diagnosis (n=9-20) and relapse (n=2-3): A) Expression fold change on CD8+ bmT cells: mean expression at initial diagnosis/mean expression at relapse. **B)** The absolute expression level of immune modulatory molecules on CD8+ bmT cells were arranged according to A. Markers with an absolute expression level <1% of CD8+ bmT cells in both groups were excluded from analysis due to high fold changes without evident biological relevance. CTLA-4 ic and PD-L1 ic were stained intracellularly. *No statistical tests were performed between the two groups due to the low number of relapse samples (n=2-3). iDx = initial diagnosis, ec = extracellular, ic = intracellular.*

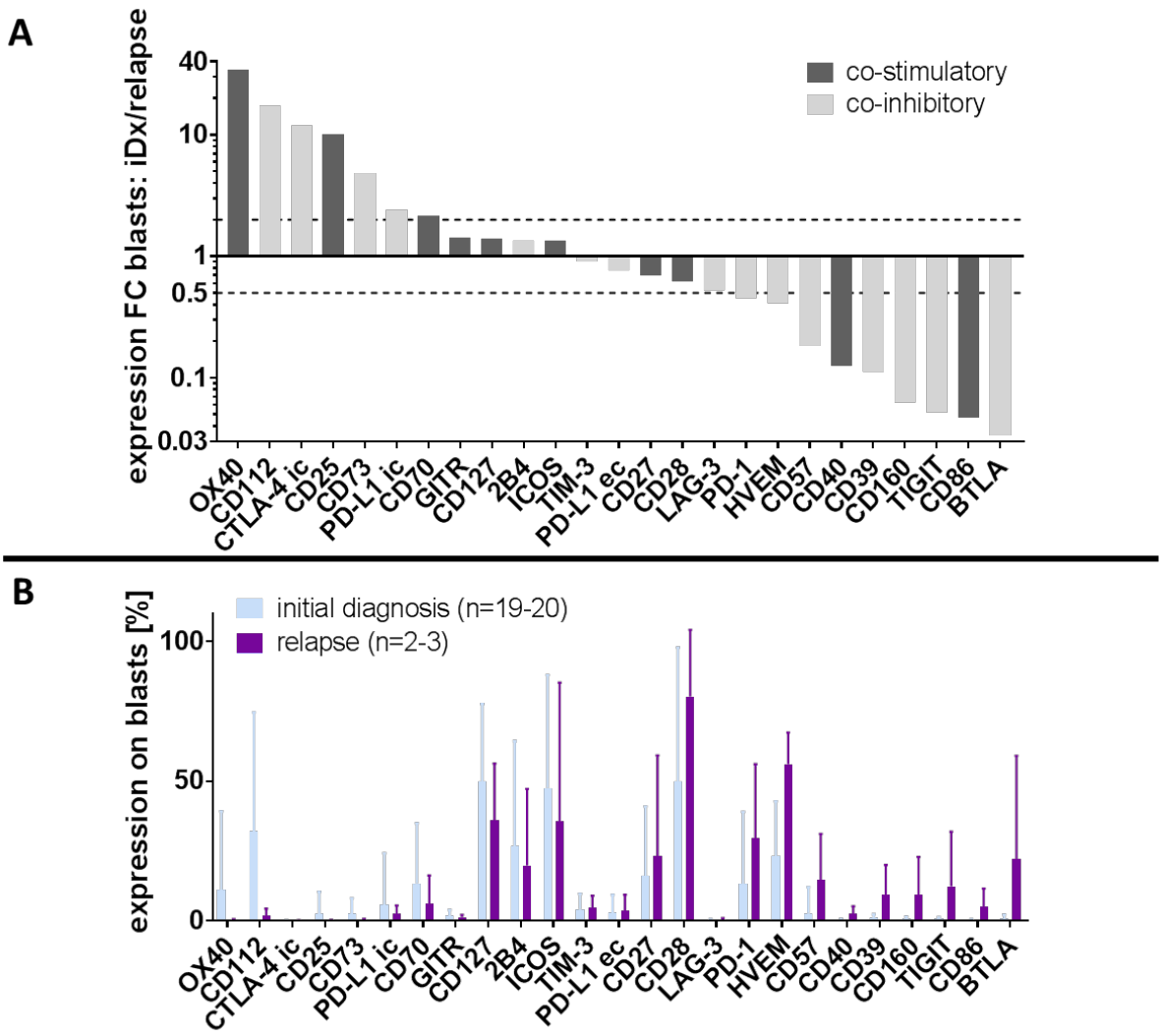

Figure 29: Expression of co-stimulatory and co-inhibitory molecules on leukemic blasts in the BM of T-ALL patients at initial diagnosis (n=9-20) and relapse (n=2-3): A) Expression fold change on leukemic blasts: mean expression at initial diagnosis/mean expression at relapse. **B)** The absolute expression levels of immune modulatory molecules on TCP were arranged according to A. CTLA-4 ic and PD-L1 ic were stained intracellularly. *No statistical tests were performed between the two groups due to the low number of relapse samples (n=2-3). iDx = initial diagnosis, ec = extracellular, ic = intracellular.*

8.4. Flow cytometric analysis: no future relapse T-ALL at initial diagnosis vs. future relapse T-ALL at initial diagnosis

The HCH T-ALL samples at initial diagnosis of no future relapse (n=15) and future relapse (n=5) patients were used as a detection cohort. T-ALL samples provided by the CoALL study center were taken at initial diagnosis of no future relapse (n=28) and future relapse patients (n=6). The CoALL samples were used as validation cohort. The expression pattern of co-stimulatory and co-inhibitory molecules on CD4+ and CD8+ bmT cells and TCP was assessed and evaluated. Since this subchapter exclusively shows data of pediatric T-ALL patients, all TCP are referred to as leukemic T-ALL blasts.

8.4.1. Limited integration of data from Hauner children´s hospital and CoALL study due to different freezing routines, storage conditions and sample heterogeneity

The samples from the CoALL study were processed differently than the HCH samples of T-ALL patients as well as of healthy BM donors. After processing, CoALL samples were stored at -80°C compared to the HCH samples that were stored in liquid nitrogen. CoALL samples were collected from different children´s hospitals in Germany and sent to the study center in Hamburg. All HCH samples were obtained and processed in the HCH. CoALL samples showed heterogeneity regarding cell count and cell viability.

Due to the differences in freezing routines and storage conditions, fold changes were evaluated within and between the following groups for a better understanding of comparability of subgroups within the CoALL cohort as well as the HCH (detection) cohort with CoALL (validation) cohort:

1) CoALL samples (therapy naïve) vs. CoALL samples (treated)
2) CoALL samples (therapy naïve) vs. HCH samples (therapy naïve)

For both comparisons, T-ALL samples at initial diagnosis were evaluated regarding their checkpoint expression. The results are represented in Figure 30 and Figure 31.

Figure 32 shows the impact of therapeutic intervention on the expression level of ICOS and OX40 on the surface of CD4+ bmT cells as well as differences in absolute checkpoint expression levels between HCH samples and CoALL samples. Data of healthy BM donors is presented as reference. ICOS expression on CD4+ bmT cells was increased in HCH T-ALL patients compared to the healthy control. A decrease was observed when comparing therapy naïve T-ALL patients from the HCH with the COALL cohort. A further downregulation on CoALL T-ALL samples could be detected in the course of therapy (therapy naïve vs. treated). OX40 expression on CD4+ bmT cells was increased for HCH T-ALL patients compared to the healthy control. However, OX40 expression was decreased on therapy naïve CoALL T-ALL patients compared to therapy naïve patients of the HCH cohort. Under therapy an upregulation was observed within the CoALL cohort (therapy naïve vs. treated). No statistical analysis was performed.

As we have documented altered bmT cells as a result of T-ALL leukemia, we wanted to determine whether these changes reflect patient prognosis (Table 6). Thus, we set up a filtering process using both data from our discovery cohort (HCH) and validation cohort (CoALL) to identify surface markers suitable for integrated analysis regarding T-ALL relapse by Kaplan-Meier analysis:

1) The trend towards down-/upregulation was comparable in the HCH and CoALL cohort
2) Absolute difference of immune checkpoint expression between groups of comparison (CoALL therapy naive vs. CoALL treated; HCH vs. CoALL therapy naïve) was >1%

3) The mean absolute expression level of the respective marker was >1 % in both cohorts (HCH and CoALL) and both groups within the cohorts (no future relapse vs. future relapse)
4) Kaplan Meier estimates showed significant differences in at least one group comparison of no future relapse patients with future relapse patients (groups: HCH, CoALL, HCH+CoALL)

As some markers showed robust surface expression, we performed combined analysis of both HCH and CoALL samples for the following surface markers in chapter 6.2: CD7, CD4, CD8, CD28, TRBC1, TCRα/β.

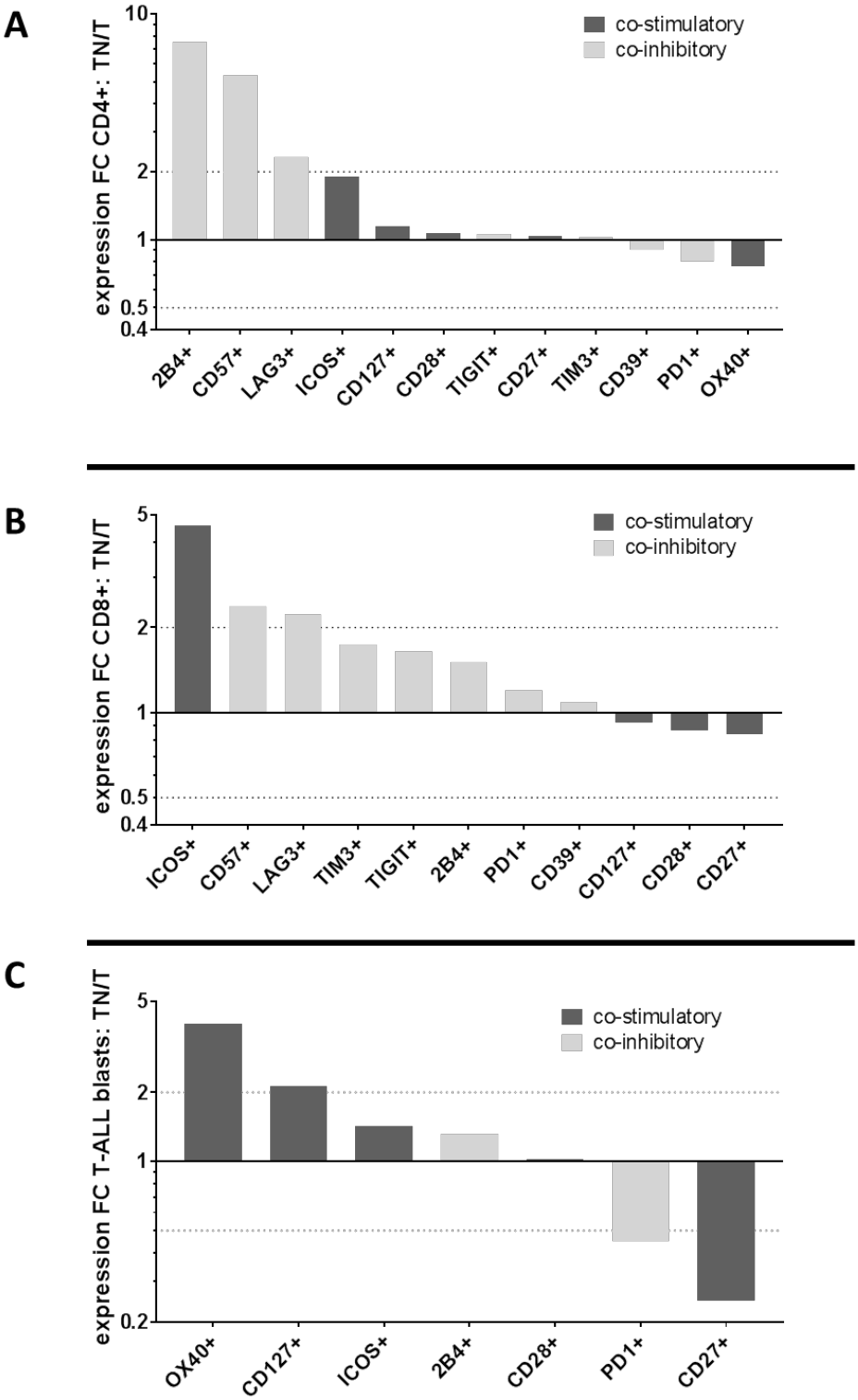

Figure 30: Expression fold change of co-stimulatory and co-inhibitory molecules on CD4+ bmT cells, CD8+ bmT cells and leukemic blasts of therapy naïve (n=18-20) and treated (n=6-7) CoALL T-ALL patients: mean expression of therapy naïve CoALL patients/mean expression of treated CoALL T-ALL patients. **A)** Expression FC of co-stimulatory and co-inhibitory markers on CD4+ bmT cells. **B)** Expression FC of co-stimulatory and co-inhibitory markers on CD8+ bmT cells. **C)** Expression of co-stimulatory and co-inhibitory markers on leukemic T-ALL blasts. *FC = fold change, blasts = leukemic T-ALL blasts, TN = therapy naïve CoALL T-ALL patients, T = treated CoALL T-ALL patients.*

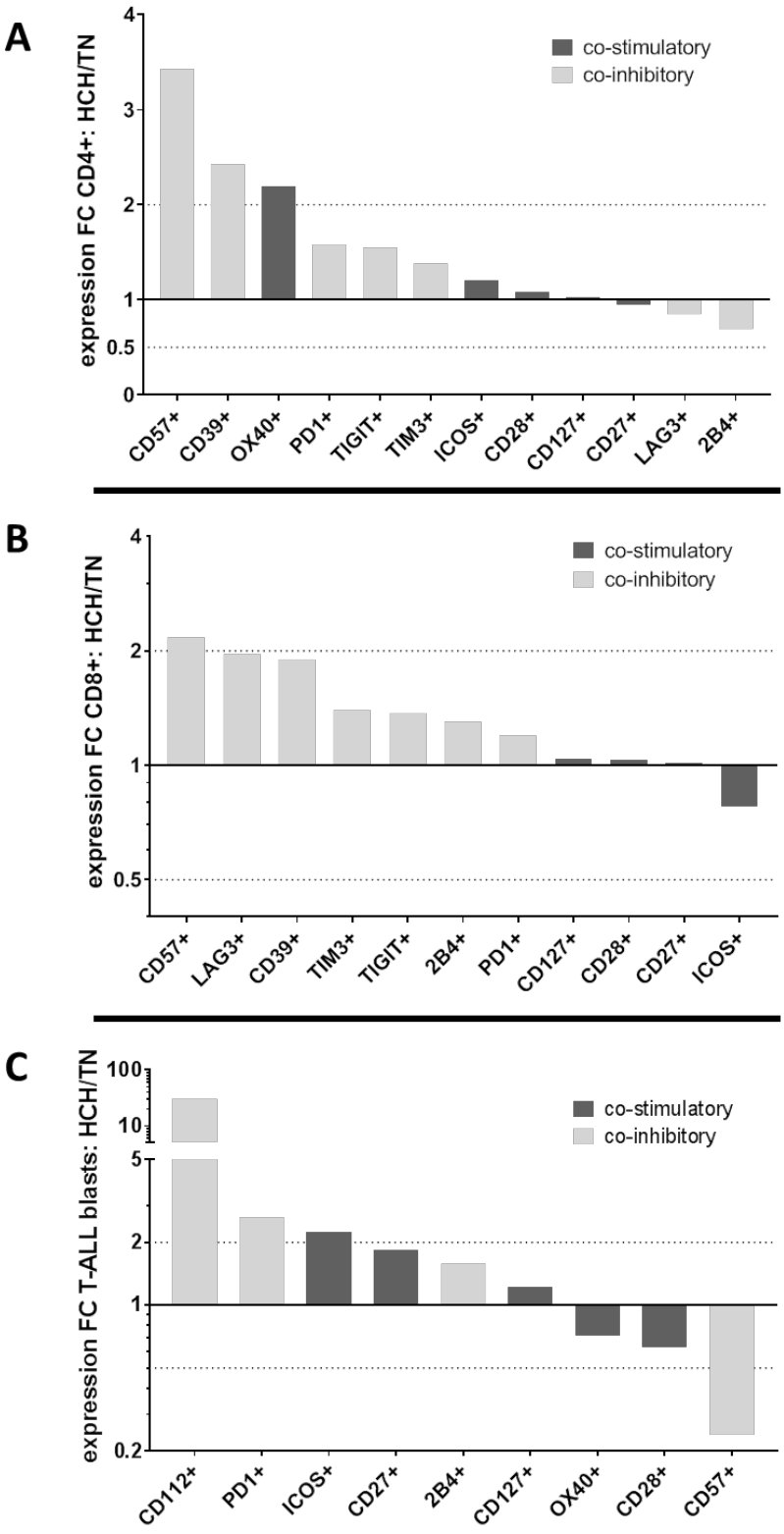

Figure 31: Expression fold change of co-stimulatory and co-inhibitory molecules on CD4+ bmT cells, CD8+ bmT cells and leukemic T-ALL blasts of the Hauner children´s hospital (n=9-20) and therapy naïve CoALL (n=18-20) T-ALL patients: mean expression of HCH T-ALL patients/ mean expression of therapy naïve CoALL T-ALL patients. **A)** Expression FC of co-stimulatory and co-inhibitory markers on CD4+ bmT cells. **B)** Expression FC of co-stimulatory and co-inhibitory markers on CD8+ bmT cells. **C)** Expression of co-stimulatory and co-inhibitory markers on leukemic T-ALL blasts. *HCH = Hauner children´s hospital, FC = fold change, TN = therapy naïve CoALL T-ALL patients.*

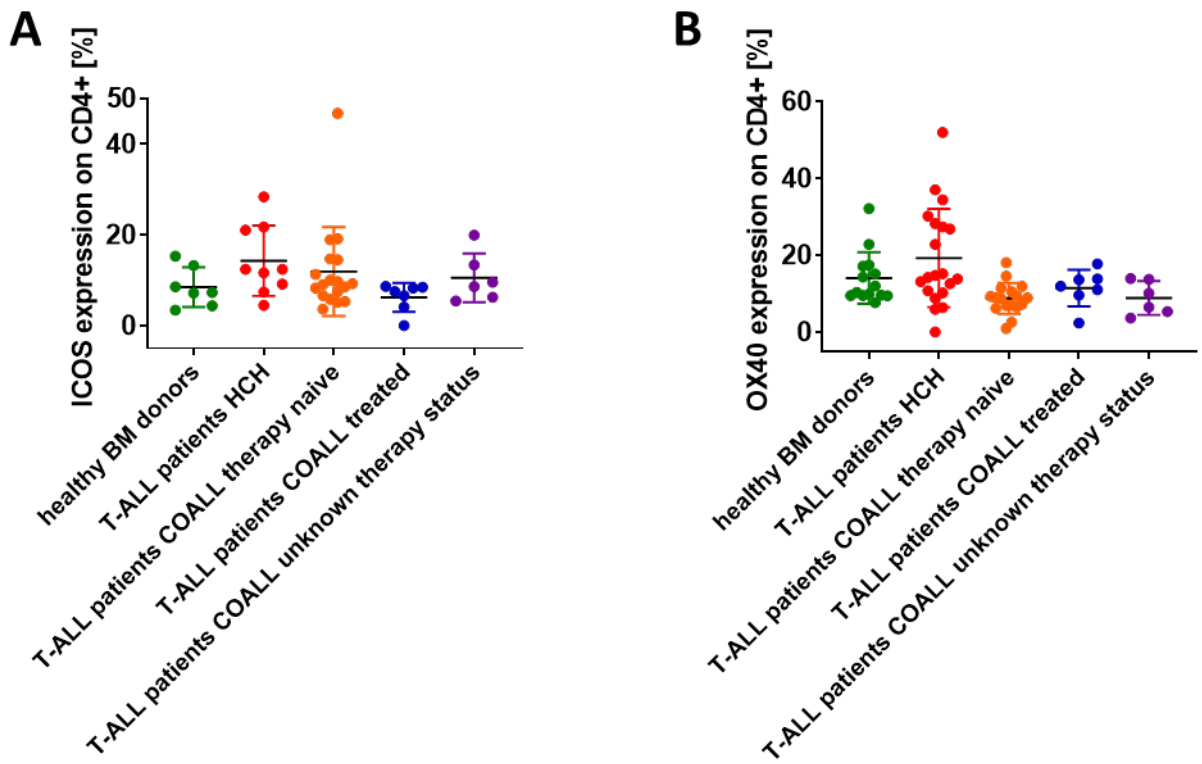

Figure 32: Impact of clinical treatment, different freezing routines and storage conditions on the expression of co-stimulatory molecules ICOS and OX40 on CD4+ bmT cells: Data of healthy BM donors (n=7-14), HCH T-ALL patients (n=9-20) and CoALL T-ALL patients (therapy naïve: n=19, treated: n=7, therapy status unknown: n=6) was included. **A)** ICOS expression on CD4+ bmT cells was increased in HCH T-ALL patients compared to the healthy control. A decrease was observed when comparing therapy naïve T-ALL patients from the HCH with the COALL cohort. There was a further decrease in ICOS expression on CD4+ bmT cells in those COALL samples that received therapy prior to sampling. **B)** OX40 expression on CD4+ bmT cells was increased for HCH T-ALL patients compared to the healthy control. OX40 expression was decreased on therapy naïve CoALL T-ALL patients compared to therapy naïve patients of the HCH cohort. Within the CoALL group, there was a decrease of OX40 expression. No statistical analysis was performed. *HCH = Hauner children´s hospital.*

	HCH			CoALL			HCH+CoALL		
Antigene	CD4+	CD8+	blasts	CD4+	CD8+	blasts	CD4+	CD8+	blasts
CD57	↑	↓	↓	↑	↑*	↓			
PD-1	→	↓	↑*	↑	↑	↑			◊
TM-3	↑	↑	↑	↑	↑	→	◊	◊	
TIGIT	↓	↓*	↓	↑	↑	→			
2B4	↓	↓	↓	↑	↑	↑			
LAG-3	↓	↓*	→	↑	↑	ne			
CD70			↓			ne			
CD28	↓	↑	↑	→	↓	↓			
ICOS	↓	↓	↑	↑*	↑	↑			
OX40	↓	→	↓	↑	↓*	↓			
CD27	↓	→	↑	↓	↑	↑			
CD112			↓			ne			
CD39	↓	↓	↑	↑*	↑	→			
CD127	↑	↑	↓	↑	↓*	↓			

integrated analysis of HCH and CoALL data
no integrated analysis of HCH and CoALL data
not of interest on respective BM population
ne not expressed (expression < 1%)
↑ marker was higher expressed in future relapse T-ALL patients
↓ marker was lower expressed in future relapse T-ALL patients
* significant differential expression in future relapse vs. no future relapse
◊ significant effect on prognosis by Kaplan-Meier analysis

Table 6: Prognostic effect of surface marker expression on CD4+ bmT cells, CD8+ bmT cells and leukemic blasts in the discovery cohort (Hauner children´s hospital) and the validation cohort (CoALL): The table shows a variety of co-stimulatory, co-inhibitory and other surface molecules (first column) measured on three BM populations (CD4+ bmT cells, CD8+ bmT cells and blasts) of HCH samples (second column, discovery cohort) and CoALL samples (third column, validation cohort). For each immune checkpoint the impact on patient prognosis (that is: relapse or no relapse) was analyzed: ↑ indicates an upregulation of the marker on primary samples of those patients with future relapse in comparison to patients without future relapse, ↓ indicates the opposite. * marks a significant difference between no future relapse and future relapse using Mann-Whitney U test. The red-green color code shows the consequence for joined analysis (red = different trend, no integrated analysis; green = comparable trend, integrated analysis). Integrated analysis was only performed for markers showing concordant changes in both HCH and CoALL samples. These markers on respective populations are marked in green in the column "HCH + CoALL", Kaplan Meier curves were generated. Those that showed significant differences in relapse free survival of no future relapse and future relapse patients using the Log-rank test were marked with ◊ (detailed analysis in chapter 8.4.3). All CoALL samples were used under the assumption that if commutated changes could be observed despite therapy there is a biological relevance. *HCH = Hauner children´s hospital, BM = bone marrow.*

8.4.2. Evaluation of BM samples of no future relapse and future relapse T-ALL patients from the Hauner children´s hospital

A significant increase in the expression level of immune modulatory markers on CD4+ bmT cells of T-ALL patients without future relapse could be observed for CD73 (4.8 % vs. 1.5 %, mean values no future relapse vs. future relapse, p=0.0437), GITR (14.6 % vs. 7.4 %, p=0.0159) and HVEM (78.1 % vs. 52.7 %, p=0.0485) (Figure 33 & Figure 34).

CD8+ bmT cells of future patients expressed most of the markers measured to a lower extent than CD8+ bmT cells of no future relapse patients at initial diagnosis. A significant increase in the expression level on CD8+ bmT cells for T-ALL patients without future relapse could be observed for LAG-3 (7.5 % vs. 1.5 %, p=0.0415), CD160 (20.8 % vs. 10.5 %, p=0.0401) and TIGIT (54.1 % vs. 29.1 %, p=0.0366) (Figure 35 & Figure 36).

A significant increase in PD-1 expression on leukemic T-ALL blasts of patients without future relapse could be observed (5.1 % vs. 37.1 %, p=0.0467, Figure 37 & Figure 38).

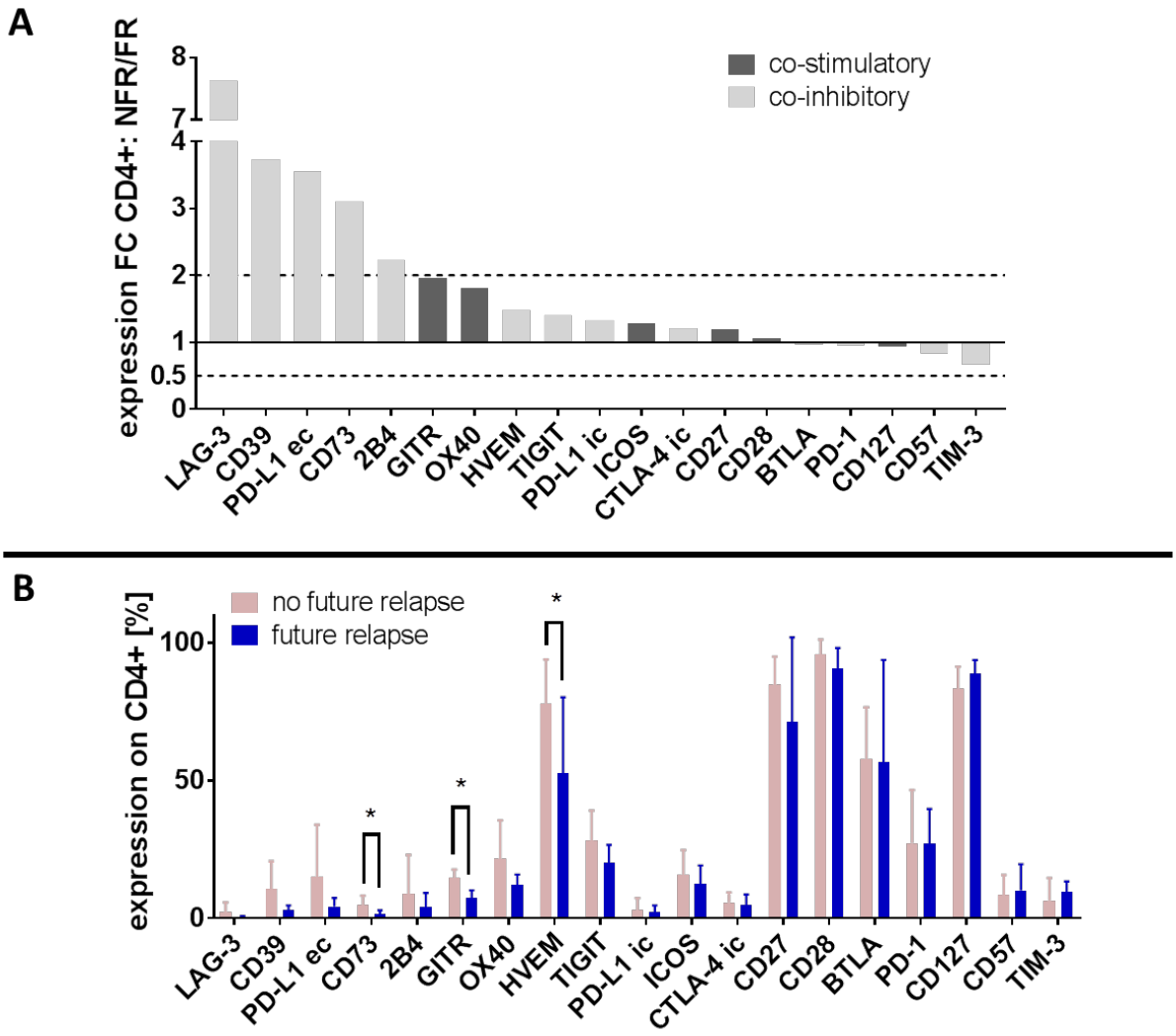

Figure 33: Expression of co-stimulatory and co-inhibitory molecules on CD4+ bmT cells of pediatric T-ALL patients of the Hauner children´s hospital without (n=5-15) and with future relapse (n=4-5) at initial diagnosis: A) Expression FC for CD4+ bmT cells: mean expression no future relapse/mean expression future relapse. **B)** The absolute expression of immune modulatory markers on CD4+ bmT cells is arranged according to A. CD4+ bmT cells of pediatric T-ALL patients without future relapse show a significantly increased expression of CD73 (p=0.0437), GITR (p=0.0159) and HVEM (p=0.0485). Markers with an expression level lower than 1% of CD4+ bmT cells in both groups were excluded from analysis due to high fold changes without biological relevance. *FC = fold change, NFR = no future relapse, FR = future relapse, ec = extracellular, ic = intracellular.*

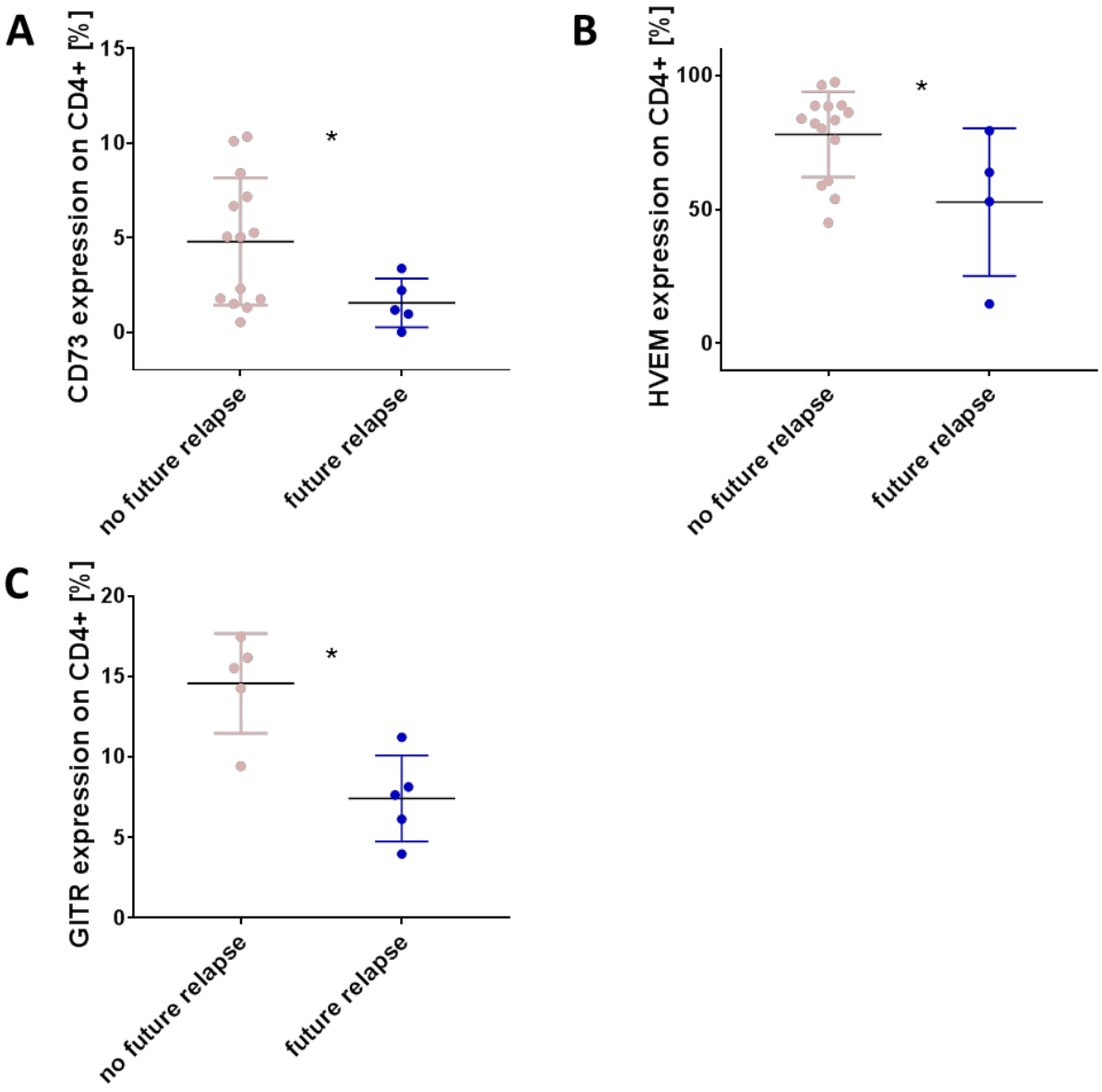

Figure 34: Expression of immune modulatory molecules on CD4+ bmT cells of patients of the Hauner children´s hospital without (n=5-15) and with future relapse (n=4-5) at initial diagnosis: The graphs show the same data set as Figure 33 in a different manner. Patients without future relapse expressed significantly higher levels of **A)** CD73 (p=0.0437), **B)** HVEM (p=0.0485) and **C)** GITR (p=0.0159).

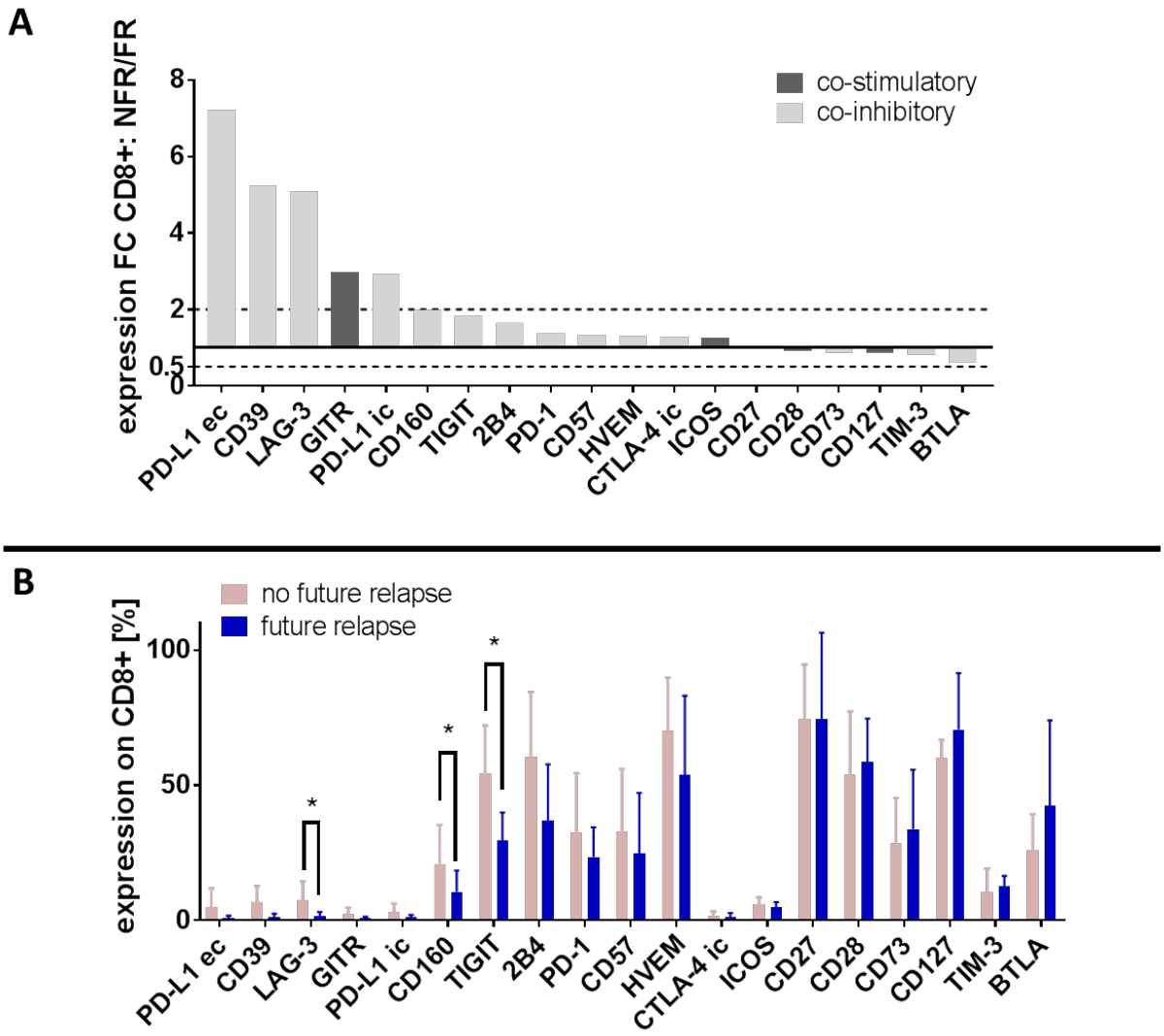

Figure 35: Expression of co-stimulatory and co-inhibitory molecules on CD8+ bmT cells of pediatric T-ALL patients of the Hauner children´s hospital without (n=5-15) and with future relapse (n=4-5) at initial diagnosis: A) Expression FC for CD8+ bmT cells: mean expression no future relapse/mean expression future relapse. The majority of markers showed an increased expression on CD8+ bmT cells of no future relapse T-ALL patients compared to future relapse patients. **B)** The absolute expression of immune modulatory markers on CD8+ bmT cells is arranged according to A. CD8+ bmT cells of pediatric T-ALL patients without future relapse show a significantly increased expression of LAG-3 (p=0.0415), CD160 (p=0.0401) and TIGIT (p=0.0366). Markers with an expression level lower than 1% of CD4+ bmT cells in both groups were excluded from analysis due to high fold changes without biological relevance. CD70 was significantly increased on future relapse T-ALL patient´s CD8+ bmT cells but excluded from this figure (p=0.0134) due to questionable relevance on T cells. FC = fold change, *NFR = no future relapse, FR = future relapse, ec = extracellular, ic = intracellular.*

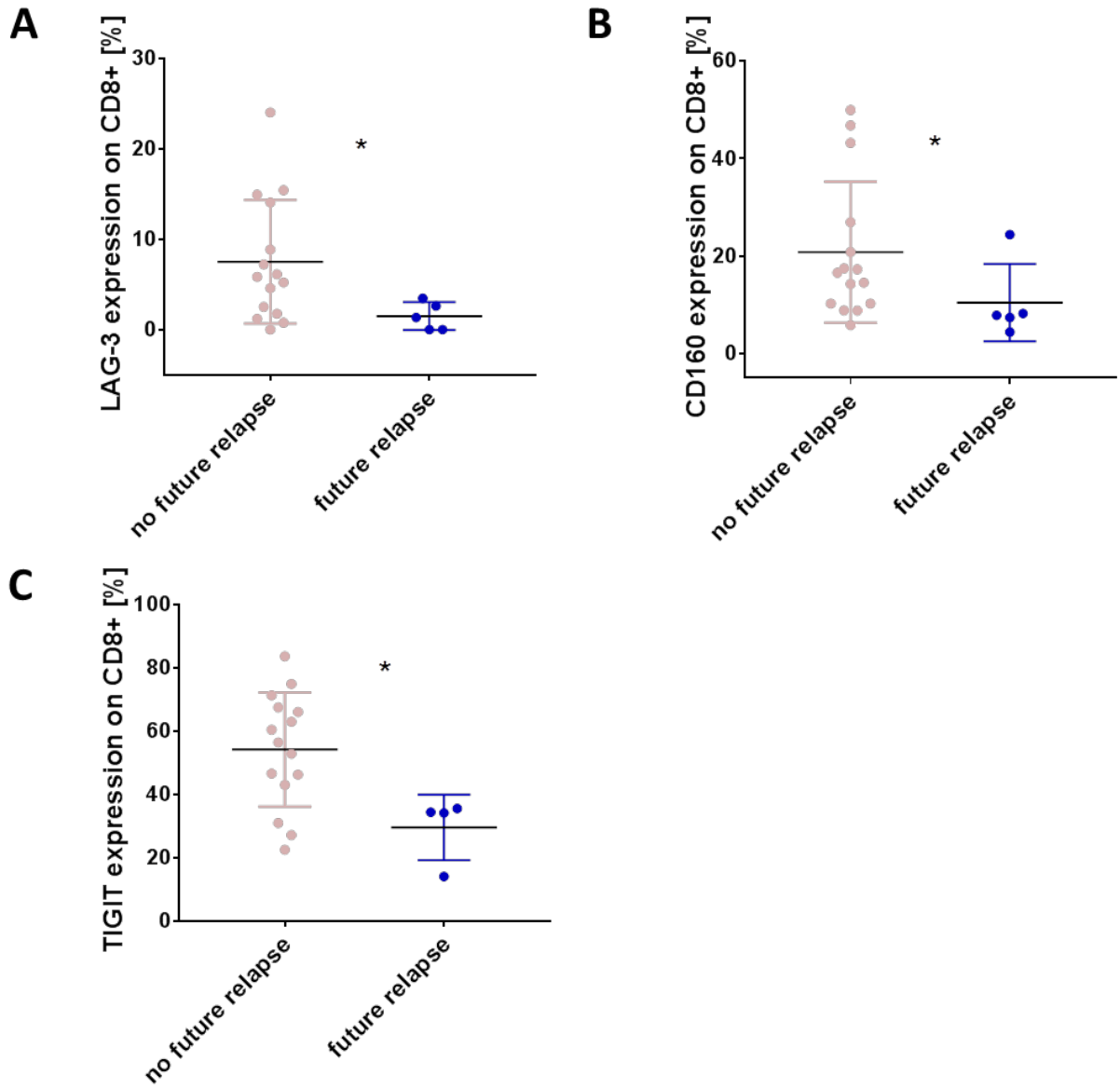

Figure 36: Differential expression of immune modulatory molecules on CD8+ bmT cells of patients without (n=15) and with future relapse (n=4-5) at initial diagnosis: The graphs show the same data set as Figure 35 but are presented in a different manner. Patients without future relapse expressed significantly higher levels of **A)** LAG-3 (p=0.0415), **B)** CD160 (p=0.0401) and **C)** TIGIT (p=0.0366).

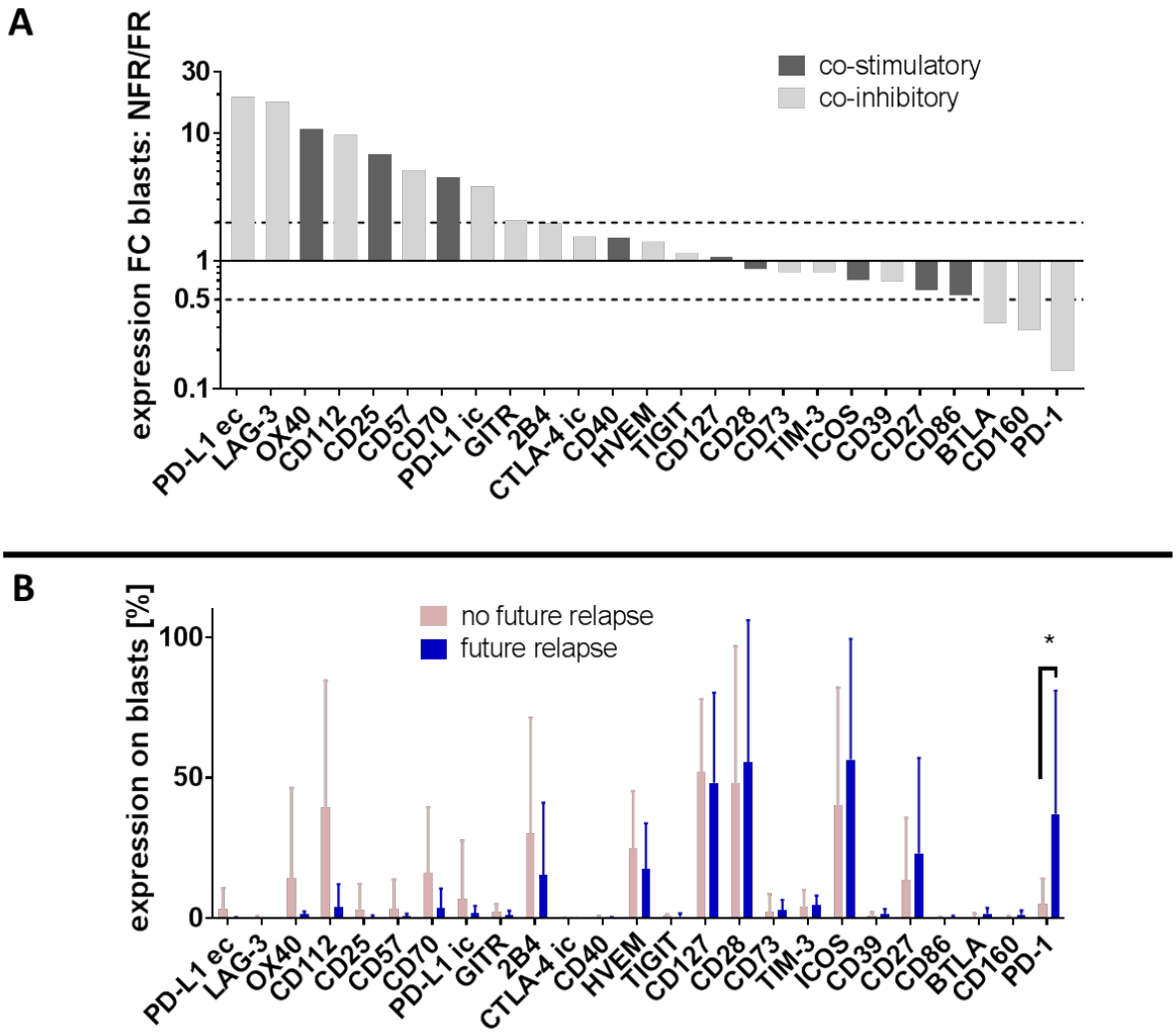

Figure 37: Expression of co-stimulatory and co-inhibitory molecules on leukemic T-ALL blasts of pediatric T-ALL patients of the Hauner children´s hospital without (n=5-15) and with future relapse (n=4-5) at initial diagnosis: A) Expression FC for leukemic T-ALL blasts: mean expression no future relapse/mean expression future relapse. The majority of markers showed an increased expression on leukemic T-ALL blasts of no future relapse T-ALL patients over future relapse patients. **B)** The absolute expression of immune modulatory markers on leukemic T-ALL blasts is arranged according to A. Leukemic T-ALL blasts of pediatric T-ALL patients with future relapse showed a significantly increased expression of PD-1 (p=0.0467). *FC = fold change, NFR = no future relapse, FR = future relapse, ec = extracellular, ic = intracellular.*

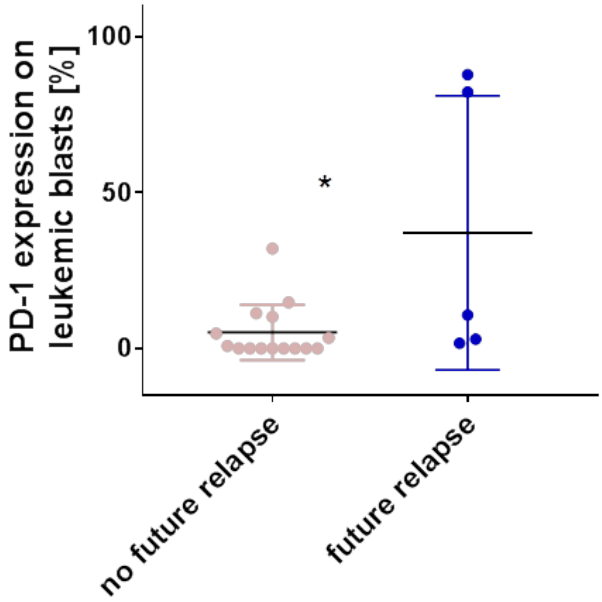

Figure 38: Increased PD-1 expression on leukemic T-ALL blasts of pediatric T-ALL patients with future relapse (n=5) over patients without future relapse (n=15): The graphs show the same data set as Figure 37 but are presented in a different manner. Future relapse patients showed significantly more PD-1 expression on leukemic blasts over patients that did suffer from future relapse (p=0.0467).

All p values of the previous chapters are not corrected for multiple testing to have a high sensitivity for differences and taking into account a low specificity of significant findings. Multiple testing correction was performed according to the original FDR method of Benjamini and Hochberg (subchapter 7.9.1). Figure 26 shows an overview of uncorrected p values and corrected p values (q values) for the BM populations CD4+ bmT cells, CD8+ bmT cells and TCP of T-ALL patients and healthy BM donors. P values of the CoALL study were not corrected. All uncorrected p values loose significance after multiple testing correction.

A

Antigen	p value	q value
PD-1	0.8521	0.8994
2B4	0.5416	0.8994
LAG-3	0.1279	0.3472
CD57	0.9613	0.9613
TIM-3	0.0996	0.317
TIGIT	0.1001	0.317
ICOS	0.6032	0.8994
BTLA	0.5965	0.8994
HVEM	0.0485	0.3072
CD28	0.3056	0.6452
GITR	0.0159	0.3021
CD27	0.8139	0.8994
OX40	0.2661	0.632
PD-L1 ec	0.7363	0.8994
CD73	0.0437	0.3072
CD39	0.0942	0.317
CD127	0.6905	0.8994
PDL-1 ic	0.8093	0.8994
CTLA-4 ic	0.6517	0.8994

B

Antigen	p value	q value
CD160	0.0401	0.2499
PD-1	0.3949	0.6598
2B4	0.0526	0.2499
LAG-3	0.0415	0.2499
CD57	0.469	0.6598
TIM-3	0.2544	0.498
TIGIT	0.0366	0.2499
ICOS	0.5556	0.6598
BTLA	0.2621	0.498
HVEM	0.2208	0.498
CD28	0.9999	0.9999
GITR	0.5397	0.6598
CD27	0.5531	0.6598
PD-L1 ec	0.096	0.3648
CD73	0.6725	0.7516
CD39	0.22	0.498
CD127	0.5476	0.6598
PDL-1 ic	0.2611	0.498
CTLA-4 ic	0.91	0.9606

C

Antigen	p value	q value
CD160	0.3048	0.9481
PD-1	0.0467	0.755
2B4	0.7354	0.9481
LAG-3	0.4181	0.9481
CD57	0.9463	0.9778
TIM-3	0.5299	0.9481
TIGIT	0.4058	0.9481
ICOS	0.4127	0.9481
BTLA	0.121	0.7563
HVEM	0.7363	0.9481
CD112	0.113	0.7563
CD28	0.672	0.9481
GITR	0.3095	0.9481
CD27	0.8798	0.9563
OX40	0.8001	0.9525
CD40	0.7585	0.9481
PD-L1 ec	0.0604	0.755
CD86	0.6801	0.9481
CD70	0.2149	0.9481
CD73	0.5677	0.9481
CD39	0.9778	0.9778
CD25	0.7383	0.9481
CD127	0.8413	0.956
PDL-1 ic	0.4538	0.9481
CTLA-4 ic	0.5049	0.9481

Figure 39: Corrected (q values) and uncorrected p values for analysis of CD4+ bmT cells (A), CD8+ bmT cells (B) and T-cell progenitors (C) in no future relapse T-ALL patients compared to future relapse patients. Multiple testing correction was performed by using the Original FDR method of Benjamini and Hochberg. P values of the CoALL study were not corrected.

8.4.3. Integration of Hauner children´s hospital data and CoALL data for examination of prognostic relevance assessing risk of relapse

Table 6 in chapter 8.4.1 identifies 11 biomarkers with putative relevance for relapse. Kaplan Meier curves were estimated for those 11 biomarkers dividing samples into two groups by mean expression level of the respective surface markers. Significance was tested using Log-rank tests.

After application of the guidelines presented in subchapter 8.4.1 only three markers (TIM-3 on CD4+ bmT cells, TIM-3 on CD8+ bmT cells and PD-1 on leukemic blasts) showed significant differences in RFS using a Log-rank test.

The Kaplan Meier in this chapter only presents those that showed significant differences in RFS comparing no future relapse and future relapse patients. No multiple testing correction was performed.

8.4.3.1. TIM-3 overexpression on CD4+ bmT cells increases risk of relapse

The cut-off at 5.9% was set according to the mean TIM-3 expression observed on the surface of CD4+ bmT cells of HCH and CoALL T-ALL patients. TIM-3 expression on CD4+ bmT cells of HCH patients with future relapse was increased in comparison to the expression levels on CD4+ bmT cells of HCH patients without future relapse (6.4 % vs. 9.5 %, ns). A similar trend was observed in the CoALL cohort (4.3 % vs. 7.8 %, ns) (Figure 40A).

Within the HCH cohort the risk of developing a relapse was insignificantly increased for patients with TIM-3 expression >5.9% on CD4+ bmT cells (60.0 % vs. 90.0 %, RFS (=RFS), ns) (Figure 40C). While individual analysis of the CoALL CD4+ bmT cells did not show a significant difference in RFS (42.9 % vs. 95.0%, ns) the integrated analysis of the HCH and CoALL CD4+ bmT cells (47.1 % vs. 93.3 %, p=0.0148) showed a significantly increased risk of relapse with TIM-3 expression levels above 5.9% compared to those patients with an expression <5.9% (Figure 40B+D). The mean follow-up period was 2.8 years for the HCH cohort and 6.0 years for the CoALL cohort.

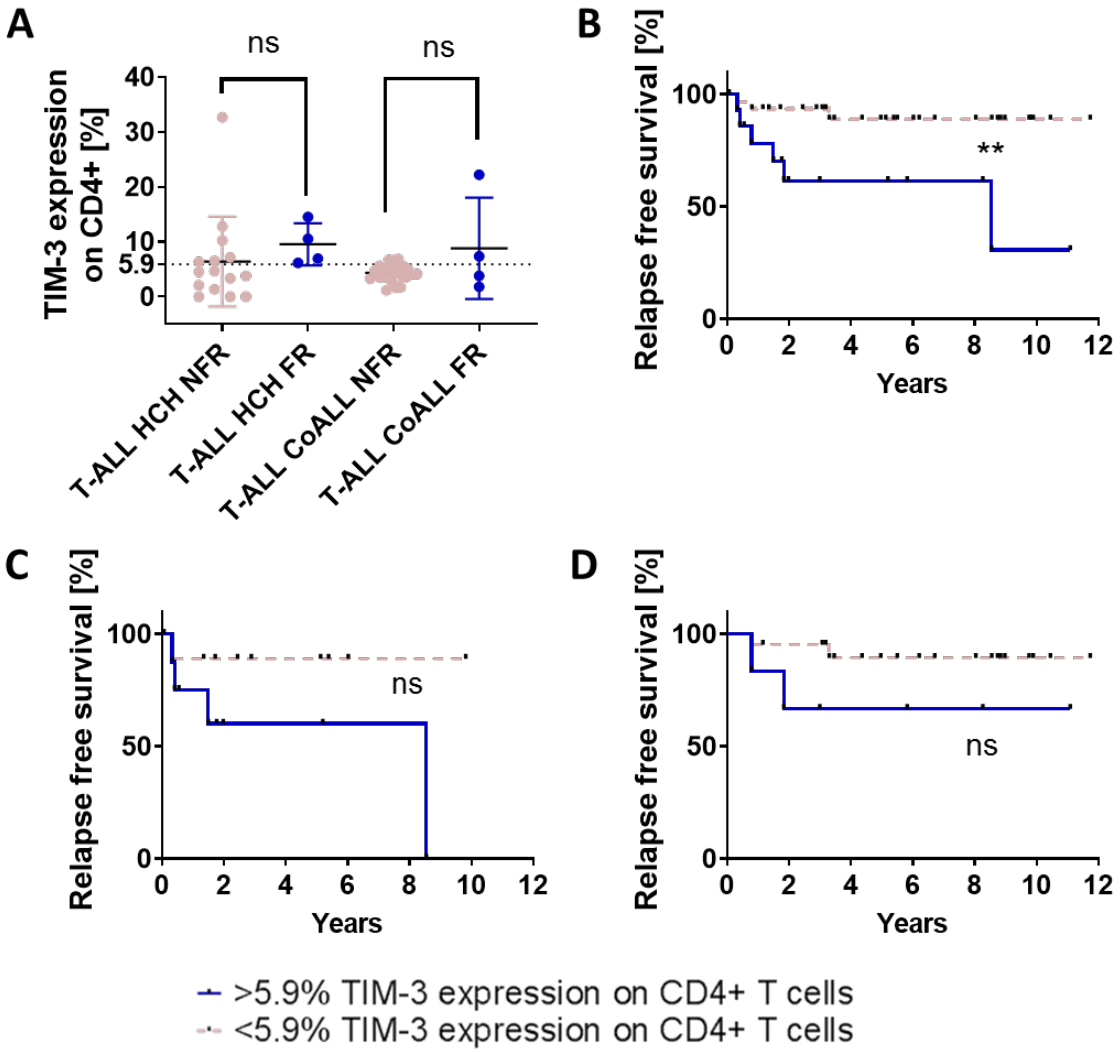

Figure 40: TIM-3 overexpression on CD4+ bmT cells as prognostic marker for risk of relapse in pediatric T-ALL: Samples from the HCH (n=20) and CoALL study (treated and untreated, n=27) were analyzed regarding TIM-3 surface expression on the CD4+ bmT-cell population. The cut-off was set at 5.9% (mean TIM-3 expression on CD4+ bmT cells of all measured patients). **A)** TIM-3 expression on CD4+ bmT cells of no future relapse T-ALL patients and future relapse T-ALL patients of the HCH and CoALL study: TIM-3 expression was increased on CD4+ bmT cells of future relapse patients compared to no future relapse patients for the HCH (ns) as well as the CoALL (ns) cohort. **B)** The Kaplan Meier curve presents the results of an integrated analysis of HCH and CoALL CD4+ bmT cells. Patients with a TIM-3 expression level <5.9% showed a higher rate of RFS. TIM-3 expression levels >5.9% correlated with a significantly higher risk of developing a relapse in the clinical course (RFS: 47.1 % vs. 93.3 %, p=0.0148). **C)** The Kaplan Meier curve presents the results of an isolated analysis of the HCH CD4+ bmT cells. The risk of relapse was increased with TIM-3 expression levels >5.9% (RFS: 60.0 % vs. 90.0 %, ns). **D)** The Kaplan Meier curve presents the results of an isolated analysis of the CoALL CD4+ bmT cells. The risk of relapsing was significantly increased for patients with TIM-3 expression levels >5.9% on CD4+ bmT cells compared to those patients with an expression <5.9% (RFS: 42.9 % vs. 95.0%, ns). *HCH = Hauner children´s hospital, RFS = relapse free survival, NFR = no future relapse, FR = future relapse, ns = not significant.*

8.4.3.2. TIM-3 overexpression on CD8+ bmT cells increases risk of relapse

The cut-off at 8.2% was set according to the mean TIM-3 expression observed on the surface of CD8+ bmT cells of HCH and CoALL T-ALL patients. TIM-3 expression on CD8+ bmT cells of CoALL patients with future relapse was significantly increased in comparison to the expression levels on CD8+ bmT cells of CoALL patients without future relapse (5.1 % vs. 16.8 %, p=0.0444). A similar tendency was observed in HCH samples (10.2 % vs. 12.6 %, ns) (Figure 41A).

Within the HCH cohort the risk of developing a relapse was slightly increased for patients with TIM-3 expression >8.2% on CD8+ bmT cells (70.0 % vs. 88.9 %, ns) (Figure 41C). However, isolated analysis of the CoALL CD8+ bmT cells (66.7 % vs. 100 %, p=0.0298) and integrated analysis of the HCH and CoALL CD8+ bmT cells (68.8 % vs. 96.7 %, p=0.0193) showed a significantly increased risk of relapse with TIM-3 expression levels above 8.2% compared to those patients with an expression <8.2% (Figure 41B+D). The mean follow-up period was 2.9 years for the HCH cohort and 6.1 years for the CoALL cohort.

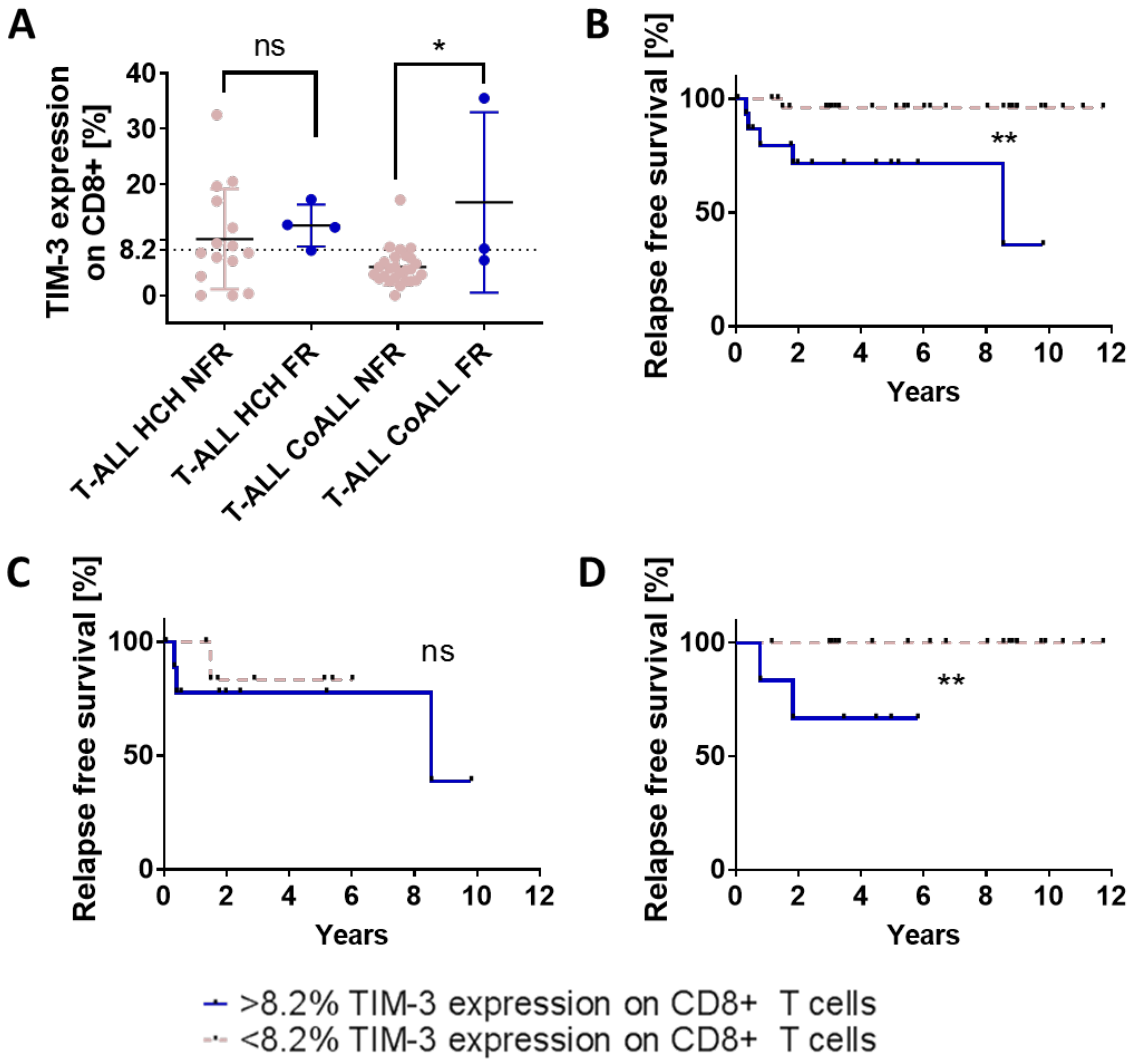

Figure 41: TIM-3 overexpression on CD8+ bmT cells as prognostic marker for risk of relapse in pediatric T-ALL: Samples from the HCH (n=19) and CoALL study (n=27) were analyzed regarding TIM-3 surface expression on the CD8+ bmT-cell population. The cut-off was set at 8.2% (mean TIM-3 expression on CD8+ bmT cells of all measured patients). **A)** TIM-3 expression on CD8+ bmT cells of no future relapse T-ALL patients and future relapse T-ALL patients of the HCH and CoALL study: TIM-3 expression was increased on CD8+ bmT cells of future relapse patients compared to no future relapse patients for the HCH (ns) as well as the CoALL (p=0.0444) cohort. **B)** The Kaplan Meier curve presents the results of an integrated analysis of HCH and CoALL CD8+ bmT cells. Patients with a TIM-3 expression level <8.2% showed a higher rate of RFS. By contrast, expression levels >8.2% correlated with a significantly higher risk of developing a relapse in the clinical course (RFS: 68.8 % vs. 96.7 %, 0.0193). **C)** The Kaplan Meier curve presents the results of an isolated analysis of the HCH CD8+ bmT cells. The risk of relapse was slightly increased with TIM-3 expression levels >8.2% (RFS: 70.0 % vs. 88.9 %, p=0.0031). **D)** The Kaplan Meier curve presents the results of an isolated analysis of the CoALL CD8+ bmT cells. The risk of a future relapse was significantly increased for patients with TIM-3 expression levels >8.2% on CD8+ bmT cells compared to those patients with an expression <8.2% (RFS: 66.7 % vs. 100 %, p=0.0298). *HCH = Hauner children´s hospital, RFS = relapse free survival, NFR = no future relapse, FR = future relapse, ns = not significant.*

8.4.3.3. PD-1 expression on leukemic blasts increases risk of relapse

The cut-off at 8.9% was set according to the mean PD-1 expression observed on the surface of leukemic T-ALL blasts of HCH and CoALL T-ALL patients. PD-1 expression on T-ALL blasts of HCH patients with future relapse was significantly increased in comparison to the expression levels on leukemic blasts of HCH patients without future relapse (5.1 % vs. 37.1 %, p=0.0467). A similar trend was observed in CoALL samples (4.2 % vs. 13.0 %, ns) (Figure 42A).

Within the CoALL cohort the risk of developing a relapse is insignificantly increased for patients with PD-1 expression >8.9% on leukemic T-ALL blasts (60.0 % vs. 84.6 %, ns) (Figure 42D). However, isolated analysis of the HCH T-ALL (50.0 % vs. 85.7 %, p=0.0071) blasts and integrated analysis of the HCH and CoALL (54.5 % vs. 85.0 %, p=0.0009) leukemic T-ALL blasts showed a significantly increased risk of relapse with PD-1 expression levels above 8.9% compared to that of patients with expression levels <8.9%. (Figure 42B+C). The mean follow-up period was 2.7 years for the HCH cohort and 5.8 years for the CoALL cohort.

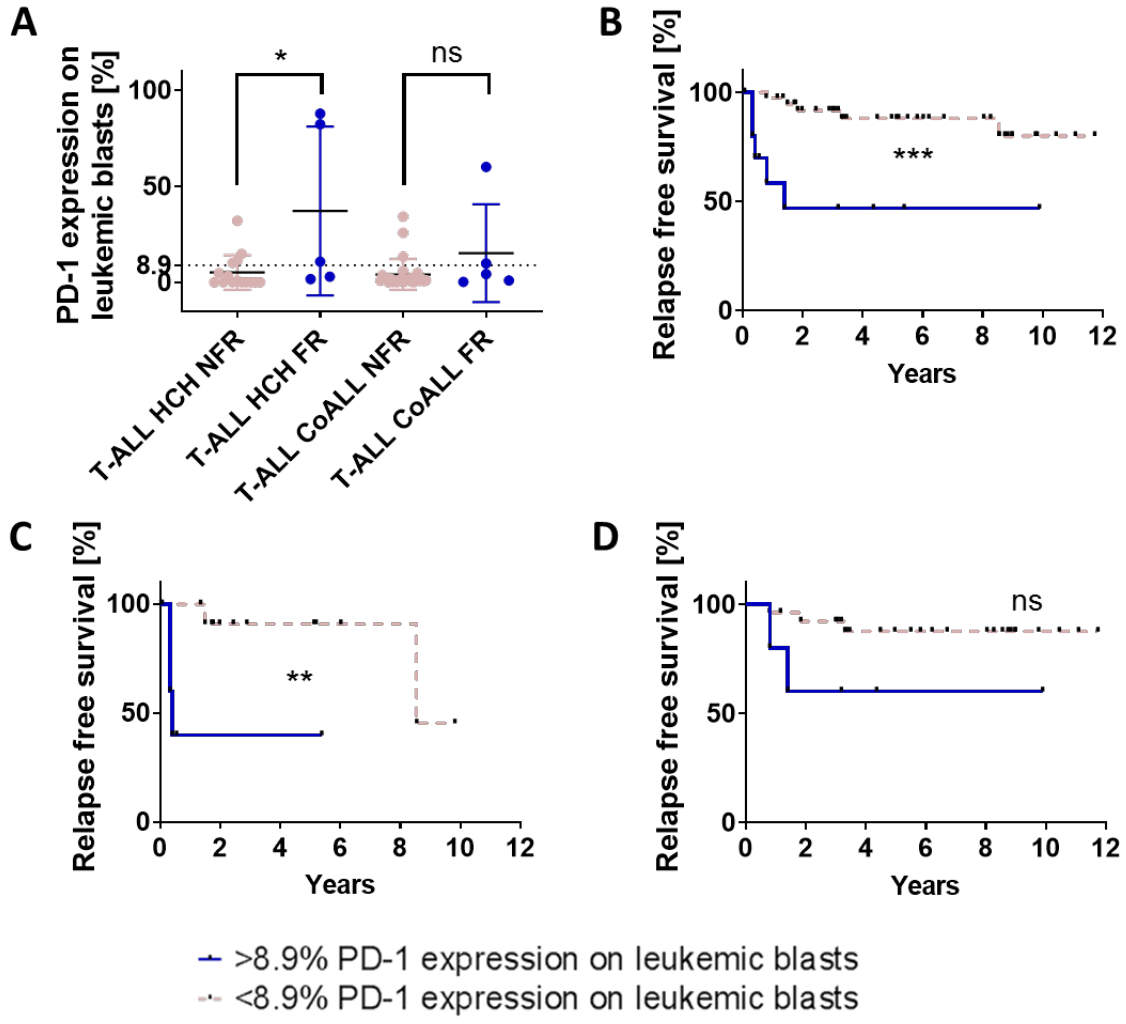

Figure 42: PD-1 overexpression on leukemic T-ALL blasts as a prognostic marker for risk of relapse in pediatric T-ALL: Samples from the HCH (therapy naïve: n=20) and CoALL study (n=31) were analyzed regarding PD-1 surface expression on leukemic T-ALL blasts. The cut-off was set at 8.9% (mean PD-1 expression on T-ALL blasts of all measured patients). **A)** PD-1 expression on leukemic T-ALL blasts of no future relapse T-ALL patients and future relapse T-ALL patients of the HCH and CoALL study center: PD-1 expression was increased on leukemic T-ALL blasts of future relapse patients compared to no future relapse patients for the HCH (ns) as well as the CoALL (p=0.0444) cohort. **B)** The Kaplan Meier curve presents the results of an integrated analysis of HCH and CoALL T-ALL blasts. Patients with PD-1 expression levels <8.9% showed higher rates of RFS. Contrarily expression levels >8.2% correlated with a significantly higher risk of developing a relapse in the clinical course (RFS: 54.5 % vs. 85.0 %, p=0.0009). **C)** The Kaplan Meier curve presents the results of an isolated analysis of the HCH T-ALL blasts. The risk of relapse was significantly increased with PD-1 expression levels >8.9% (RFS: 50.0 % vs. 85.7 %, p=0.0071). **D)** The Kaplan Meier curve presents the results of an isolated analysis of the CoALL T-ALL blasts. The risk of relapse was increased with PD-1 expression levels >8.9% on leukemic T-ALL blasts compared to those patients with an expression <8.2% (RFS: 60.0 % vs. 84.6 %, ns). *HCH = Hauner children´s hospital, RFS = relapse free survival, NFR = no future relapse, FR = future relapse, ns = not significant.*

8.5. Flow cytometric analysis of T-cell interaction with leukemic T-ALL blasts: interaction of TIGIT+ bmT cells with CD112+ T-ALL blasts

With the intent of understanding the interaction between bmT cells and leukemic T-ALL blasts, the following known interacting receptors and ligands were examined within the HCH T-ALL patients for signs of interaction between leukemic blasts and bmT cells: (1) CD80/CD86 and CD28/CTLA4, (2) CD112 and TIGIT and (3) CD70 and CD27. The results suggest an interaction via the CD112-TIGIT axis. No signs of interaction were observed regarding the CD80/CD86 and CD28/CTLA-4 axis.

CD112 expression on leukemic T-ALL blasts showed a bimodal distribution. An overexpression of CD112 on pediatric T-ALL blasts at initial diagnosis compared to the healthy control was observed (31.9 % vs. 3.5 %, ns). We arbitrarily set a cutoff at 10% CD112 expression on T-ALL blasts as a visually selected cut-off: 8/19 patients showed high (>10%) CD112 expression ($CD112_{high}$) and 11/19 patients showed low (<10%) CD112 expression ($CD112_{low}$).

BmT cells (CD4+ and CD8+) of each of the established groups of patients were analyzed for TIGIT surface expression. The expression level of TIGIT on bmT cells (CD4+ and CD8+) of T-ALL patients with $CD112_{low}$ T-ALL blasts and healthy BM donors was comparable (CD4+: 21.0 % vs. 21.4 %, ns; CD8+: 42.5 % vs. 41.0 %, ns). Patients with $CD112_{high}$ blasts showed increased TIGIT expression levels on CD4+ (34.0 % vs. 21.4 %, p=0.0012) and CD8+ (57.8 % vs. 41.0 %, p=0.0421) bmT cells over healthy BM donors. While patients with $CD112_{high}$ blasts expressed significantly more TIGIT on CD4+ bmT cells (34.0 % vs. 21.0 %, p=0.0050) than $CD112_{low}$ patients, the respective comparison was not significant for CD8+ bmT cells (57.8 % vs. 42.5 %, ns) (Figure 43).

CD112 expression on T-ALL blasts of CoALL samples was negative. Only the data available for the HCH cohort allowed an analysis of the TIGIT-CD112 axis.

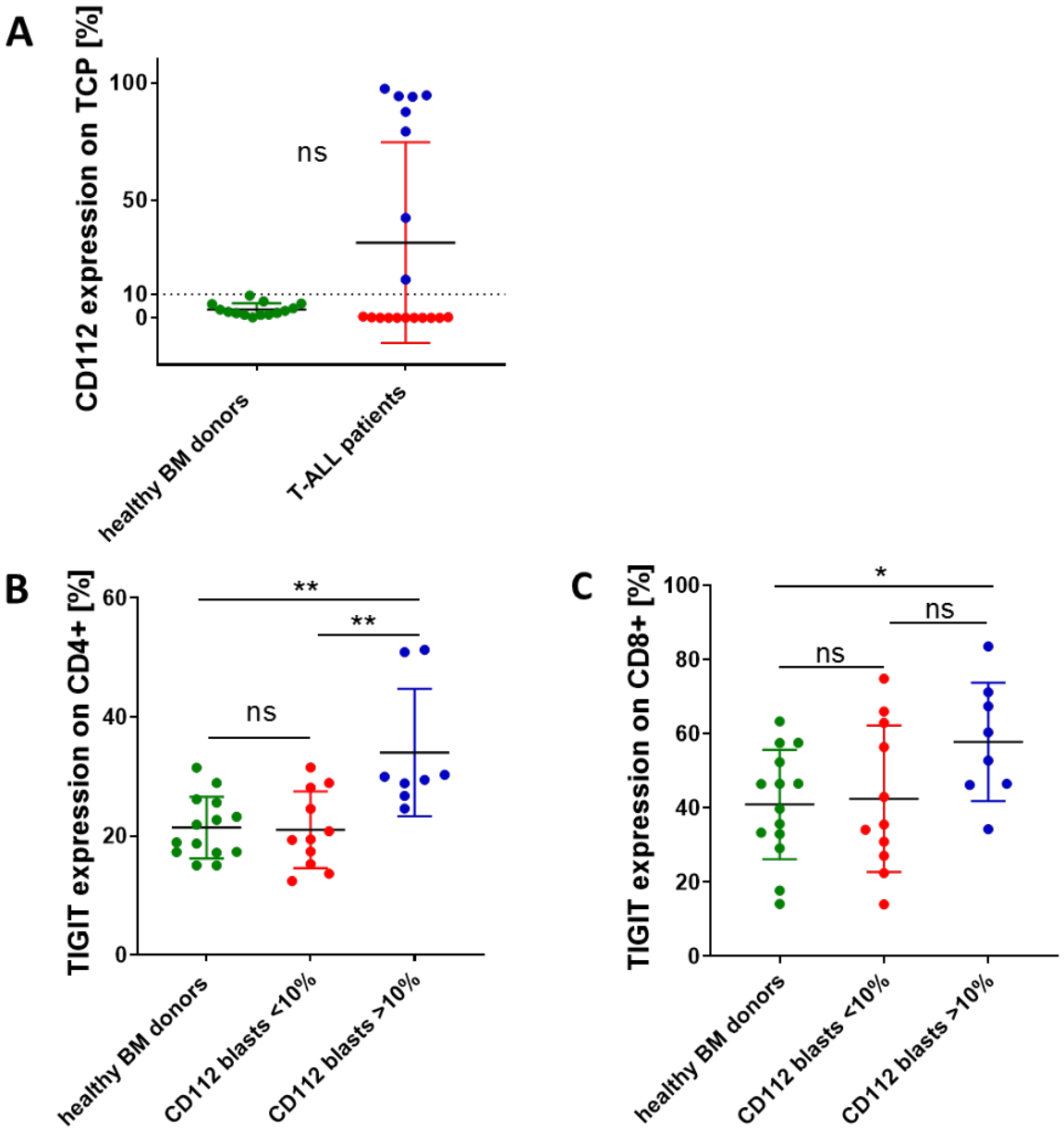

Figure 43: CD112 expression on leukemic blasts correlated with TIGIT expression on CD4+ and CD8+ bmT cells in T-ALL patient´s samples of the Hauner children´s hospital (n=19): A) An overexpression of CD112 on leukemic T-ALL blasts in comparison to healthy BM donors could be observed (ns). CD112 expression on leukemic T-ALL blasts showed a bimodal distribution: 8/19 patients showed high (>10%) CD112 expression ($CD112_{high}$) and 11/19 patients showed low (<10%) expression of CD112 ($CD112_{low}$). **B)** The bmT cells (CD4+ and CD8+) were analyzed regarding their TIGIT surface expression according to the two determined groups. The expression level of TIGIT on bmT cells (CD4+ and CD8+) of healthy BM donors and T-ALL patients with $CD112_{low}$ T-ALL blasts was comparable (ns). Patients with $CD112_{high}$ blasts showed increased TIGIT expression levels on CD4+ (p=0.0012) and CD8+ (p=0.0421) bmT cells over healthy BM donors. While patients with $CD112_{high}$ blasts expressed significantly more TIGIT on CD4+ bmT cells (p=0.0050) than those of $CD112_{low}$ patients the respective comparison was not significant for CD8+ bmT cells. *TCP = T-cell progenitors, ns = not significant.*

8.6. Other findings

8.6.1. Further significant differences

Co-stimulatory markers CD25 (2.4 % vs. 4.5 %, p=0.0001) and CD40 (0.3 % vs. 2.7 %, p<0.0001) were significantly higher expressed on healthy TCP compared to expression on leukemic T-ALL blasts of pediatric T-ALL patients (Figure 44).

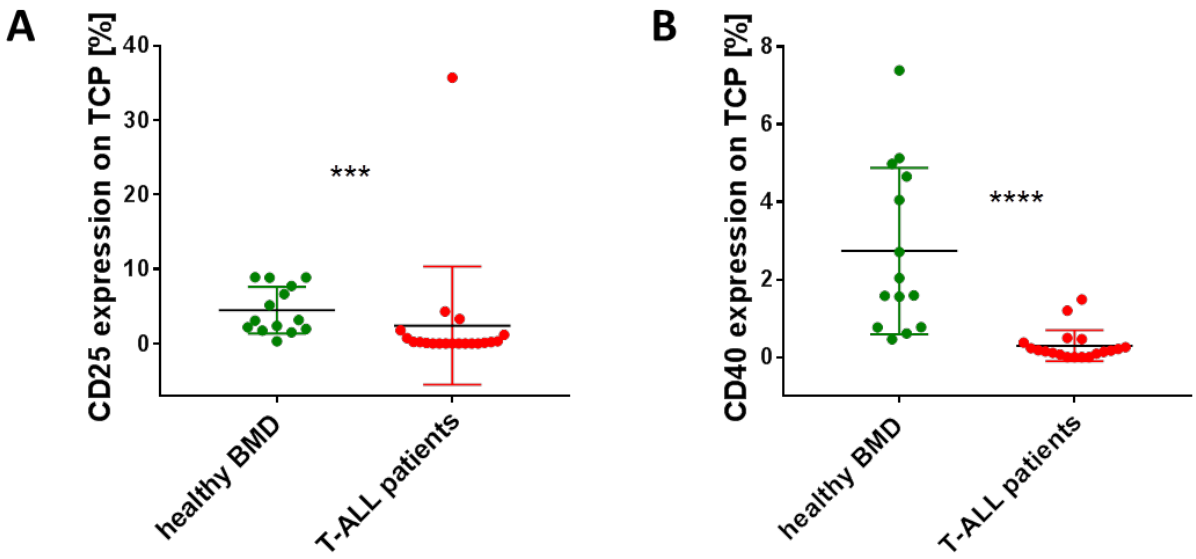

Figure 44: Downregulation of co-stimulatory markers on T-cell progenitors of pediatric T-ALL patients (n=10-20) compared to healthy BM donors (n=7-14): The graph emerged from the same data set as Figure 20. A significant upregulation of co-stimulatory markers **A)** CD25 (p=0.0001) and CD40 **B)** (p<0.0001) could be observed on the side of healthy BM donors´ TCP compared to expression levels on leukemic blasts of pediatric T-ALL patients. *TCP = T-cell progenitors, healthy BMD = healthy BM/bone marrow donors.*

The data for surface markers CD40, CD70, CD86 and CD112 expression on the surface of CD4+ and CD8+ bmT cells was not presented in the previous chapters for either of the following reasons:

1) mean expression levels <1% in the respective cohort.
2) no estimated relevance on cells of the respective BM population (CD4+ or CD8+ bmT cells)

Markers that showed a significantly differential expression comparing two groups are presented in Figure 45. CD40 expression at initial diagnosis was significantly increased on CD4+ bmT cells of future relapse T-ALL patients compared to those patients without future relapse (0.6 % vs. 0.9 % ,p=0.0196). CD70 expression was significantly upregulated on the CD8+ bmT cells of pediatric T-ALL patients without future relapse compared to those patients with future relapse (4.4 % vs. 0.3 %, p=0.0134).

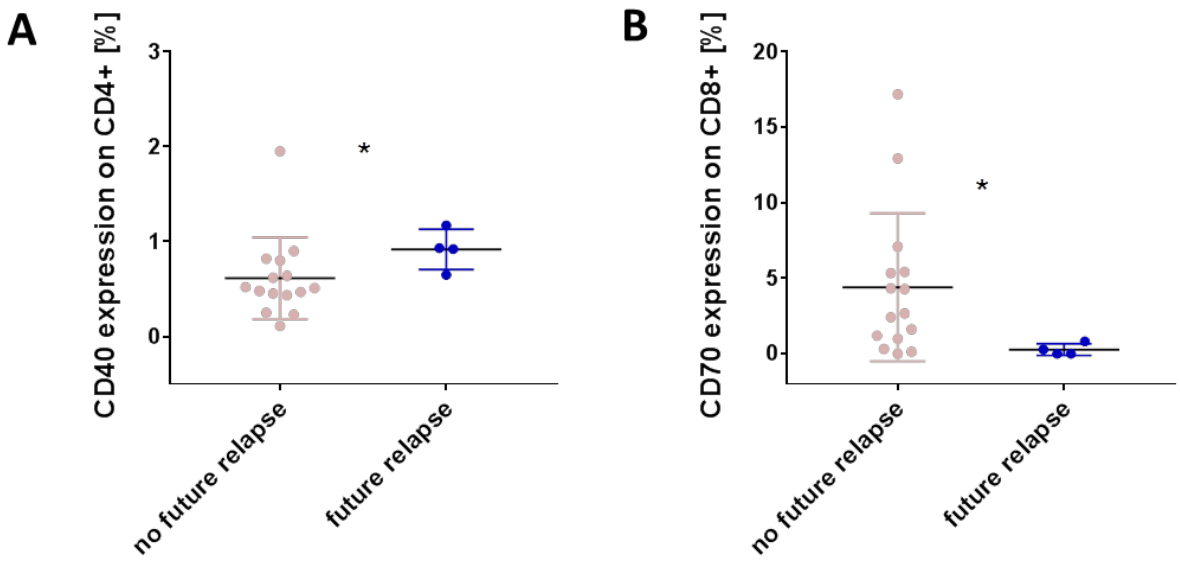

Figure 45: Differential expression of CD40 on CD4+ bmT cells and CD70 on CD8+ bmT cells. A) CD40 expression was significantly overexpressed on CD4+ bmT cells of pediatric T-ALL patients with future relapse compared to those patients without future relapse (p=0.0196). **B)** CD70 expression was significantly increased on CD8+ bmT cells in cases of patients with future relapse compared to those patients without future relapse (p=0.0134).

8.6.2. Negative findings

Several markers were stained for patients B002-B011 and healthy BM donors B101-B110. They were excluded from further analysis due to non-expression on bmT cells as well as on TCP (not shown).

As already mentioned in chapter 8.2.1.4, staining of T_{regs} within the CD4+ bmT-cell population did not work sufficiently using the intracellular transcription factor FoxP3 (fluorochrome: AF647) for characterization. As a result, evaluation of T_{regs} was not possible for patients B002-B011 and healthy BM donors B101-B110. For further measurements T_{regs} definition was performed via extracellular staining of CD25 and CD127.

Table 7 shows an overview over the markers that were excluded from further analysis including their function and problems.

Fluorochrome	Antigen	Cell type	Function	Problem
FITC	CTLA-4	bmT cells	T-cell inhibition	No extracellular expression
BV421	CD137	bmT cells	T-cell activation	No differential expression
BV421	CD80	T-ALL blasts	T-cell activation	Lack of expression
APC	VISTA	bmT cells	T-cell inhibition	Lack of expression
APC	MUC1 5E5	T-ALL blasts	Possible target	Lack of expression
PE	MUC1 5E10	T-ALL blasts	Control for MUC1 5E5	Lack of expression
AF647	FoxP3 ic	CD4+ bmT cells	Definition of regulatory T cells	Not feasible for BM samples

Table 7: Exclusion of molecules due to non-expression (CTLA-4, CD137, CD80, VISTA, MUC1 5E15, MUC1 5E10) and technical difficulties with measurement (intracellular staining of FoxP3). *ic = intracellular.*

8.6.3. Overlapping CD56 expression on T-cell progenitors (of healthy BM donors and pediatric T-ALL patients) and natural killer cells prohibits NK-cell evaluation

Cell characterization of natural killer cells (NK cells) via surface marker CD56 was highly expressed on TCP of healthy BM donors as well as on leukemic T-ALL blasts. It was not possible to define a suitable pre-gate using the markers CD3 and CD45 to differentiate between healthy or leukemic TCP and CD56+ NK cells. As a result, no NK cell characterization and analysis were performed in terms of the project.

8.7. Connecting flow cytometric data to RNA-sequencing data of CD8+ bmT cells

As already mentioned in subchapter 7.6.2 the flow cytometric analysis showed profound differences when comparing the immune checkpoint expression of CD8+ bmT cells of pediatric T-ALL patients and healthy BM donors. To validate flow cytometry results, RNA of the CD8+ bmT-cell populations of pediatric T-ALL patients and healthy BM donors was sequenced after cell sorting and RNA isolation. A total of 11076 genes were filtered according to the following criteria: (1) RPKM≥2 in T-ALL patient samples, (2) RPKM≥2 in healthy BM donor samples, (3) FC≤0.5, FC≥2 (4) multiple testing corrected $p<0.05$. Subsequently, 258 genes were filtered and examined for their relevance for CD8+ bmT-cell function and organized into groups. The antigens measured via flow cytometry and the corresponding genes (RNA-sequencing) are presented in Table 8.

Gene (RNA)	Antigen (Flow)	Gene (RNA)	Antigen (Flow)
CTLA4 *	CTLA-4 *	**PDCD1**	PD-1
LAG3 *	LAG-3 *	**TNFRSF18**	GITR
HAVCR2	TIM-3 *	**TNFSF14**	HVEM
ICOS	ICOS *	**IL7R**	CD127
B3GAT1	CD57	**CD27**	CD27
CD244	2B4	**BTLA**	BTLA
CD274	PD-L1	**CD28**	CD28
ENTPD1	CD39	**CD160**	CD160
TIGIT	TIGIT	**NT5E**	CD73 *

Table 8: Overview of protein coding genes from RNA-sequencing and respective antigens measured via flow cytometry: The asterisks (*) were used for genes/antigens when a significant differential expression was observed via RNA-sequencing (genes: CTLA4, LAG3)/flow cytometry measurement (antigens: CTLA-4, LAG-3, TIM-3, ICOS, CD73). The gene-antigen combinations CTLA4/CTLA-4 and LAG3/LAG-3 were significant in case of flow cytometric measurement as well as RNA-sequencing.

The genes CTLA4 (CTLA-4, p=0.0221, FC=7.95) and LAG3 (LAG-3, p<0.0001, FC=3.87) were overexpressed in CD8+ bmT cells of pediatric T-ALL patients compared to those of healthy BM donors. CTLA-4 and LAG-3 are known to be involved in the process of T-cell inhibition and the mechanism of T-cell exhaustion (Jiang et al., 2015). Those results match the flow cytometry data of CD8+ bmT cells. PFR1 (Perforin 1, p= 0.0015, FC=3.30), GZMB (Granzyme B, p<0.0001, FC 8.06) and GRLY (Granulysin, p= 0.0040, FC=3.24) were higher expressed in the CD8+ bmT cells of pediatric T-ALL patients. The respective proteins are known to be involved in the CD8+ T-cell effector function upon interleukin stimulation and/or specific antigen exposure (Voskoboinik, Whisstock, & Trapani, 2015). The gene expression of FAS (FAS cell surface death receptor, p=0.0046, FC=2.00) and TXN (Thioredoxin, p=0.0001, FC=2.78) was upregulated in CD8+ bmT cells of pediatric T-ALL patients. FAS is part of the death receptor family and responsible for apoptosis upon ligand binding (Condo & Testi, 2000). The Thioredoxin system has antioxidant functions and regulates mechanisms like gene expression, cell differentiation and apoptosis (Muri et al., 2018). MYB (MYB proto-oncogene, p=0.0301, FC=2.89) was higher expressed in CD8+ bmT cells of pediatric T-ALL patients. The MYB proto-oncogene was shown to encode essential regulators of cell proliferation and NF-κB signaling. It was also discussed in relation to different adult T-cell malignancies (Nakano, Uchimaru, Utsunomiya, Yamaguchi, & Watanabe, 2016).

IL21R (Interleukin 21 Receptor, p=0.0469, FC=0.44) and RARA (Retinoic acid receptor alpha, p=0.0339, FC=0.44) expression was reduced in CD8+ bmT cells of pediatric T-ALL patients compared to healthy BM donors. IL21R is known to be involved in the development and maturation process of the CD4+

and CD8+ T-cell subsets (Andorsky & Timmerman, 2008; Tian & Zajac, 2016). RARA was shown to mediate expansion, differentiation, and survival of cytotoxic CD8+ T cells (Guo et al., 2014).

Figure 46A shows the differential gene expression of CD8+ bmT cells of pediatric T-ALL patients and healthy BM donors. Figure 46B presents a selection of genes from Figure 46A for better visualization. Genes coding for antigens measured on CD8+ bmT cells via flow cytometry are presented in Figure 47A. Figure 47B shows the fold change (FC, T-ALL vs. healthy BM donors) of the expression levels from flow cytometric analysis (x-axis) and gene expression on RNA level (y-axis): LAG-3 and CTLA-4 showed significant upregulation on RNA level and in flow cytometric analysis.

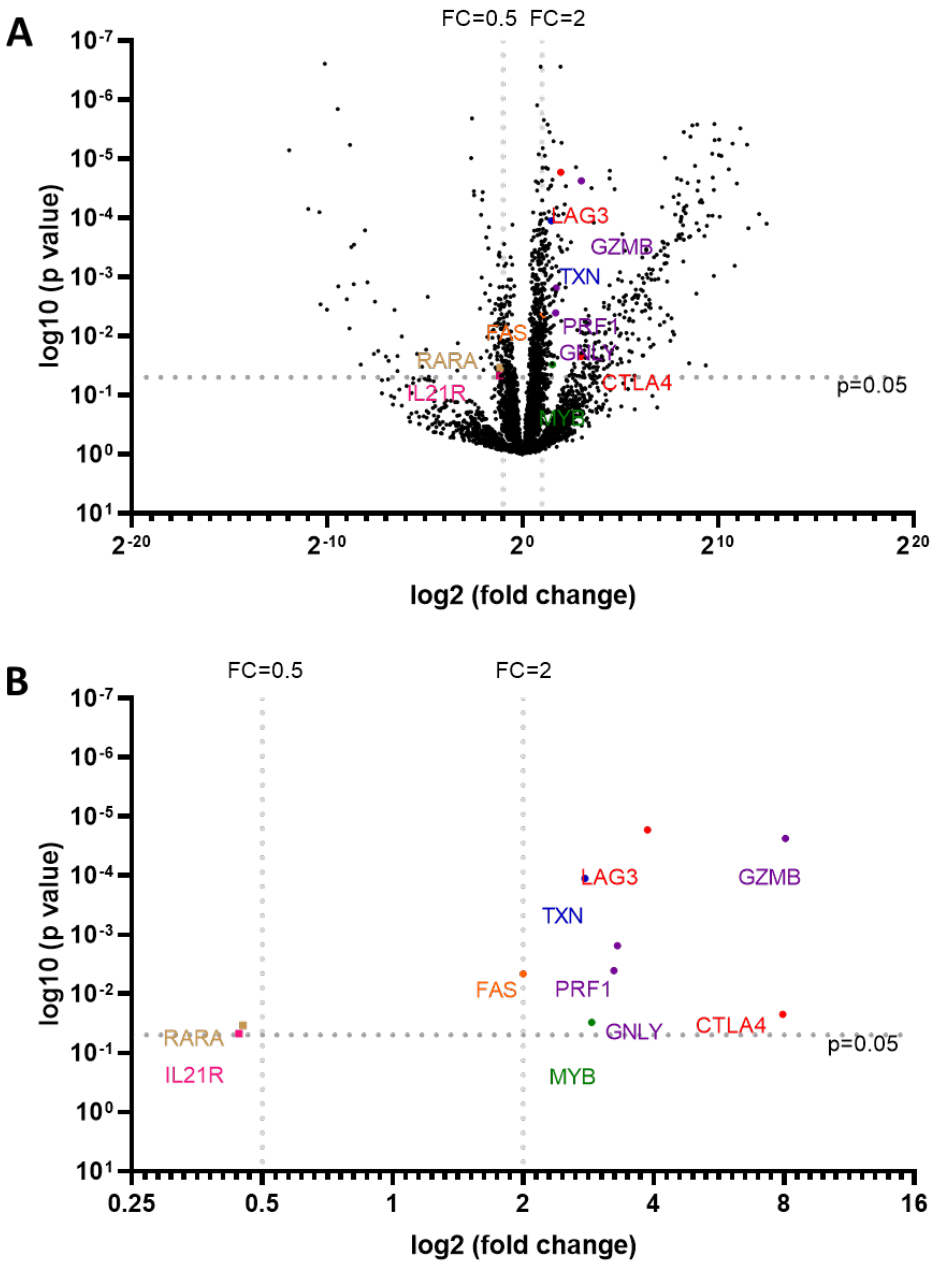

Figure 46: Differential gene expression of CD8+ bmT cells in the BM of pediatric T-ALL patients (N=12) in comparison to healthy BM donors (N=14): A) Differential mRNA expression of 11076 genes in T-ALL patients and healthy BM donors. The following genes were overexpressed in the CD8+ bmT cells of pediatric T-ALL patients compared to healthy BM donors: LAG3, CTLA4 (red; co-inhibitory immune checkpoint molecules); GZMB, PRF1, GNLY (purple; cytolytic effector function of CD8+ bmT-cells); FAS (orange; induction of apoptosis); TXN (blue; antioxidant functions); MYB (green; proto-oncogene mediating cell proliferation and NF-κB signaling). The following genes were lower expressed in the CD8+ bmT cells of T-ALL patients compared to healthy BM patients: IL21R (pink; CD8+ T-cell development and maturation); RARA (beige; expansion, differentiation and survival of CD8+ bmT cells). **B)** The volcano plot depicts the selection of color-coded gens from Figure 46A for better visualization (same data set as A). *RPKM = reads per kilo base per million mapped reads, FC = Fold change, LAG3 = Lymphocyte-activation gene 3, CTLA4 = Cytotoxic T-lymphocyte-associated antigen 4, GZMB = Granzyme B, PRF1 = Perforin A, GNLY = Granulysin, TXN = Thioredoxin, MYB = MYB proto-oncogene, IL21R = Interleukin 21 Receptor, RARA = Retinoic acid receptor alpha.*

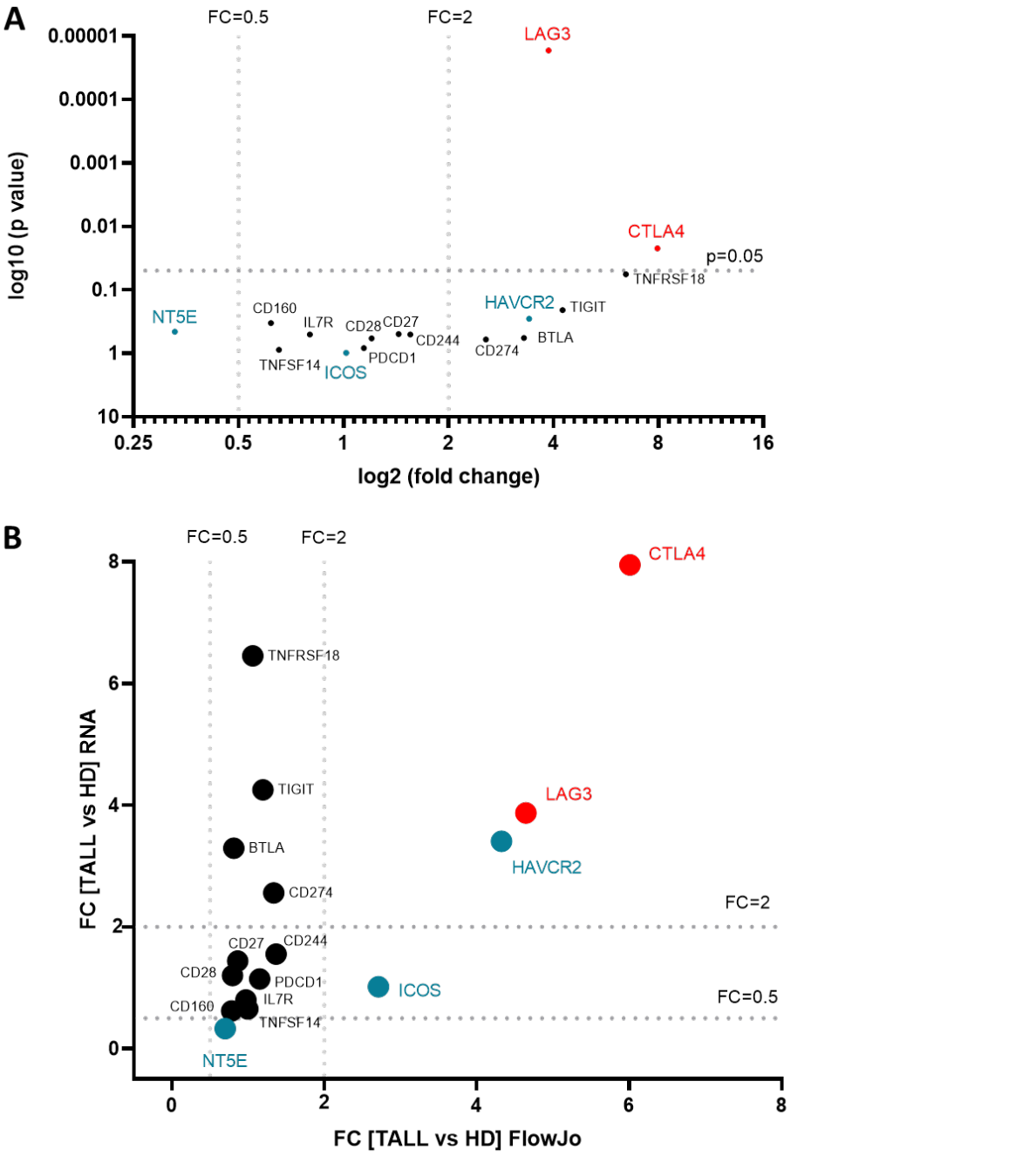

Figure 47: Differential gene expression of CD8+ bmT cells in T-ALL patients (N=12) in comparison to healthy BM donors (N=14): RNA-sequencing was performed via DNASTAR – Lasergene. 11076 genes were filtered according to the following criteria: (1) RPKM≥2 in T-ALL patient samples, (2) RPKM≥2 in healthy BM donor samples, (3) FC≤0.5, FC≥2 (4) p<0.05. The volcano plots show the corresponding genes of antigens measured in terms of flow cytometric analysis. The genes were divided in three groups: 1) Significant upregulation on CD8+ bmT cells in pediatric T-ALL patients compared to healthy BM donors on RNA level and in flow cytometric analysis (red; LAG3 and CTLA4); 2) Significant overexpression on CD8+ bmT cells of pediatric T-ALL patients compared to healthy BM donors only in case of flow cytometric analysis (blue; HAVCR2, ICOS and NT5E); 3) Antigens and genes that showed no significantly altered expression levels on RNA level or in flow cytometry. **A)** The dotted lines present the fold change cut-offs (vertical; FC≤0.5; FC≥2) and the p-value cut-off (p<0.05). *FC = Fold change, LAG3 = Lymphocyte-activation gene 3, CTLA4 = Cytotoxic T-lymphocyte-associated antigen 4, HAVCR2 = Hepatitis A virus cellular receptor 2, ICOS = Inducible T-cell co-stimulator, NT5E = Ecto-5'-nucleotidase.*

9. Discussion

9.1. Challenges of this project

9.1.1. Disease related challenges – cell count and gating strategy

As pediatric T-ALL is a rare disease, patient sample selection was a first challenge we were confronted with. High count of leukemic blasts in the bone marrow (BM) of pediatric T-ALL patients resulted in low frequency of physiological BM populations such as CD4+ and CD8+ bone marrow T cells (bmT cells), which were of particular interest in this study. Differentiation between healthy lymphocytes and leukemic blasts was difficult in some cases via CD45 vs. CD3 gating due to CD45hi CD3+ leukemic blasts. Consequently, evaluation of CD4+ and CD8+ bmT-cell populations was occasionally not possible. T_{regs} numbers were generally too low for evaluation of surface markers of interest. Finally, expression of the natural killer cell (NK cell) marker CD56 on leukemic blasts prevented a reliable evaluation of NK cells (also see subchapter 8.6.3).

9.1.2. Project related challenges - two sources of T-ALL BM samples

Two different sources of samples were analyzed, as a discovery cohort and a validation cohort. However, we were confronted with challenges in relation to sample measurement and evaluation. Due to different processing and storage routines, limitations included differences in cell count, cell viability and expression of lineage markers as well as potentially differential expression of immune checkpoints (IC) comparing the Hauner children´s Hospital (HCH) samples (detection cohort) and the Cooperative Acute Lymphoblastic Leukemia study (CoALL study) samples (validation cohort). While the expression of IC remained stable independently of processing and storage routines, other markers were altered (see Figure 32). Consequently, CoALL samples were only included into analysis if justifiable for a specific IC (this was decided individually for each marker).

9.2. Fundamental background information from published literature

9.2.1. T cells in the microenvironment BM in healthy individuals

For a better understanding of the projects´ objective knowledge of T-cell populations resident in the BM of healthy individuals and their role is of paramount importance. According to Di Rosa and Gebhardt, T cells (including regulatory CD4+ T cells) make up for 3-8% of all nucleated BM cells. In context with infections, autoimmune reactions and neoplastic diseases antigens are presented by dendritic cells (DC). T cells react to these signals via differentiation into effector and memory T cells. After an effective antigen-specific immune response the respective memory T cells persist in the BM (BM-resident memory T cells) as well as in tissues of the pathogen entry (tissue-resident memory, TRM, T cells). Di Rosa and Gebhardt could show that the majority of memory-phenotype T-cell subsets is motile circulating in the blood between BM and peripheral lymphatic tissues. Although most of the circulating BM memory T cells are quiescent their local proliferation is higher than in the spleen or lymph nodes. Therefore, the BM forms an important reservoir for long-lived memory T cells including central memory and effector memory T cells which become re-activated upon antigen presentation – all deriving from the same set of precursors. Infectious agents and cytokines promote the recirculation of T cells from the BM to the blood. TRM cells are quiescent and sessile in skin/mucosal tissues (Di Rosa & Gebhardt, 2016).

9.2.2. CD8+ tumor-infiltrating lymphocytes in acute lymphoblastic leukemia

Pediatric tumors are known to present lower numbers of somatic mutations and consequently less tumor-associated antigens (TAA). However, in their publication Zamora et al. emphasized the relevance of a neoantigen-specific anti-tumor response in context with acute lymphoblastic leukemia (ALL) after processing and presentation of mutant proteins. The authors stated that immunodominance (CD8+ T cells restricted to one or two neoepitopes) plays an important role in shaping an effective anti-tumor T-cell response leading to highly functional CD8+ effector T cells, which thus function as tumor-infiltrating lymphocytes (TIL). It was shown that 5-28 neoantigens per patient were sufficient to elicit an effective T-cell response despite a low mutational burden. CD8+ TILs were identified in all six samples of pediatric ALL patients and showed expression of markers indicating antigen-specific stimulation (PD-1, TIM-3, CD137). CD8+ TIL effector function itself was monitored by the production of Interferon-γ (IFN-γ) and tumor necrosis factor (TNF-α) (Zamora et al., 2019).

The results of Zamora et al. strongly suggest the ALL to be an immunogenic disease despite low mutational burden despite low mutational burden. CD8+ TILs in the BM of ALL patients seem to be

specific for the tumor-neoepitopes leading to tumor-antigen specific interaction of ALL blasts and CD8+ T cells located in the microenvironment BM (therefore referred to as TILs).

9.2.3. T-cell exhaustion and impaired T-cell function

One of the questions at hand was whether physiological T cells can detect malignant T-ALL blasts and whether an interaction occurs between these two populations (p.e. in sense of T-cell exhaustion). T-cell exhaustion can be the outcome of continuous antigen presentation to T-cells and might result from blast-T cell interaction in the BM. T-cell exhaustion is a common phenomenon observed in connection with chronic viral infections and tumor diseases and describes a differentiation of T cells towards a hyporesponsive state (Philip & Schietinger, 2019). As mentioned by Jiang et al., the complex process of T-cell exhaustion in the tumor microenvironment (TME) presents a common problem when assessing the mechanisms of tumor development and treatment options for malignancies (Jiang et al., 2015). Zarour concluded that effective tumor elimination requires functional effector T cells after showing the paradox of CD8+ T-cell infiltration and insufficient tumor elimination in cases of advanced malignancies (Zarour, 2016). Common characteristics of exhausted T cells include the overexpression of co-inhibitory molecules such as PD-1, LAG-3, TIM-3, CTLA-4, BTLA and TIGIT (Jiang et al., 2015).

The process of T-cell exhaustion is known to be accompanied by impaired cytokine secretion and decreased cytolytic activity leading to insufficient tumor elimination. As a result, the upregulation of co-inhibitory markers such as CTLA-4 and TIM-3 go hand in hand with decreased proliferation and cytokine secretion such as IL-2, TNF-α, IFN-γ and Granzyme B (Jiang et al., 2015).

9.3. Discussion of detected alterations in bmT cells of pediatric T-ALL patients

9.3.1. BmT-cell exhaustion of CD4+ and CD8+ bmT cells of pediatric T-ALL patients

CD4+ and CD8+ bmT cells of pediatric T-ALL patients showed alterations in the distribution of maturation stages towards a more matured phenotype indicating a chronic immune response. Flow cytometry analysis of HCH T-ALL patients showed a significant upregulation of extracellular LAG-3 and TIM-3 and intracellular CTLA-4 on/in CD8+ bmT cells compared to the expression levels on/in bmT cells of healthy BM donors. Observed effects on CD4+ bmT cells were similar and included the significant upregulation of co-inhibitory markers 2B4, TIM-3 and CD57. Aside of increased co-inhibitory markers we could observe an upregulation of co-stimulatory marker ICOS on CD4+ bmT cells. This led us to the question whether T-cell exhaustion and upregulation of co-inhibitory molecules can be seen as the results of chronic T-cell activation via tumor specific antigens (TSA).

These findings in flow cytometry may point towards CD4+ and CD8+ bmT-cell exhaustion and could be supported by RNA-sequencing data of CD8+ bmT cells (significant overexpression of the genes LAG3 and CTLA4 in HCH patients).

Until now, no experiments regarding effector function of exhausted bmT cells in pediatric T-ALL were performed. However, the RNA-sequencing data of CD8+ bmT cells showed increased gene expression of Granzyme B, Perforin 1 and Granulysin in cases of T-ALL patients compared to healthy controls (compare subchapter 8.7). This led to the question why CD8+ bmT cells lose their ability to effectively destroy tumor cells despite increased RNA levels of Granzyme B, Perforin 1 and Granulysin on gene level within the cell cytoplasm. Decreased proliferation and thereby BM frequency of T cells and impaired cytokine secretion could present a possible explanation for T-cell hyporesponsiveness and impaired T-cell function (Jiang et al., 2015).

As the exhaustion of CD4+ and CD8+ TILs is known to cause insufficient tumor elimination reversing the T-cell anergy and restoring T-cell effector function by targeting responsible receptors and mechanisms of T-cell exhaustion shows a promising approach and will be further discussed (Zarour, 2016). This will be further discussed in subchapter 9.5.1.

9.3.2. Blast-T cell interactions via TIGIT-CD112 axis

One of our projects´ main objectives was the identification of possible specific blast-T cell interactions which might indicate a direct interaction between blasts and bmT cells. As mentioned in subchapter 8.2.1, TIGIT was one of the co-inhibitory molecules upregulated on the surface of bmT cells (not significant). TIGIT is known to decrease of T-cell proliferation, proinflammatory cytokine production; therefore, mediating T-cell inhibition and exhaustion (Joller et al., 2011; Yu et al., 2009).

T-ALL blasts in the BM of pediatric T-ALL patients repeatedly expressed high levels of CD112 on their surface which presents one of possible ligand for TIGIT mediating T-cell inhibition. The combination of CD112 upregulation on the leukemic blasts surface combined with the TIGIT upregulation on CD4+ and CD8+ bmT cells suggests a possible interaction and supports the hypothesis that the malign cells actively develop mechanisms inducing T-cell inhibition.

However, this possible blast-T cell interaction raises further questions due to following limitations:

1) CD226 and CD112R – alternative binding partners of CD112 – and CD155 – an alternative binding partner of TIGIT – were not measured (Solomon & Garrido-Laguna, 2018).

2) In cases of the CoALL samples CD112 was not expressed on the blasts surface suggesting CD112 to be instable depending on freezing and storage conditions. Therefore, a validation of using the CoALL group as validation cohort.
3) Since NK-cells could not be assessed a possible mechanism of NK cell suppression in the BM of pediatric T-ALL patients can neither be proven nor excluded. In literature a suppressive role of TIGIT on NK cells could be shown (Xu et al., 2017).

Following those limitations many questions regarding the relevance of the blast-T cell interaction via the CD112-TIGIT axis remain unanswered. Prior to proposing a clear working hypothesis about the interaction there is a great need for further testing. However, if there is indeed an interaction via the named axis the blockade could present an alternative treatment strategy.

9.3.3. TIM-3 upregulation on CD4+ and CD8+ bmT cells correlates with increased risk of relapse

In subchapter 8.4.3 we could show that upregulation of the surface marker TIM-3 on CD4+ and CD8+ bmT-cells might be co-responsible for the insufficient tumor elimination leading to increased risk of disease recurrence. By comparing initial diagnosis of future relapse and no future relapse T-ALL patients we could detect that pediatric T-ALL patients with high TIM-3 expression levels on the CD4+ and CD8+ bmT cells also seemed to have a higher risk of relapse development.

Sakuishi could show that PD-1 and TIM-3 are expressed in approximately 50% of CD8+ TILs in various tumor entities. PD-1+TIM-3+ CD8+ T cells were unable to proliferate and produce IL-2, TNF-α and IFN-γ in vitro as well as in mouse models (Sakuishi et al., 2010). In melanoma patients the BTLA+PD-1+TIM-3+ CD8+ T-cell population produced less IFN-γ, TNF-α and IL-2. The combined blockade of above-named IC could increase proliferation, expansion of CD8+ T-cells (Fourcade et al., 2012). These findings match with the publication of Zhou et al. who could further show that increased expression levels of TIM-3 are associated with a poor survival prognosis for patients with solid tumors such as colon cancer (Zhou et al., 2015). Similar results were published by Cheng et al. examining the expression of TIM-3 in gastric cancer and its relationship with prognosis (Cheng et al., 2015).

The analysis of TIM-3 expression levels on CD4+ and CD8+ bmT cells at initial diagnosis as such could possibly present an additional parameter for T-ALL risk stratification. Depending on a prior selected cut off an intensification of treatment could be used to lower the risk of relapse in high-risk patients with high TIM-3 expression levels on bmT-cell subsets. However, further prospective analysis and a better understanding of mechanisms involved are necessary for integrating TIM-3 in clinical routine.

9.3.4. Decreased frequency of regulatory T cells in the BM of pediatric T-ALL patients compared to healthy BM donors

T_{regs} are known to suppress effector T-cell function and therefore induce poor anti-tumor immune response and clinical prognosis (Tanaka & Sakaguchi, 2017). According to Wherry et al. increased T_{regs} infiltration in the TME induces dysfunction of cytotoxic T lymphocytes as well as T-cell exhaustion (Wherry & Kurachi, 2015). In their review Dees et al. described the T_{regs} accumulation in the tumor tissue and peripheral blood as part of the tumor´s escape from the immune system (Dees, Ganesan, Singh, & Grewal, 2021). Due to those publications and the presence of exhaustion markers (TIM-3, LAG-3 and CTLA-4) on/in CD4+ and CD8+ bmT cells we anticipated increased T_{regs} frequencies in the TME BM. Contrary to expectations, pediatric T-ALL patients without future relapse showed decreased T_{regs} percentages in the BM at initial diagnosis compared to the healthy control. In cases of pediatric T-ALL patients with future relapse T_{regs} frequencies at initial diagnosis were further downregulated. According to Niedźwiecki et al. T_{regs} have the capacity to suppress functionality of B cells, NK cells, T-cell subpopulations as well as macrophages and dendritic cells. In their review the authors point towards increased T_{regs} levels in a variety of cancers including different leukemia entities compared to the healthy control. Initial chemotherapy led to a significant decrease of the T_{regs}- frequency correlating remission. High expression of T_{regs} correlated with disease progression in solid tumors. The authors even propose to include the determination of T_{regs} levels for assessing disease severity and prognosis of pediatric ALL (Niedźwiecki et al., 2019). Those results stand in contrast to our findings. In cases of pediatric T-ALL patients low T_{regs} frequencies might cohere with less suppression of the bmT cells as well as the leukemic T cell blasts. Possibly, the blasts benefit even more from the decreased T_{regs} frequency than the bmT cells.

The upregulation of ectoencymes CD39 and CD73 and surface marker CD25 were shown to have a negative impact on effector T-cell functionality (Jiang et al., 2015). However, as mentioned in subchapter 8.2.1.4 the total number of T_{regs} was too low for a more detailed analysis regarding expression of surface markers on T_{regs}. Further characterization could have provided more information about their role in the involvement and mechanisms of pediatric T-ALL including possible targets for an immunotherapeutic approach.

As T-ALL is a malignancy deriving from T cell progenitors, T_{regs} could play a fundamentally different role in this disease: they might impact both physiological T cells and leukemic T cells and consequently might lead to impaired T-cell functionality and reduced leukemia proliferation at the same time. Hatzioannou et al. argue that an antigen specific therapy (e.g., checkpoint inhibition) could lead to tumor regression (Hatzioannou et al., 2021). In general, the blockade of specific receptors on the T_{regs}

surface could enhance an anti-tumor response but also result in severe autoimmune responses. Proof of this hypothesis is still missing underlining the need for further research in this area. There are several Phase I trials researching alternative treatment options targeting T_{regs} (Dees et al., 2021).

9.4. Alterations of leukemic T-ALL blasts in the BM of pediatric T-ALL patients

9.4.1. Disbalance of co-stimulatory and co-inhibitory molecules on the blasts surface

While most of the publications on malignancies in the TME blood or BM comment on the expression of co-stimulatory and co-inhibitory molecules on the surface of T cells in leukemia patients we could observe an altered checkpoint profile of leukemic blasts compared to the physiological TCP of healthy BM donors. The malignant T-ALL blasts showed:

1) Upregulation of co-stimulatory surface molecules: CD28, CD27, OX40, CD70, ICOS, CD127.
2) Downregulation of co-inhibitory surface molecules: CD160, TIGIT, 2B4, TIM-3, CD57, HVEM, BTLA, CD39.

Here the downregulation of co-inhibitory markers was more prominent than the upregulation of co-stimulatory markers. Biologically both mechanisms seem very logical and could be leading to continuous stimulation, growth, proliferation, and increased survival of the leukemic blasts. The sum of upregulation of co-stimulatory markers and downregulation of co-inhibitory molecules could play an essential role in the leukemia biology.

As this study only comprises descriptive data, the functional relevance of co-stimulatory and co-inhibitory molecules in T-ALL will have to be analyzed in future studies.

9.4.2. Upregulation of co-stimulatory molecule CD28 on the surface of T-ALL blasts

One of the most prominent results was the upregulation of the co-stimulatory marker CD28: Leukemic blasts showed a CD28 expression level above 50% in 38 out of 50 cases. Healthy BM donors showed expression levels below 5% on the surface of physiological TCP.

CD28 is known to be a co-stimulatory receptor on T cells binding to the surface markers CD80 and CD86 that are commonly expressed by dendritic cells (DC), macrophages and eosinophils. Murray et al. (2014) could show that CD28 overexpression on multiple myeloma (MM) cells (also expressing CD80 and CD86) leads to pro-survival signaling and chemotherapy resistance. The authors argue that MM cell survival is dependent on the interaction between MM cells and the stromal/cellular compartment of the BM. CD28 activation leads to a proliferative signaling via the PI3K/Akt/FoxO3a/Bim pathway which is known to be involved in the development of many malignancies (Murray et al., 2014). For

pediatric T-ALL we could not detect a prognostic relevance of CD28 expression levels on the blasts surface on the events relapse or death.

Interestingly, 13/24 HCH samples and 30/32 CoALL samples showed CD28 expression levels >50% on the surface of leukemic T-ALL blasts. This difference can, however, be partly explained by the difference in storage and freezing conditions (also see subchapter 9.1.2). The concept of T cell malignancies being fueled by CD28 signaling is supported by Rohr et al. who identified recurrent activating mutations in CD28 in peripheral T-cell lymphomas (Rohr et al., 2016). Sakamoto et al. could show that CD28 gene alterations are common in adult T-cell leukemia/lymphoma (ATL), in general 33% of the patients showed alterations involving the CD28 gene. The authors connected CD28 activating mutations with an aggressive clinical course and chemotherapy resistance in ATL patients without hematopoietic stem cell transplantation (Sakamoto et al., 2021).

There is a need for further experiments examining the role of CD28 expression in T-ALL and the question regarding an interaction of CD28+ T-ALL blasts with CD80/CD86 expressing cell populations in the TME BM (flow cytometric evaluation not included in the project). Sequencing of sorted T-ALL blast DNA (which have been generated during this project) could provide further information about the interplay between genotype, transcriptome and CD28 surface expression.

9.4.3. PD-1 upregulation on T-ALL blasts correlates with increased risk of relapse

Pediatric T-ALL patients at initial diagnosis with PD-1 expression levels >8.9% on the blasts surface showed a significantly higher risk of developing a relapse than those with expression levels <8.9%. A significantly increased risk could be observed for the entirety of measured T-ALL samples as well as the isolated analysis of the HCH samples (the CoALL cohort showed the same trend, ns).
According to Jiang at al. PD-1 is one of the main regulators of T-cell exhaustion (Jiang et al., 2015). PD-1 overexpression is known to be overexpressed on the surface of CD8+ TILs in various tumor entities (including Hodgkin´s lymphoma, melanoma, hepatocellular carcinoma, and gastric cancer) (Ahmadzadeh et al., 2009; Fourcade et al., 2009; Gehring et al., 2009; Saito, Kuroda, Matsunaga, Osaki, & Ikeguchi, 2013; Yamamoto et al., 2008). The downstream intracellular signal transduction indicates involvement of SHP-2 phosphorylation and resulting decreased IFN-γ production (Yamamoto et al., 2008). Mahoney et al. state that T-cells upregulate PD-L1 after chronic immune response, consequently leading to maintenance of immunosuppression in the TME by binding to its receptor PD-1. This mechanism was described as one possible explanation of why direct stimulation of the immune system often fails (Mahoney, Rennert, & Freeman, 2015). Regarding tumor entities in the TME BM

Kong et al. could show an increased risk of relapse in AML patients post allogeneic stem cell transplantation in combination with increased PD-1 expression levels on T cells (Kong et al., 2015).

Data examining the role of PD-1/PD-L1 in pediatric T-ALL is still missing. However, in analogy to mentioned reports on PD-1 in activated T cells, a role for cellular functions seems plausible in pediatric T-ALL. Wartewig et al. could prominently demonstrate PD-1 to be a haploinsufficient suppressor of T-cell lymphomagenesis frequently altered in T-cell lymphomas. PD-1 is known to be involved in the prevention of immunopathology after antigen-induced T-cell activation. This includes the limitation of antigen-driven T-cell proliferation and survival in suppressive environments (e.g., in cancer and chronic infection). PD-1 activation led to increased levels of the tumor suppressor PTEN and attenuated signaling via the kinases AKT and PKC in pre-malignant cells. Homo- or heterozygous deletion of PD-1 was shown to induce unrestricted T-cell growth and rapid development of highly aggressive lymphomas (Wartewig et al., 2017).

The strong involvement of PD-1 in T-cell exhaustion, in maintenance of the immunosuppressive TME and the role of a PD-1 gene locus mutation underline the need for further examination of the origin and mechanisms of PD-1 in the development of pediatric T-ALL. In summary, one attractive scenario emerges in context with the data on PD-1 as tumor suppressor by Wartewig et al. (2017): PD-1 expression is a reaction of leukemic blasts to strong proliferative signals originating from genetic driver mutations. Thus, PD-1 expression is an epiphenomenon that resonates the genetic landscape of T-ALL blasts and indicates an inferior outcome.

9.5. Perspective and therapeutic implications

Highly toxic salvage chemotherapy commonly used in leukemia treatment protocols is known to result in severe long-term side effects including graft versus host disease and the development of secondary malignancies. Immunotherapy presents a promising alternative approach to the salvage chemotherapy in T-ALL treatment protocols (especially for relapse and refractory T-ALL patients) and aims to reduce the risk of severe off-target effects (Durinck et al., 2015).

In terms of our project, the checkpoint profile of physiological CD4+ and CD8+ bmT cells was comparable for all leukemia patients showing signs of T-cell exhaustion, respective chronic activation. However, the leukemic T-cell blasts of pediatric T-ALL patients were found to be highly heterogeneous regarding expression of co-stimulatory and co-inhibitory IC as well as lineage (CD45, CD3, CD4, CD8, CD56) and maturation markers (CD45R0, CD62l).

T-ALL in general is seen as the result of a multistep process caused by accumulating mutations in tumor suppressor genes and oncogenes (Sanchez-Martin & Ferrando, 2017). ALL blasts are known for a low mutational burden compared to other tumor entities such as malign melanoma (Alexandrov et al., 2013). As such the identification and targeting of possible tumor specific antigens (TSA) on the blasts surface might present as more challenging than in other tumor entities with high immunogenicity.
This issue is further complicated since tumor antigens are self-molecules and therefore show weak immunogenicity. High-avidity T cells are deleted in the selection process (Kim & Ahmed, 2010).

9.5.1. Antibody mediated immunotherapy for pediatric T-ALL

Since mechanisms of T-cell exhaustion are known to lead to an immunosuppressing TME therapeutic approaches targeting tumor TSA directly tend to fail. For many malignancies including the pediatric BCP-ALL, melanoma, Hodgkin lymphoma and non-small-cell lung cancer immune checkpoint inhibitors (CPI) blocking co-inhibitory molecules on the surface (such as PD-1 and CTLA-4) of physiological T cells have already been successfully used for treatment (Mahoney et al., 2015).

Representative for the treatment via checkpoint inhibitors, the blockade of CTLA-4 via Ipilimumab in patients with advanced melanoma received FDA approval in 2010 (Pardoll, 2012). For instance a phase III trial of patients with metastasized melanoma showed a survival benefit including long-term control after treatment with Ipilimumab (medial overall survival: 10.1 months in Ipilimumab-only group compared to 6.4 months in gp100-alone group) (Hodi et al., 2010).
A clinical case report gave account to a 12-year-old patient with refractory BCP-ALL who was treated with Blinatumomab (CD3/CD19 bispecific T cell engager, BiTE) and Pembrolizumab (anti PD-L1 antibody). The side effects were limited, and anti-leukemic response was observed. The patient unfortunately suffered from relapse 2 months after the treatment (Feucht et al., 2016).
First data referring to Adult T-ALL (ATLL) suggests a controversy of PD-1/PD-L1 blockade. According to Jalili-Nik, Soltani, Mashkani, Rafatpanah, & Hashemy the blockade also led to clonal expansion of leukemic blasts and ineffective anti-tumor response due to PD-L1 3´-UTR disruption. (Jalili-Nik, Soltani, Mashkani, Rafatpanah, & Hashemy, 2021).

The combination of chemotherapy and immunotherapy is already in use in terms of standard treatment protocols, e.g., anti-CD20 monoclonal antibody Rituximab as part of R-CHOP, as such presenting a possibility to increase response rates and induce complete remission (Mahoney et al., 2015). After proving the presence of various exhaustion markers on the surface of CD4+ and CD8+ bmT cells in our project the combinatorial blockade of T-cell exhaustion mediating receptors could partially revert T-cell exhaustion and immune escape: Zarour et al. proposed combinations such as anti PD-1 or

anti PD-L1 antibodies plus CTLA-4, LAG-3, TIM-3 or TIGIT blockade (Zarour, 2016). According to Pauken and Wherry a combinatorial therapy seems expedient to improve the outcome. Approaches could include the targeting of inhibitory receptors, as well as soluble agents and adoptive immune cell therapy (Pauken & Wherry, 2015). Mahoney et al. claimed timing and choice of chemotherapeutic treatment to be of importance; prior lymphocyte depleting chemotherapy regimens would prevent the effects of checkpoint inhibitors (Mahoney et al., 2015).

Prior to therapy PD-1+TIM-3+BLTA+ CD8+ T cells in melanoma were unable to proliferate and produce IL-2, TNF-α, IFN-y and Granzyme B. A combined blockade increased expansion, proliferation, and cytokine production (Fourcade et al., 2012). Johnston et al. reported that blockade of PD-L1 and TIGIT could restore CD8+ T-cell effector function and result in tumor clearance (Johnston et al., 2014). In two clinical trials melanoma patients receiving Nivolumab (PD-1) and Ipilimumab (CTLA-4) showed better response rates as well as longer progression free survival compared to the Ipilimumab-only group (Postow et al., 2015; Wolchok et al., 2013). However, combined checkpoint blockade increased the risk of toxicity; grade 3 and 4 adverse events were observed in 54% of the patients receiving CTLA-4 plus PD-1 antibodies compared to 24% in patients with Ipilimumab-only (Postow et al., 2015).

Since physiological bmT cells and leukemic T-ALL blasts derive from the same lineage we presume that both populations have the same capacity of checkpoint expression. Therefore, the identification of a co-inhibitory marker that is exclusively expressed on the physiological bmT cells and precursors but not on the leukemic blasts seems challenging. However, this is a necessity to guarantee a specific blocking of co-inhibitory IC exclusively on physiological bmT cells. Blocking co-inhibitory pathways in case of malignant T-ALL blasts would be counterproductive.

9.5.2. Synthetic Immunotherapy

According to Novikov at al. the analysis of the TCR gives limited information about clonality. Therefore the authors identified TRBC1 as a suitable parameter to determine T-cell clonality (Novikov et al., 2019). Maciocia et al. investigated TRBC1 as target for CAR T-cell therapy in matured T-cell malignancies. The authors summarize matured T-cell malignancies to be restricted to either TRBC1 or TRBC2 expression and developed anti-TRBC1 CAR T cells that eradicated all TRBC1+ cells including physiological T cells. The TRBC1 specific approach resulted in an eradication of tumor cells while enough functional T cells (those with TRBC2) remained (Maciocia et al., 2017). The findings of Maciocia et al. stand in contrast to the data we obtained in our project regarding pediatric T-ALL patients. TRBC1 was only expressed by the T-ALL blasts of 2 patient samples. The expression level was comparable to that of healthy CD4+ or CD8+ bmT cells (30-35% TRBC1+). The percentage of TRBC1+ cells itself showed to be variable when comparing the blasts of initial diagnosis with those from relapses which suggests

the co-existence of different malign clones. Therefore, application of an anti-TRBC1 CAR T cell mediated approach seems insufficient for pediatric T-ALL patients since the disease seems to be polyclonal and therefore therapy would target only part of the blast population.

Transferring the CAR T-cell approach to T-cell malignancies targeting CD7 presents another possibility. CD7 is expressed on the surface of more than 95% of all T-cell malignancies. According to Li et al. CD7-targeted CAR-T cells could effectively eliminate T-ALL including long-term duration of response (Li et al., 2021). In our project, 53/53 T-ALL blasts populations evaluated were strongly positive for CD7 (>90%) whereas expression levels on physiological TCP were below 10%. Therefore, a CAR T cell approach would primarily target T-ALL blasts and physiological CD4+/CD8+ bmT cells and NK cells (also high levels of CD7 expression). Gomes-Silva et al. could show that the genomic disruption of the target antigen CD7 on T cells could overcome CAR T-cell fratricide. The CD7 knock-out did not confer a functional disadvantage in T cells; the T cells showed high cytotoxicity against malignant T cells in leukemia cell lines and primary T-cell malignancies in vitro and in vivo. Low off-target-organ toxicity was observed - limited to CD4+ and CD8+ T cells and NK cells (Gomes-Silva et al., 2017). Safety and efficacy will have to be examined in further studies (Li et al., 2021).

As such, the CAR T cell mediated therapy presents another promising alternative to salvage therapy. However, the fact that T-ALL blasts and physiological bmT cells derive from the same lineage and in general have the same repertoire of surface molecules seems to complicate the selection of possible antigens suitable for a blast specific CAR T cell approach.

Facing this issue Driouk et al. examined the functionality as well as off target effects of CAR T-cells targeting NKG2D-ligands in vitro. NKG2D is expressed on AML and T-ALL blasts but not on healthy T cells. The authors could show a specific increase of T-cell efficacy including increased degranulation and cytokine production. The authors proposed a pretreatment via HDAC-inhibitors to enhance NKG2D-ligand expression on AML or T-ALL blasts prior to treatment via NKG2D CAR T-cells to increase the therapeutic potential (Driouk et al., 2020).

9.5.3. Perspective – emerging project: functional relevance of co-signaling molecules in T-ALL cell lines

As mentioned above the upregulation of co-stimulatory (e.g., CD28, ICOS) and downregulation of co-inhibitory molecules (e.g., TIGIT, CD160) on the surface of T-ALL blasts was one of the projects´ main findings (compare subchapter 9.4.1).

Murray et al. could show that a blockade of the CD28 – CD80/CD86 axis via CTLA-4 could reduce disease progression, restore chemotherapy sensitivity, and reduce tumor burden in Multiple Myeloma (MM). (Murray et al., 2014). In pediatric BCP-ALL the blockade of a co-stimulatory marker like CD80/CD86 led to a decreased proliferation, IL2 and IFN-y secretion (Feucht et al., 2016). Rohr et al. claimed the targeting of CD28 in CD28-mutated peripheral lymphomas could be one possible alternative approach (Rohr et al., 2016). Considering CD28 blockade as possible treatment option for T-ALL patients, the question concerning an interaction of CD28+ T-ALL blasts with CD80/CD86 expressing cell populations in the TME BM and side effects of CD28 depletion on physiological CD28+ T cells remains unanswered. Since CD28 is highly expressed on the physiological CD4+ and CD8+ bmT cells only an isolated knock-out/knock-down of CD28 on the leukemic cells seems expedient and might result in apoptosis induction.

In this context possible future experiments include the investigation of co-signaling molecules in T-ALL cell lines and of the disbalance of co-stimulatory and co-inhibitory molecules in pediatric T-ALL.

Future scope:

1) How does a knock-out and doxycycline dependent knockdown of CD28, ICOS and LCK affect the blast´s viability, proliferation, cell cycle and cellular senescence?
2) How does a doxycycline dependent knock-in of CD28, ICOS, CD160 and TIGIT affect the blast´s proliferation, viability, cell cycle and senescence?
3) Is there a possibility to target the blasts with kinase inhibitors (Imatinib, PP1, Saracatinib)?

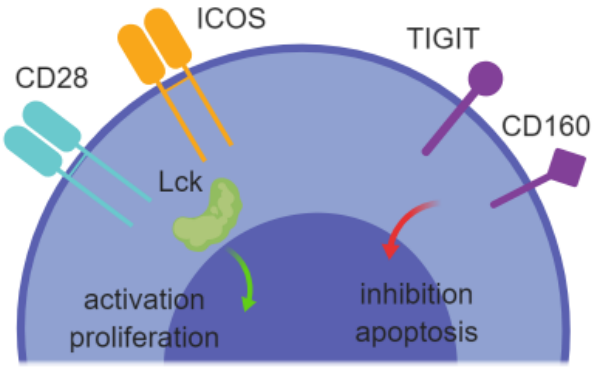

Figure 48: Model of co-stimulatory and co-inhibitory molecules on leukemic cells in T-ALL cell lines

10. Literature

Agnusdei, V., Minuzzo, S., Pinazza, M., Gasparini, A., Pezzè, L., Amaro, A. A., . . . Indraccolo, S. (2020). Dissecting molecular mechanisms of resistance to NOTCH1-targeted therapy in T-cell acute lymphoblastic leukemia xenografts. *Haematologica, 105*(5), 1317-1328. doi:10.3324/haematol.2019.217687

Ahmadzadeh, M., Johnson, L. A., Heemskerk, B., Wunderlich, J. R., Dudley, M. E., White, D. E., & Rosenberg, S. A. (2009). Tumor antigen-specific CD8 T cells infiltrating the tumor express high levels of PD-1 and are functionally impaired. *Blood, 114*(8), 1537-1544. doi:10.1182/blood-2008-12-195792

Alexandrov, L. B., Nik-Zainal, S., Wedge, D. C., Aparicio, S. A., Behjati, S., Biankin, A. V., . . . Stratton, M. R. (2013). Signatures of mutational processes in human cancer. *Nature, 500*(7463), 415-421. doi:10.1038/nature12477

Andorsky, D. J., & Timmerman, J. M. (2008). Interleukin-21: biology and application to cancer therapy. *Expert Opin Biol Ther, 8*(9), 1295-1307. doi:10.1517/14712598.8.9.1295

Arber, D. A., Orazi, A., Hasserjian, R., Thiele, J., Borowitz, M. J., Le Beau, M. M., . . . Vardiman, J. W. (2016). The 2016 revision to the World Health Organization classification of myeloid neoplasms and acute leukemia. *Blood, 127*(20), 2391-2405. doi:10.1182/blood-2016-03-643544

Basso, K., Mussolin, L., Lettieri, A., Brahmachary, M., Lim, W. K., Califano, A., . . . Rosolen, A. (2011). T-cell lymphoblastic lymphoma shows differences and similarities with T-cell acute lymphoblastic leukemia by genomic and gene expression analyses. *Genes Chromosomes Cancer, 50*(12), 1063-1075. doi:10.1002/gcc.20924

Belver, L., & Ferrando, A. (2016). The genetics and mechanisms of T cell acute lymphoblastic leukaemia. *Nat Rev Cancer, 16*(8), 494-507. doi:10.1038/nrc.2016.63

Berg, S. L., Blaney, S. M., Devidas, M., Lampkin, T. A., Murgo, A., Bernstein, M., . . . Harris, M. B. (2005). Phase II study of nelarabine (compound 506U78) in children and young adults with refractory T-cell malignancies: a report from the Children's Oncology Group. *J Clin Oncol, 23*(15), 3376-3382. doi:10.1200/jco.2005.03.426

Bernbeck, B., Wüller, D., Janssen, G., Wessalowski, R., Göbel, U., & Schneider, D. T. (2009). Symptoms of childhood acute lymphoblastic leukemia: red flags to recognize leukemia in daily practice. *Klin Padiatr, 221*(6), 369-373. doi:10.1055/s-0029-1239538

Boekstegers, A. M., Blaeschke, F., Schmid, I., Wiebking, V., Immler, S., Hoffmann, F., . . . Feuchtinger, T. (2017). MRD response in a refractory paediatric T-ALL patient through anti-programmed cell death 1 (PD-1) Ab treatment associated with induction of fatal GvHD. *Bone Marrow Transplant, 52*(8), 1221-1224. doi:10.1038/bmt.2017.107

Cheng, G., Li, M., Wu, J., Ji, M., Fang, C., Shi, H., . . . Jiang, J. (2015). Expression of Tim-3 in gastric cancer tissue and its relationship with prognosis. *Int J Clin Exp Pathol, 8*(8), 9452-9457.

Condo, I., & Testi, R. (2000). Intracellular mediators of programmed cell death initiated at the cell surface receptor Fas. *Transpl Int, 13 Suppl 1*, S3-6.

Curran, K. J., Margossian, S. P., Kernan, N. A., Silverman, L. B., Williams, D. A., Shukla, N., . . . Brentjens, R. J. (2019). Toxicity and response after CD19-specific CAR T-cell therapy in pediatric/young adult relapsed/refractory B-ALL. *Blood, 134*(26), 2361-2368. doi:10.1182/blood.2019001641

Dees, S., Ganesan, R., Singh, S., & Grewal, I. S. (2021). Regulatory T cell targeting in cancer: Emerging strategies in immunotherapy. *Eur J Immunol, 51*(2), 280-291. doi:10.1002/eji.202048992

Di Rosa, F., & Gebhardt, T. (2016). Bone Marrow T Cells and the Integrated Functions of Recirculating and Tissue-Resident Memory T Cells. *Front Immunol, 7*, 51. doi:10.3389/fimmu.2016.00051

Driouk, L., Gicobi, J. K., Kamihara, Y., Rutherford, K., Dranoff, G., Ritz, J., & Baumeister, S. H. C. (2020). Chimeric Antigen Receptor T Cells Targeting NKG2D-Ligands Show Robust Efficacy Against Acute Myeloid Leukemia and T-Cell Acute Lymphoblastic Leukemia. *Front Immunol, 11*, 580328. doi:10.3389/fimmu.2020.580328

Dunsmore, K. P., Winter, S. S., Devidas, M., Wood, B. L., Esiashvili, N., Chen, Z., . . . Hunger, S. P. (2020). Children's Oncology Group AALL0434: A Phase III Randomized Clinical Trial Testing Nelarabine in Newly Diagnosed T-Cell Acute Lymphoblastic Leukemia. *Journal of Clinical Oncology, 38*(28), 3282-3293. doi:10.1200/jco.20.00256

Durinck, K., Goossens, S., Peirs, S., Wallaert, A., Van Loocke, W., Matthijssens, F., . . . Van Vlierberghe, P. (2015). Novel biological insights in T-cell acute lymphoblastic leukemia. *Exp Hematol, 43*(8), 625-639. doi:10.1016/j.exphem.2015.05.017

Fattizzo, B., Rosa, J., Giannotta, J. A., Baldini, L., & Fracchiolla, N. S. (2020). The Physiopathology of T-Cell Acute Lymphoblastic Leukemia: Focus on Molecular Aspects. *Frontiers in Oncology, 10*. doi:10.3389/fonc.2020.00273

Ferreira, J. A. (2007). The Benjamini-Hochberg method in the case of discrete test statistics. *Int J Biostat, 3*(1), Article 11. doi:10.2202/1557-4679.1065

Feucht, J., Kayser, S., Gorodezki, D., Hamieh, M., Doring, M., Blaeschke, F., . . . Feuchtinger, T. (2016). T-cell responses against CD19+ pediatric acute lymphoblastic leukemia mediated by bispecific T-cell engager (BiTE) are regulated contrarily by PD-L1 and CD80/CD86 on leukemic blasts. *Oncotarget, 7*(47), 76902-76919. doi:10.18632/oncotarget.12357

Fielding, A. K., Richards, S. M., Chopra, R., Lazarus, H. M., Litzow, M. R., Buck, G., . . . Group, t. E. C. O. (2006). Outcome of 609 adults after relapse of acute lymphoblastic leukemia (ALL); an MRC UKALL12/ECOG 2993 study. *Blood, 109*(3), 944-950. doi:10.1182/blood-2006-05-018192

Fourcade, J., Kudela, P., Sun, Z., Shen, H., Land, S. R., Lenzner, D., . . . Zarour, H. M. (2009). PD-1 is a regulator of NY-ESO-1-specific CD8+ T cell expansion in melanoma patients. *J Immunol, 182*(9), 5240-5249. doi:10.4049/jimmunol.0803245

Fourcade, J., Sun, Z., Pagliano, O., Guillaume, P., Luescher, I. F., Sander, C., . . . Zarour, H. M. (2012). CD8(+) T cells specific for tumor antigens can be rendered dysfunctional by the tumor microenvironment through upregulation of the inhibitory receptors BTLA and PD-1. *Cancer Res, 72*(4), 887-896. doi:10.1158/0008-5472.Can-11-2637

Gehring, A. J., Ho, Z. Z., Tan, A. T., Aung, M. O., Lee, K. H., Tan, K. C., . . . Bertoletti, A. (2009). Profile of tumor antigen-specific CD8 T cells in patients with hepatitis B virus-related hepatocellular carcinoma. *Gastroenterology, 137*(2), 682-690. doi:10.1053/j.gastro.2009.04.045

Gomes-Silva, D., Srinivasan, M., Sharma, S., Lee, C. M., Wagner, D. L., Davis, T. H., . . . Mamonkin, M. (2017). CD7-edited T cells expressing a CD7-specific CAR for the therapy of T-cell malignancies. *Blood, 130*(3), 285-296. doi:10.1182/blood-2017-01-761320

Guo, Y., Lee, Y. C., Brown, C., Zhang, W., Usherwood, E., & Noelle, R. J. (2014). Dissecting the role of retinoic acid receptor isoforms in the CD8 response to infection. *J Immunol, 192*(7), 3336-3344. doi:10.4049/jimmunol.1301949

Hatzioannou, A., Boumpas, A., Papadopoulou, M., Papafragkos, I., Varveri, A., Alissafi, T., & Verginis, P. (2021). Regulatory T Cells in Autoimmunity and Cancer: A Duplicitous Lifestyle. *Front Immunol, 12*, 731947. doi:10.3389/fimmu.2021.731947

Hodi, F. S., O'Day, S. J., McDermott, D. F., Weber, R. W., Sosman, J. A., Haanen, J. B., . . . Urba, W. J. (2010). Improved survival with ipilimumab in patients with metastatic melanoma. *N Engl J Med, 363*(8), 711-723. doi:10.1056/NEJMoa1003466

Hong, M., Clubb, J. D., & Chen, Y. Y. (2020). Engineering CAR-T Cells for Next-Generation Cancer Therapy. *Cancer Cell, 38*(4), 473-488. doi:10.1016/j.ccell.2020.07.005

Jalili-Nik, M., Soltani, A., Mashkani, B., Rafatpanah, H., & Hashemy, S. I. (2021). PD-1 and PD-L1 inhibitors foster the progression of adult T-cell Leukemia/Lymphoma. *Int Immunopharmacol, 98*, 107870. doi:10.1016/j.intimp.2021.107870

Jiang, Y., Li, Y., & Zhu, B. (2015). T-cell exhaustion in the tumor microenvironment. *Cell Death Dis, 6*, e1792. doi:10.1038/cddis.2015.162

Jiménez-Morales, S., Aranda-Uribe, I. S., Pérez-Amado, C. J., Ramírez-Bello, J., & Hidalgo-Miranda, A. (2021). Mechanisms of Immunosuppressive Tumor Evasion: Focus on Acute Lymphoblastic Leukemia. *Front Immunol, 12*, 737340. doi:10.3389/fimmu.2021.737340

Johnston, R. J., Comps-Agrar, L., Hackney, J., Yu, X., Huseni, M., Yang, Y., . . . Grogan, J. L. (2014). The immunoreceptor TIGIT regulates antitumor and antiviral CD8(+) T cell effector function. *Cancer Cell, 26*(6), 923-937. doi:10.1016/j.ccell.2014.10.018

Joller, N., Hafler, J. P., Brynedal, B., Kassam, N., Spoerl, S., Levin, S. D., . . . Kuchroo, V. K. (2011). Cutting edge: TIGIT has T cell-intrinsic inhibitory functions. *J Immunol, 186*(3), 1338-1342. doi:10.4049/jimmunol.1003081

Karrman, K., & Johansson, B. (2017). Pediatric T-cell acute lymphoblastic leukemia. *Genes Chromosomes Cancer, 56*(2), 89-116. doi:10.1002/gcc.22416

Kim, P. S., & Ahmed, R. (2010). Features of responding T cells in cancer and chronic infection. *Curr Opin Immunol, 22*(2), 223-230. doi:10.1016/j.coi.2010.02.005

Kong, Y., Zhang, J., Claxton, D. F., Ehmann, W. C., Rybka, W. B., Zhu, L., . . . Zheng, H. (2015). PD-1(hi)TIM-3(+) T cells associate with and predict leukemia relapse in AML patients post allogeneic stem cell transplantation. *Blood Cancer J, 5*, e330. doi:10.1038/bcj.2015.58

Lato, M. W., Przysucha, A., Grosman, S., Zawitkowska, J., & Lejman, M. (2021). The New Therapeutic Strategies in Pediatric T-Cell Acute Lymphoblastic Leukemia. *Int J Mol Sci, 22*(9). doi:10.3390/ijms22094502

Laumont, C. M., Vincent, K., Hesnard, L., Audemard, E., Bonneil, E., Laverdure, J. P., . . . Perreault, C. (2018). Noncoding regions are the main source of targetable tumor-specific antigens. *Sci Transl Med, 10*(470). doi:10.1126/scitranslmed.aau5516

Li, S., Wang, X., Yuan, Z., Liu, L., Luo, L., Li, Y., . . . Wang, S. (2021). Eradication of T-ALL Cells by CD7-targeted Universal CAR-T Cells and Initial Test of Ruxolitinib-based CRS Management. *Clin Cancer Res, 27*(5), 1242-1246. doi:10.1158/1078-0432.Ccr-20-1271

Liu, Y., Easton, J., Shao, Y., Maciaszek, J., Wang, Z., Wilkinson, M. R., . . . Mullighan, C. G. (2017). The genomic landscape of pediatric and young adult T-lineage acute lymphoblastic leukemia. *Nat Genet, 49*(8), 1211-1218. doi:10.1038/ng.3909

Maciocia, P. M., Wawrzyniecka, P. A., Philip, B., Ricciardelli, I., Akarca, A. U., Onuoha, S. C., . . . Pule, M. A. (2017). Targeting the T cell receptor beta-chain constant region for immunotherapy of T cell malignancies. *Nat Med, 23*(12), 1416-1423. doi:10.1038/nm.4444

Mahoney, K. M., Rennert, P. D., & Freeman, G. J. (2015). Combination cancer immunotherapy and new immunomodulatory targets. *Nat Rev Drug Discov, 14*(8), 561-584. doi:10.1038/nrd4591

Majzner, R. G., Heitzeneder, S., & Mackall, C. L. (2017). Harnessing the Immunotherapy Revolution for the Treatment of Childhood Cancers. *Cancer Cell, 31*(4), 476-485. doi:10.1016/j.ccell.2017.03.002

Maude, S. L., Frey, N., Shaw, P. A., Aplenc, R., Barrett, D. M., Bunin, N. J., . . . Grupp, S. A. (2014). Chimeric antigen receptor T cells for sustained remissions in leukemia. *N Engl J Med, 371*(16), 1507-1517. doi:10.1056/NEJMoa1407222

Miller, B. C., Sen, D. R., Al Abosy, R., Bi, K., Virkud, Y. V., LaFleur, M. W., . . . Haining, W. N. (2019). Subsets of exhausted CD8(+) T cells differentially mediate tumor control and respond to checkpoint blockade. *Nat Immunol, 20*(3), 326-336. doi:10.1038/s41590-019-0312-6

Mroczek, A., Zawitkowska, J., Kowalczyk, J., & Lejman, M. (2021). Comprehensive Overview of Gene Rearrangements in Childhood T-Cell Acute Lymphoblastic Leukaemia. *Int J Mol Sci, 22*(2). doi:10.3390/ijms22020808

Muri, J., Heer, S., Matsushita, M., Pohlmeier, L., Tortola, L., Fuhrer, T., . . . Kopf, M. (2018). The thioredoxin-1 system is essential for fueling DNA synthesis during T-cell metabolic reprogramming and proliferation. *Nat Commun, 9*(1), 1851. doi:10.1038/s41467-018-04274-w

Murray, M. E., Gavile, C. M., Nair, J. R., Koorella, C., Carlson, L. M., Buac, D., . . . Lee, K. P. (2014). CD28-mediated pro-survival signaling induces chemotherapeutic resistance in multiple myeloma. *Blood, 123*(24), 3770-3779. doi:10.1182/blood-2013-10-530964

Nakano, K., Uchimaru, K., Utsunomiya, A., Yamaguchi, K., & Watanabe, T. (2016). Dysregulation of c-Myb Pathway by Aberrant Expression of Proto-oncogene MYB Provides the Basis for Malignancy in Adult T-cell Leukemia/lymphoma Cells. *Clin Cancer Res, 22*(23), 5915-5928. doi:10.1158/1078-0432.Ccr-15-1739

Niedźwiecki, M., Budziło, O., Adamkiewicz-Drożyńska, E., Pawlik-Gwozdecka, D., Zieliński, M., Maciejka-Kembłowska, L., . . . Trzonkowski, P. (2019). CD4(+)CD25(high)CD127(low/-)FoxP(3)(+) Regulatory T-Cell Population in Acute Leukemias: A Review of the Literature. *J Immunol Res, 2019*, 2816498. doi:10.1155/2019/2816498

Novikov, N. D., Griffin, G. K., Dudley, G., Drew, M., Rojas-Rudilla, V., Lindeman, N. I., & Dorfman, D. M. (2019). Utility of a Simple and Robust Flow Cytometry Assay for Rapid Clonality Testing in Mature Peripheral T-Cell Lymphomas. *Am J Clin Pathol, 151*(5), 494-503. doi:10.1093/ajcp/aqy173

Pardoll, D. M. (2012). The blockade of immune checkpoints in cancer immunotherapy. *Nat Rev Cancer, 12*(4), 252-264. doi:10.1038/nrc3239

Pauken, K. E., & Wherry, E. J. (2015). Overcoming T cell exhaustion in infection and cancer. *Trends Immunol, 36*(4), 265-276. doi:10.1016/j.it.2015.02.008

Philip, M., & Schietinger, A. (2019). Heterogeneity and fate choice: T cell exhaustion in cancer and chronic infections. *Curr Opin Immunol, 58*, 98-103. doi:10.1016/j.coi.2019.04.014

Postow, M. A., Chesney, J., Pavlick, A. C., Robert, C., Grossmann, K., McDermott, D., . . . Hodi, F. S. (2015). Nivolumab and ipilimumab versus ipilimumab in untreated melanoma. *N Engl J Med, 372*(21), 2006-2017. doi:10.1056/NEJMoa1414428

Raetz, E. A., & Teachey, D. T. (2016). T-cell acute lymphoblastic leukemia. *Hematology Am Soc Hematol Educ Program, 2016*(1), 580-588. doi:10.1182/asheducation-2016.1.580

Rohr, J., Guo, S., Huo, J., Bouska, A., Lachel, C., Li, Y., . . . Chan, W. C. (2016). Recurrent activating mutations of CD28 in peripheral T-cell lymphomas. *Leukemia, 30*(5), 1062-1070. doi:10.1038/leu.2015.357

Saito, H., Kuroda, H., Matsunaga, T., Osaki, T., & Ikeguchi, M. (2013). Increased PD-1 expression on CD4+ and CD8+ T cells is involved in immune evasion in gastric cancer. *J Surg Oncol, 107*(5), 517-522. doi:10.1002/jso.23281

Sakamoto, Y., Ishida, T., Masaki, A., Takeshita, M., Iwasaki, H., Yonekura, K., . . . Inagaki, H. (2021). Clinical significance of CD28 gene-related activating alterations in adult T-cell leukaemia/lymphoma. *Br J Haematol, 192*(2), 281-291. doi:10.1111/bjh.17211

Sakuishi, K., Apetoh, L., Sullivan, J. M., Blazar, B. R., Kuchroo, V. K., & Anderson, A. C. (2010). Targeting Tim-3 and PD-1 pathways to reverse T cell exhaustion and restore anti-tumor immunity. *J Exp Med, 207*(10), 2187-2194. doi:10.1084/jem.20100643

Sanchez-Martin, M., & Ferrando, A. (2017). The NOTCH1-MYC highway toward T-cell acute lymphoblastic leukemia. *Blood, 129*(9), 1124-1133. doi:10.1182/blood-2016-09-692582

Schrappe, M., Valsecchi, M. G., Bartram, C. R., Schrauder, A., Panzer-Grümayer, R., Möricke, A., . . . Conter, V. (2011). Late MRD response determines relapse risk overall and in subsets of childhood T-cell ALL: results of the AIEOP-BFM-ALL 2000 study. *Blood, 118*(8), 2077-2084. doi:10.1182/blood-2011-03-338707

Solomon, B. L., & Garrido-Laguna, I. (2018). TIGIT: a novel immunotherapy target moving from bench to bedside. *Cancer Immunol Immunother, 67*(11), 1659-1667. doi:10.1007/s00262-018-2246-5

Tanaka, A., & Sakaguchi, S. (2017). Regulatory T cells in cancer immunotherapy. *Cell Res, 27*(1), 109-118. doi:10.1038/cr.2016.151

Teachey, D. T., & O'Connor, D. (2020). How I treat newly diagnosed T-cell acute lymphoblastic leukemia and T-cell lymphoblastic lymphoma in children. *Blood, 135*(3), 159-166. doi:10.1182/blood.2019001557

Thaxton, J. E., & Li, Z. (2014). To affinity and beyond: harnessing the T cell receptor for cancer immunotherapy. *Hum Vaccin Immunother, 10*(11), 3313-3321. doi:10.4161/21645515.2014.973314

Tian, Y., & Zajac, A. J. (2016). IL-21 and T Cell Differentiation: Consider the Context. *Trends Immunol, 37*(8), 557-568. doi:10.1016/j.it.2016.06.001

Voskoboinik, I., Whisstock, J. C., & Trapani, J. A. (2015). Perforin and granzymes: function, dysfunction and human pathology. *Nat Rev Immunol, 15*(6), 388-400. doi:10.1038/nri3839

Wang, Z., Wu, Z., Liu, Y., & Han, W. (2017). New development in CAR-T cell therapy. *J Hematol Oncol, 10*(1), 53. doi:10.1186/s13045-017-0423-1

Wartewig, T., Kurgyis, Z., Keppler, S., Pechloff, K., Hameister, E., Ollinger, R., . . . Ruland, J. (2017). PD-1 is a haploinsufficient suppressor of T cell lymphomagenesis. *Nature, 552*(7683), 121-125. doi:10.1038/nature24649

Weng, A. P., Ferrando, A. A., Lee, W., Morris, J. P. t., Silverman, L. B., Sanchez-Irizarry, C., . . . Aster, J. C. (2004). Activating mutations of NOTCH1 in human T cell acute lymphoblastic leukemia. *Science, 306*(5694), 269-271. doi:10.1126/science.1102160

Wherry, E. J., & Kurachi, M. (2015). Molecular and cellular insights into T cell exhaustion. *Nat Rev Immunol, 15*(8), 486-499. doi:10.1038/nri3862

Wolchok, J. D., Kluger, H., Callahan, M. K., Postow, M. A., Rizvi, N. A., Lesokhin, A. M., . . . Sznol, M. (2013). Nivolumab plus ipilimumab in advanced melanoma. *N Engl J Med, 369*(2), 122-133. doi:10.1056/NEJMoa1302369

Xu, F., Sunderland, A., Zhou, Y., Schulick, R. D., Edil, B. H., & Zhu, Y. (2017). Blockade of CD112R and TIGIT signaling sensitizes human natural killer cell functions. *Cancer Immunol Immunother, 66*(10), 1367-1375. doi:10.1007/s00262-017-2031-x

Yamamoto, R., Nishikori, M., Kitawaki, T., Sakai, T., Hishizawa, M., Tashima, M., . . . Uchiyama, T. (2008). PD-1-PD-1 ligand interaction contributes to immunosuppressive microenvironment of Hodgkin lymphoma. *Blood, 111*(6), 3220-3224. doi:10.1182/blood-2007-05-085159

Yu, X., Harden, K., Gonzalez, L. C., Francesco, M., Chiang, E., Irving, B., . . . Grogan, J. L. (2009). The surface protein TIGIT suppresses T cell activation by promoting the generation of mature immunoregulatory dendritic cells. *Nat Immunol, 10*(1), 48-57. doi:10.1038/ni.1674

Zamora, A. E., Crawford, J. C., Allen, E. K., Guo, X. J., Bakke, J., Carter, R. A., . . . Thomas, P. G. (2019). Pediatric patients with acute lymphoblastic leukemia generate abundant and functional neoantigen-specific CD8(+) T cell responses. *Sci Transl Med, 11*(498). doi:10.1126/scitranslmed.aat8549

Zarour, H. M. (2016). Reversing T-cell Dysfunction and Exhaustion in Cancer. *Clin Cancer Res, 22*(8), 1856-1864. doi:10.1158/1078-0432.Ccr-15-1849

Zhou, E., Huang, Q., Wang, J., Fang, C., Yang, L., Zhu, M., . . . Dong, M. (2015). Up-regulation of Tim-3 is associated with poor prognosis of patients with colon cancer. *Int J Clin Exp Pathol, 8*(7), 8018-8027.

11. Tables

12. Figures

13. Acknowledgements

I would like to express my gratitude to Prof. Dr. Tobias Feuchtinger for giving me the opportunity to perform my doctoral thesis in his laboratory and entrusting me with this highly interesting and challenging research project.
Further, I would like to emphasize my sincerest appreciation to my supporting supervisor Dr. Semjon Willier. With his positivity as well as with his creative skills and ambitious thinking Semjon always guided the way and maintained a clear head even in the most challenging situations.

I am extremely grateful for the trustworthy collaboration with my lab partner Paula Rothämel which included facing challenges and solving problems as a team and enjoyable moments.
Furthermore, I would also like to express my deepest gratitude to Prof. Dr. Dr. Christoph Klein and his working group for their technical and financial support. In this context, I would like to extend my sincere appreciation to Raffaele Conca and Susanne Wullinger for patiently sorting the patient samples and for providing required technical devices with the FACS.
Also, I would like to offer a special thanks to Dr. Meino Rohlfs for his support with the RNA- and ATAC-Sequencing, as well as operating the bioanalyzer with our samples.
Moreover, I would like to thank Nicola Habjan for supporting me repeatedly in the flow cytometric measurement of the CoALL samples.
I would also like to thank Dr. Matthias Heinig, Dr. Thomas Walzthöni, and Dr. Lukas Friedrich for their expertise in the bioinformatic evaluation of the RNA-samples.

I would also like to extend my thanks to all members of my working group: Dr. Franziska Blaeschke, Dr. Theresa Käuferle, Dana Stenger, Tanja Stief, Tanja Weißer, Nadine Stoll, Florian Jurgeleit, Tanja Rossmann, Larissa Deisenberger, Jasmin Mahdawi, Lena Jablonowski, as well as Antonia Apfelbeck.

I would like to express my thanks the CoALL study center in Hamburg for providing the extremely rare and valuable CoALL samples as well as for enabling a cooperation guaranteeing an optimal use of the samples.
During the twelve-month research period I was financially supported by a promotional scholarship of the *José Carreras Leukämie-Stiftung*. I am grateful for this support as it enabled me to fully focus on the research project.

Finally, I am particularly grateful for all the mental support and encouragements given by my friends and family as well as their forgiving attitude regarding my unavailability.

14. Affidavit (Eidesstaatliche Erklärung)

Eidesstattliche Versicherung

Wilhelm, Jonas

_____

Name, Vorname

Ich erkläre hiermit an Eides statt, dass ich die vorliegende Dissertation mit dem Titel:

T-cell interaction with leukemia in the bone marrow of pediatric patients with T-cell acute lymphoblastic leukemia

selbständig verfasst, mich außer der angegebenen keiner weiteren Hilfsmittel bedient und alle Erkenntnisse, die aus dem Schrifttum ganz oder annähernd übernommen sind, als solche kenntlich gemacht und nach ihrer Herkunft unter Bezeichnung der Fundstelle einzeln nachgewiesen habe.

Ich erkläre des Weiteren, dass die hier vorgelegte Dissertation nicht in gleicher oder in ähnlicher Form bei einer anderen Stelle zur Erlangung eines akademischen Grades eingereicht wurde.

Thusis, 02.08.2022 — Jonas Wilhelm

Ort, Datum — Unterschrift Doktorandin bzw. Doktorand